

AUS DEM WALTER-BRENDEL-ZENTRUM FÜR EXPERIMENTELLE MEDIZIN

LUDWIG-MAXIMILIANS-UNIVERSITÄT MÜNCHEN



Excessive ageing of neutrophils in cancer accelerates tumor progression

Dissertation
zum Erwerb des Doctor of Philosophy (Ph.D.)
an der Medizinischen Fakultät der
Ludwig-Maximilians-Universität zu München

Vorgelegt von
Laura Alice Mittmann
aus Prien am Chiemsee

München, 2020

Supervisor: Prof. Dr. med. Christoph Reichel

Second expert: Prof. Dr. med. Christian Schulz

Dean: Prof. Dr. med. dent. Reinhard HICKEL

Date of oral defense: 16.06.2020

Abbreviations

4T1	mammary carcinoma cell line
AIM2	absent in melanoma 2
Arg-1	arginase-1
ASC	apoptosis-associated speck-like protein containing a CARD
ATP	adenosine triphosphate
BrdU	5-Bromdesoxyuridin
BSA	bovine serum albumin
CAR	chimeric antigen receptor
CARD	caspase activation and recruitment domain
CD4 ⁺	CD4-positive
CD8 ⁺	CD8-positive
CTLA-4	cytotoxic T lymphocyte-associated protein-4
DAMPs	damage-associated molecular patterns
DNA	deoxyribonucleic acid
ds	double-stranded

ECM	extracellular matrix
ESL-1	E-selectin ligand-1
FDA	Food and Drug Administration
FLA-ST	flagellin
G-CSF	granulocyte-colony stimulating factor
HER-2	human epidermal growth factor receptor-2
HMGB1	high-mobility group box 1
HNSCC	head and neck squamous cell carcinoma
HPV	human papillomavirus
IL	interleukin
IRS-1	insulin receptor substrate-1
i.p.	intraperitoneal
i.s.	intrascrotal
i.v.	intravenous
IVM	intravital / <i>in vivo</i> microscopy
LPS	lipopolysaccharides
LRR	leucine-rich repeat
mAb	monoclonal antibody

<i>M. cremaster</i>	<i>musculus cremaster</i>
MDP	muramyl dipeptide
MHC	major histocompatibility complex
MMP9	matrix metalloproteinase 9
MSU	monosodium urate
NE	neutrophil elastase
NETs	neutrophil extracellular traps
NF- κ B	nuclear factor 'kappa-light-chain-enhancer' of activated B cells
NLR	NOD-like receptor
NLRP1	NLR family pyrin domain-containing 1
NLRP3	NLR family pyrin domain-containing 3
NLRC4	NLR family CARD domain-containing protein 4
NOD	nucleotide-binding oligomerization domain
PAMPs	pathogen-associated molecular patterns
PD-1	programmed cell death protein-1
PI3K	phosphoinositol-3-kinase

PMA	phorbol-12-myristat-13-acetat
PBS	phosphate buffered saline
PRR	pattern recognition receptor
PSGL-1	P-selectin glycoprotein ligand-1
RLR	retinoic acid inducible gene-1 like receptor
ROS	reactive oxygen species
SCC VII	squamous cell carcinoma VII cell line
SEM	standard error of the mean
ss	single-stranded
TGF- β	transforming growth factor-beta
T _H	T-helper cells
TNF	tumor necrosis factor
T _{reg}	regulatory T cell
TLR	toll-like receptor
VEGF	vascular endothelial growth factor
WHO	World Health Organization
WT	wildtype

Table of contents

1	Introduction	11
1.1	Cancer.....	11
1.1.1	Breast cancer.....	11
1.1.2	Head and neck cancer	12
1.2	Therapeutic approaches of cancer	13
1.3	Immunotherapy	15
1.4	The immune system.....	17
1.4.1	The adaptive immune system.....	17
1.4.2	The innate immune system.....	19
1.5	Neutrophil functions in acute inflammatory conditions.....	24
1.6	Neutrophil functions in tumors.....	25
1.6.1	Recruitment of neutrophils to tumors.....	30
1.7	Aged neutrophils	31
1.8	The inflammasomes.....	34
1.8.1	The NLRP3 inflammasome.....	35
1.8.2	The NLRP3 inflammasome in tumors.....	37
2	Objective.....	39
3	Material and Methods	40
3.1	Ethics	40
3.2	Animals	40
3.3	Anesthesia	40
3.4	Cell lines.....	41

3.4.1	Thawing of cells.....	41
3.4.2	Splitting of cells.....	42
3.4.3	Determination of cell numbers	42
3.5	Animal models.....	42
3.5.1	Orthotopic tumor models	42
3.5.2	Heterotopic tumor models.....	47
3.5.3	<i>M. Cremaster</i> assay.....	51
3.5.4	Peritonitis assay.....	53
3.6	Flow cytometry	55
3.7	<i>In vivo</i> microscopy.....	55
3.8	Tumorigenicity of neutrophils	57
3.9	Activation of neutrophils	58
3.9.1	Analysis of integrin expression on neutrophils in the blood	58
3.9.2	Analysis of ICAM-1/CD54-Fc binding properties of neutrophils	58
3.10	Activation of endothelial cells	59
3.11	Immunohistochemistry and confocal microscopy	60
3.11.1	Analysis of ICAM-1/CD54 and VCAM-1/CD106 expression in cremasteric venules.....	60
3.11.2	Visualizing neutrophils in tumor sections.....	61
3.12	Assessment of tumor development	62
3.13	Cell proliferation assay	62
3.13.1	Investigating the effect of tumor-primed neutrophils on cell proliferation.....	63

3.14	Endothelial cell migration	64
3.15	Multiplex immunoassays	64
3.16	ELISA	65
3.16.1	HMGB1.....	65
3.16.2	S100A8/A9	65
3.17	MSU measurements.....	65
3.18	TLR2 and 4 activity assay	66
3.19	Statistics.....	66
4	Results.....	67
4.1	Cytokines in supernatants of cultured tumor cells, solid tumors, and serum samples.....	67
4.2	Neutrophils in the circulation of tumor-bearing mice	68
4.3	CXCR4 expression levels on blood neutrophils in tumor-bearing mice ...	69
4.4	The fate of excessively aged neutrophils in tumor-bearing mice	70
4.4.1	Accumulation of aged neutrophils in the peritumoral microvasculature	70
4.4.2	Leukocyte subsets in solid SCC VII and 4T1 tumors	71
4.5	The recruitment of aged neutrophils.....	73
4.5.1	The release of DAMPs by tumor cells.....	73
4.5.2	The effect of DAMPs on myeloid leukocyte recruitment	74
4.5.3	The effect of tumor-released mediators on TLR2 and TLR4 activity.	75
4.5.4	The effect of MSU on inflammasome activation.....	76
4.5.5	The effect of inflammasome activation on myeloid leukocyte recruitment.....	77

4.5.6	The effect of NLRP3 inflammasome activation on neutrophils	78
4.5.7	The effect of NLRP3 inflammasome activation on endothelial cells..	80
4.5.8	The effect of DAMPs on endothelial cells	81
4.5.9	Cytokine release upon NLRP3 inflammasome activation	82
4.5.10	ICAM-1/CD54 and VCAM-1/CD106 expression on cremasteric endothelial cells after activation of the NLRP3 inflammasome	83
4.5.11	Myeloid leukocyte trafficking in the cremaster muscle after NLRP3 inflammasome activation	84
4.5.12	The effect of NLRP3 inflammasome inhibition on neutrophil trafficking in tumors.....	86
4.6	The role of aged neutrophils in tumor progression	87
4.6.1	The effect of depleting neutrophils in tumor-bearing mice	87
4.6.2	The effect of NLRP3, CXCR4, or CXCR2 inhibitors on tumor weight and neutrophil infiltration of tumors.....	89
4.6.3	Direct effects on tumor cell proliferation.....	91
4.7	The mechanisms underlying tumor growth mediated by aged neutrophils	92
4.7.1	Expression of N1 and N2 phenotype-associated molecular markers in neutrophils recruited by NLRP3 inflammasome activation.....	92
4.7.2	The effect of tumor-primed neutrophils on tumor cell proliferation	93
4.7.3	The effect of tumor-primed neutrophils on microvascular endothelial cell proliferation.....	94

4.7.4	The effect of tumor-primed on the migration of microvascular endothelial cells	94
4.7.5	The effect of neutrophil depletion on the microvascular network of tumors	95
4.7.6	The effect of depleting neutrophils on T cell infiltration into tumors ..	96
5	Discussion	98
5.1	Material and Methods.....	98
5.2	Results	103
5.2.1	The fate of excessively ageing neutrophils in cancer.....	105
5.2.2	The recruitment of excessively ageing neutrophils to tumors	106
5.2.3	The role of excessively ageing neutrophils in tumor progression ...	111
5.2.4	The mechanisms excessively ageing neutrophils employ to mediate tumor growth.....	114
6	Conclusion.....	117
7	Table of figures and tables.....	119
8	References	123
9	Acknowledgements.....	143
10	Publications and scientific presentations	144
11	Affidavit.....	147
12	Confirmation of congruency between printed and electronic version of the doctoral thesis	148

Abstract

Neutrophils have always been recognized as key players in the acute inflammatory response. Their contribution to the pathogenesis of malignant tumors, however, is an emerging concept. Recent findings revealed that neutrophils undergo phenotypic changes during their time in the circulation, a process referred to as biological ageing. Whereas these changes have been shown to be crucial for their anti-infectious functions, studies also revealed these highly reactive immune cells can oppose a threat to the vascular health. The role of neutrophil biological ageing in cancer, however, remains unknown. In the present study, we now demonstrate that due to specific chemokines released during early tumorigenesis, biological ageing of circulating neutrophils is further accelerated, allowing these innate immune cells to accumulate in malignant lesions. This is facilitated by DAMPs derived from the tumor, which activate the NLRP3 inflammasome in peritumoral macrophages and, in turn, microvascular endothelial cells, ultimately facilitating the recruitment of neutrophils to the malignancies. Once present in the neoplastic lesions, neutrophils supported tumor progression by stimulating tumor cell proliferation through release of neutrophil elastase. Counteracting neutrophil ageing (*via* blockade of the chemokine receptor CXCR2) or neutrophil recruitment to the tumor (*via* inhibition of NLRP3 inflammasome activation) in tumor-bearing mice severely compromised tumor growth. In conclusion, our data uncover a self-sustaining mechanism of malignant tumors that induces excessive biological ageing of circulating neutrophils and thereby promotes the progression of these neoplastic lesions. This process represents a particularly promising therapeutic target as first clinical studies already revealed encouraging results of using CXCR2 inhibitors in breast cancer.

1 Introduction

1.1 Cancer

Cancer is a disease defined by cells that are able to proliferate indefinitely, resist cell death, secrete self-sustaining growth signals, withstand anti-growth signals, as well as enhance angiogenesis and invade and metastasize (Hanahan & Weinberg, 2011). As healthy tissue successfully manages to control all these aspects, cancer is considered a disease that is caused by genome instability (Hanahan & Weinberg, 2000). These neoplastic cells can arise from different tissues and organs. However, since mortality rates vary among different types of cancer, it becomes apparent that tumors are not merely clones of malignant cells, but rather complex organs (Egeblad, Nakasone, & Werb, 2010).

1.1.1 Breast cancer

Breast cancer develops from any cell of the mammary gland. However, most breast tumors (95 %) belong to the group of adenocarcinomas which means they developed from epithelial cells of the gland (Makki, 2015). Breast cancer accounts for about 25.1 % of all cancers and is the most common malignancy in women worldwide (Ghoncheh, Pournamdar, & Salehiniya, 2016). According to the World Health Organization (WHO), this disease is impacting 2.1 million women per year (WHO, 2018a).

Apart from the female sex, the major risk factor for this disease is age. About 80 % of the cases are diagnosed in women above the age of 50 (Benson et al., 2009). With up to 10 % of breast cancer cases in western countries being linked to

mutations in certain genes, genetic predisposition also plays its part in developing this disease (McPherson, Steel, & Dixon, 2000). For instance, with breast cancer gene-1 (BRCA1) and -2 (BRCA2), two genes have been identified in which inherited mutations cause a higher risk of developing breast cancer (Ford et al., 1998; King, Marks, & Mandell, 2003). Moreover, studies revealed that increased concentrations of endogenous estrogens in the serum are strongly associated with a higher risk for breast cancer in postmenopausal women (Key, Verkasalo, & Banks). Hence, as prevention it has already been suggested to influence the hormonal milieu of women at risk (McPherson et al., 2000). As several studies revealed that incidence rates are higher in more developed countries, corresponding rates in less developed countries are still lower. However, even in these countries rates are rising, suggesting external factors such as diet and alcohol consumption may also contribute to the pathogenesis of this oncological disorder (Key et al., 2001).

1.1.2 Head and neck cancer

More than 90 % of all head and neck cancers are squamous cell carcinomas. These can arise from squamous cells in mucous membranes in various subsites of the head and neck region: the hypopharynx, oropharynx, lip, oral cavity, nasopharynx, or larynx (Marur & Forastiere, 2008; Vigneswaran & Williams, 2014). Contrary to breast cancer, the squamous cell carcinoma of the head and neck only accounts for about 5-10 % of all cancers (Vigneswaran & Williams, 2014).

Continuous exposure to tobacco and alcohol has been linked to the development of these malignancies (Marur & Forastiere, 2008). However, recently the infection

with high-risk human papillomaviruses (HPV), especially type 16, has also been shown to be implicated in the pathology of malignancies in the upper airway, such as respiratory papillomatosis and oropharyngeal cancer (Gillison et al., 2012; Sturgis & Cinciripini, 2007). Previously, these specific types of HPV were only linked to malignancies of the anogenital area (McKaig, Baric, & Olshan, 1998), as for instance, 80 % of cervical tumors are caused by these viruses (Bosch et al., 1995).

1.2 Therapeutic approaches of cancer

In localized stage I tumors, surgery is still the most effective way of treatment, as it removes 100 % of all tumor cells. However, in many cases, with stage II or stage III malignancies, surgical approaches are combined with radiotherapy. Clinical radiotherapy had its debut in 1896 when Emil Grubbé treated advanced ulcerated breast cancer with X-rays (Bernier, Hall, & Giaccia, 2004). The aim of this form of therapy is to use high doses of radiation in order to eliminate cancer cells and shrink tumors. This method can either be employed pre-surgery ('neo-adjuvant'), post-surgery ('adjuvant'), or intraoperative. Radiotherapy alone is used in early stage or non-metastasized advanced head and neck cancers (Urruticoechea et al., 2010). In case of more advanced tumors or stage IV malignancies, where the tumor has spread from its place of origin to another organ, systemic treatment is necessary.

One example of a systemic treatment approach is the use of chemotherapeutics. The first cancer chemotherapeutics were developed in 1940. Whereas the early agents, the alkylating agents, were based on highly electrophilic reagents that

have the ability to react with cellular nucleophiles, the second group of cancer chemotherapeutics were antimetabolites (A. Baudino, 2015). Both reagents interfere with deoxyribonucleic acid (DNA) synthesis, thus, lead to cancer cell death. Nowadays, chemotherapy usually comprises a cocktail of many different reagents (Shewach & Kuchta, 2009) and can be used in several different ways: as neoadjuvant therapy (pre-surgery) in order to reduce the size of the tumor that has to be removed, adjuvant therapy (post-surgery) to ensure any tumor cells that might be left in patient are removed as well or concomitant without any surgery (A. Baudino, 2015).

However, since chemotherapeutic reagents are used to treat the entire body, they also target and damage healthy tissue. Hence, side effects are usually quite severe (A. Baudino, 2015). It has become apparent that each tumor needs to be targeted directly and in unique ways in order to further reduce mortality, salvage healthy tissue and reduce side effects. Thus, the concept of targeted therapy evolved. These new targets include growth factors, signaling molecules, cell-cycle proteins, modulators of apoptosis, as well as molecules enhancing angiogenesis (Urruticoechea et al., 2010). In breast cancer, blocking the human epidermal growth factor receptor-2 (HER-2) has been shown to potently inhibit proliferation of breast cancer cells and is already used to treat HER-2 positive breast cancer patients (Plosker & Keam, 2006). Another example is the approach of targeting the epidermal growth factor receptor (Jablonska, Leschner, Westphal, Lienenklaus, & Weiss) with Cetuximab, a monoclonal antibody (mAb). It binds to the epidermal growth factor receptor with high affinity which has been shown to inhibit cell proliferation, enhance apoptosis, reduce angiogenesis, as well as invasiveness and metastasis (Harding, 2005). Another systemic treatment approach aiming to

target the tumor without causing severe side effects, is hormonal therapy. This treatment modality is often used in breast cancer, as certain subtypes were shown to be affected by hormone levels. The most common types of hormone therapy either aim to lower estrogen level within the entire system or to block estrogen from binding to its receptor on breast cancer cells (Burstein et al., 2018; Fabian, 2007).

1.3 Immunotherapy

The most recent advances in treating cancer were made in the field of cancer immunotherapy. In order to develop solid tumors, cancer cells have to find mechanisms to avoid immune recognition and their subsequent elimination. The aim of immunotherapy is to use these mechanisms, interfere with them, and thereby inhibit tumor growth (Farkona, Diamandis, & Blasutig, 2016). For instance, blocking immune checkpoints which cancer cells employ to activate immune-inhibitory pathways (Pardoll & Topalian, 1998). One of these is the cytotoxic T lymphocyte-associated protein-4 (CTLA-4), a receptor that down-regulates T cell activation upon binding one of its ligands, CD80 or CD86. By administering mAbs against CTLA-4, cancer cells can no longer attach to the immune checkpoint and anti-cancer T cell responses are fostered (Leach, Krummel, & Allison, 1996; Ribas et al., 2016). Indeed, clinical trials revealed promising results for melanoma patients with metastatic disease (Hodi et al., 2010) and led to the approval by the Food and Drug Administration (FDA) in 2011 (Farkona et al., 2016). Another checkpoint molecule is the programmed cell death protein-1 (PD-1) receptor, which is also expressed on T cells and inhibits proliferation, cytokine release, as

well as reduces their cytotoxic properties upon binding (Ishida, Agata, Shibahara, & Honjo, 1992; Keir, Butte, Freeman, & Sharpe, 2008). The most prominent ligand for PD-1 is PD-L1 which can be found on healthy, but also on cancer cells. Inhibiting the interaction of PD-1 and PD-L1 was shown to enhance T cell function and, thereby, increase antitumor activity of these immune cells (Topalian et al., 2012). Several mAbs targeting PD-1 and PD-L1 have already been approved by the FDA after successful clinical trials. Recent studies also revealed other potential pathways such as lymphocyte activation gene 3 (Triebel et al., 1990) or the T cell immunoglobulin and mucin domain-containing 3 protein (Sakuishi et al., 2010), that could evolve as future therapeutic targets. Apart from the immune checkpoint inhibitors, another promising approach aiming to train the immune system to attack cancer, is the chimeric antigen receptor (CAR) T cell therapy. It involves isolating T cells from the patient, equipping these isolated immune cells with man-made antigen receptors that target the tumor, and transferring the improved T cells back into the patient (Almåsbaek, Aarvak, & Vemuri, 2016; Farkona et al., 2016). Especially when it comes to hematologic cancers, this approach has shown very encouraging results (Chavez, Bachmeier, & Kharfan-Dabaja, 2019). Cancer immunotherapy also involves the use of monoclonal antibodies in order to target cancer-specific antigens, or of non-specific adjuvants in order to boost the immune system in general (Circelli, Tornesello, Buonaguro, & Buonaguro, 2017; Weiner, Surana, & Wang, 2010). Moreover, the development of cancer vaccines has been another immunotherapeutic strategy. This approach aims to initiate the process of activating the immune system through administering tumor antigens (Yaddanapudi, Mitchell, & Eaton, 2013). Despite all these advances, further

progress still needs to be made in this area. In order to continue this progress, it is of utter importance to understand how the immune system works.

1.4 The immune system

In a world full of pathogenic as well as non-pathogenic threats to the homeostasis of our bodies, the immune system is essential to ensure our wellbeing. Being a highly conserved system among many species, highlights once more its importance for our survival. Consequently, dysfunctions of the immune system can oppose a severe threat to our health: whereas overactivity can lead to allergies or autoimmune diseases, underactivity causes the body to be susceptible to infections or even the development of tumors (Parkin & Cohen, 2001). Hence, understanding the underlying mechanisms of immune responses is of great importance to be able to combat its dysfunctions.

Historically, the immune system is divided into two parts: the innate and the adaptive immune system (Medzhitov & Janeway, 2000).

1.4.1 The adaptive immune system

Comparing the two parts of the immune system, the adaptive immune system represents the more fine-tuned immune response, meaning it operates with a small number of cells that possess high specificity for an individual threat (Bonilla & Oettgen, 2010; Chaplin, 2010). These immune responses are performed by T and B lymphocytes that are equipped with antigen specific receptors. Antigen presenting cells, such as macrophages and dendritic cells, phagocytose

pathogens and present small pieces on major histocompatibility complex (MHC) molecules on their surface. Subsequently, T and B lymphocytes can bind these *via* their specific receptors and thus, become activated. These cells against a specific antigen are able to persist within the body for the entire life which creates an immune memory that can be reactivated after another encounter with the target antigen and consequently, provide a rapid response when necessary (Bonilla & Oettgen, 2010). After developing in the bone marrow from hematopoietic stem cells that give rise to their lymphoid progenitor, T cells mature in the thymus and can be differentiated into the two types: cytotoxic CD8-positive (CD8⁺) T cells, with the primary function to eliminate infected cells, and CD4-positive (CD4⁺) T cells which are mainly responsible for the regulation of cellular and humoral immune responses (Chaplin, 2010; Cooper & Alder, 2006). CD4⁺ T cells can further be divided into T-helper (T_H) cells and regulatory (T_{reg}) T cells (Bonilla & Oettgen, 2010). B lymphocytes are also developed from the lymphoid progenitor in the bone marrow. After activation, naive B cells can either develop into effector cells or plasma cells (Pieper, Grimbacher, & Eibel, 2013). Through becoming plasma cells, they are responsible for the humoral part of the adaptive immunity by producing and secreting antibodies (LeBien & Tedder, 2008). Antibodies can bind to their respective antigen, neutralize it, activate the complement system, and thereby, recruit more phagocytosing cells (Forthal, 2014).

As both cell types are depending on the exposure to antigen presenting cells from the innate immune system and can also influence the innate response by secreting cytokines, it becomes apparent that the separation between the two immune responses is rather historical than just functional.

1.4.2 The innate immune system

The innate immune system represents the body's first line of defense against potential threats and provides a rapid, yet more unspecific response (Medzhitov & Janeway, 2000). In addition to physical barriers or defense mechanisms such as saliva or gastric acid, the innate immune system has to determine what represents a threat to the homeostasis in order to protect the body. Therefore, three ways of immune recognition have been proposed (Medzhitov & Janeway, 2002). For example, the host is able to determine "microbial non-self" by binding conserved microbial products only produced by microorganisms which are not part of the body. They are referred to as pathogen-associated molecular patterns, called PAMPs (Mogensen, 2009). Moreover, "missing self" is identified by applying markers that are always part of the "normal self", which are unique for the host and not part of microorganisms. Several studies revealed that the immune system eliminates cells that do not express higher levels of the MHC class I protein. Consequently, the concept of missing self was introduced. MHC class I is expressed on all nucleated cells and only downregulated by viral infection or cellular damage, hence, serving as an fundamental marker for self-recognition (Ljunggren & Kärre, 1990). In order to detect "induced and altered self" the host relies on certain markers that are released upon infection or cellular damage, so called damage-associated molecular patterns (DAMPs) (Bianchi, 2007; Matzinger, 2002). These three mechanisms are the door opener to activating the innate immune response.

1.4.2.1 Pathogen-associated molecular patterns, Damage-associated molecular patterns and their pattern-recognition receptors

In order to recognize these structures and distinguish PAMPs as well as DAMPs, the host immune system has a set of receptors, called the pattern-recognition receptors (PRR). These receptors can either be membrane-associated, inside the cell, or present in a secreted form. Consequently, several different types of PRR can be distinguished: transmembrane toll-like receptors (TLR), cytosolic receptors such as nucleotide-binding oligomerization domain (NOD)-like receptors (NLR) or retinoic acid inducible gene-I like receptors (RLR), and the secreted PRR (A. Iwasaki & Medzhitov, 2010).

In total, 11 human TLRs and 13 TLRs in mice have been identified so far (X. Zhang & Mosser, 2008). TLRs located on the cell surface such as TLR4, TLR1 and 2, TLR6, and TLR5 largely recognize PAMPs on the surface of microbes, whereas endosomal TLRs such as TLR3, TLR7, TLR8, and TLR9 recognize microbial nucleic acids, double-stranded (ds) (Srikrishna & Freeze), ribonucleic acid (RNA), single-stranded (ss) RNA, and dsDNA (Takeda & Akira, 2005). Examples for PAMPs expressed on the surface of pathogens include lipopolysaccharides (LPS) of gram-negative bacteria or peptidoglycan of gram-negative and gram-positive bacteria (Mogensen, 2009). These receptors are mainly found on macrophages and dendritic cells but also on neutrophils, eosinophils, and epithelial cells (Chaplin, 2010; Akiko Iwasaki & Medzhitov, 2004). Cytosolic TLRs have been shown to detect viral proteins (Pichlmair & Reis e Sousa, 2007). Since the NLRs are cytosolic as well, they also bind soluble intracellular ligands. There are over 20 NLR encoding genes, all containing the following three domains: the C-terminal leucine-rich repeat (LRR) domain which is

responsible for binding microbial patterns, the NOD domain that is used to form multimeric complexes, and the N-terminal effector domain (Kanneganti, Lamkanfi, & Núñez, 2007). The NLRs are all able to sense pathogens but also recognize DAMPs released from injured or stressed tissue (Gallucci & Matzinger, 2001; Martinon, Mayor, & Tschopp, 2009). These DAMPs are molecules that are chemically completely unrelated, however, are all potent triggers of sterile inflammation (Hernandez, Huebener, & Schwabe, 2016). The secreted PRR are pattern-recognition proteins that contribute to initiating an immune response by mediating opsonization and activating the complement system: For instance, Dectin-1 can be activated through components of yeast. Collectins have the ability to recognize microbial carbohydrates and consequently, opsonize the microbe for phagocytosis. Pentraxins and Ficolins also recognize PAMPs and activate complement system (Bottazzi, Doni, Garlanda, & Mantovani, 2010).

1.4.2.2 The innate immune response

Once the host system has sensed danger, either by the binding of PAMPs or DAMPs to PRR, an inflammatory response is triggered, resulting in the recruitment of immune cells. The innate immune system comprises dendritic cells, mast cells, natural killer cells, as well as phagocytes such as macrophages, monocytes, and neutrophils (Chaplin, 2010). Together with eosinophils and basophils, neutrophils also belong to the group of polymorphonuclear leukocytes or granulocytes. Hence, these cells do not only display a varying shape of their nucleus but also contain antimicrobial granules in their cytoplasm (Geering, Stoeckle, Conus, & Simon, 2013). Regarding the timescale of the immune response, neutrophils are recruited

to the site of infection first. Next, monocytes reach the target destination. All of these cells are highly phagocytic and therefore play an important role in the clearance of pathogens (S. Nourshargh & Alon, 2014; Zuchtriegel et al., 2015).

1.4.2.2.1 The leukocyte recruitment cascade

In order to get to sites of inflammation, leukocytes follow a distinct cascade of events which is referred to as the leukocyte adhesion cascade (Ley, Laudanna, Cybulsky, & Nourshargh, 2007) (**Fig. 1.1**). First, these immune cells are captured and roll on the luminal surface of postcapillary venular vessel walls (S. Nourshargh & Alon, 2014; Sperandio et al., 2003). This weak adhesive interaction is mostly mediated through a family of transmembrane glycoproteins: the selectins. L-selectin/CD62L is known to be expressed on leukocytes, whereas E-selectin is found on endothelial cells and P-selectin/CD62P is expressed on activated endothelial cells and platelets (Kansas, 1996). All these selectins interact with P-selectin glycoprotein ligand 1 (PSGL-1) (McEver & Cummings, 1997; Sperandio, 2006), a ligand expressed on leukocytes and other cells. Hence, endothelial cells capture circulating leukocytes *via* interaction of E- and P-selectin with PSGL-1, despite constant blood flow. Several studies revealed that the shear stress arising from blood flow is even required for successful capturing of leukocytes (Lawrence, Kansas, Kunkel, & Ley, 1997). Furthermore, E-selectin/CD62E was also shown to bind to glycosylated CD44 and E-selectin ligand-1 (ESL-1) (Hidalgo, Peired, Wild, Vestweber, & Frenette, 2007). The binding of L-selectin to PSGL-1 results in leukocyte-leukocyte interactions, leading to secondary leukocyte capturing by already adhesive immune cells. Apart from their role in capturing and rolling,

studies revealed selectins also activate immune cells (Zarbock & Ley, 2009). Subsequently, this first weak adhesion is further strengthened by inflammatory cytokines that activate endothelial cells and thereby, cause an upregulation in adhesion molecules as well as chemokines and lipid chemoattractants (Campbell, Qin, Bacon, Mackay, & Butcher, 1996). These chemokines and chemoattractants are very strong activators of integrins - the main molecules responsible for the firm intravascular adherence of leukocytes. Inside-out signaling pathways from chemokines binding to chemokine receptors, result in switching their conformation from low-affinity to extended-intermediate and finally high-affinity conformation with its open ligand-binding pocket (Arnaout, Mahalingam, & Xiong, 2005). This, for instance, allows the β 2 integrins LFA-1/CD11a and Mac-1/CD11b, expressed on leukocytes, to bind to ICAM-1/CD54 or ICAM-2/CD102 on endothelial cells. The β 1 integrin VLA-4/CD49d can bind to VCAM-1/CD106 both facilitating firm adhesion of the leukocytes to the endothelium (Ley et al., 2007). Moreover, it has been shown that further downstream this interaction activates the non-receptor tyrosine kinase Syk which has been shown to play an important role for neutrophil activation (Mócsai, Ruland, & Tybulewicz, 2010; Schymeinsky, Then, & Walzog, 2005). Subsequently, leukocytes are crawling along the endothelial surface to find appropriate sites of transmigration. Guided by adherent platelets (Zuchriegel et al. PLOS Biol 2016), leukocytes then transmigrate either *via* the transcellular route (roughly 10%), directly through the cell, or the paracellular pathway (roughly 90%) through endothelial-cell junctions. However, the route of transmigration seems to be dependent of the type of the underlying tissue, therefore, percentages vary (Maas, Soehnlein, & Viola, 2018; Phillipson et al., 2006; Woodfin et al., 2011). In order to arrive in the inflamed tissue, three different barriers have to be crossed:

first the endothelial cells (passage time 2-5 min) guided by adhesion and signaling molecules such as JAM-A, PECAM-1, CD99, CD99L2, and ESAM (Bixel et al., 2010; Muller, Weigl, Deng, & Phillips, 1993; Sussan Nourshargh, Krombach, & Dejana, 2006; Woodfin et al., 2007), second the endothelial-cell basement membrane, mainly consisting of collagen type IV and laminins (passage time 5-15min), and finally the pericyte sheath. Once leukocytes have overcome that barrier, they move through the interstitium along a chemokine gradient to their target destination (S. Nourshargh, Hordijk, & Sixt, 2010).

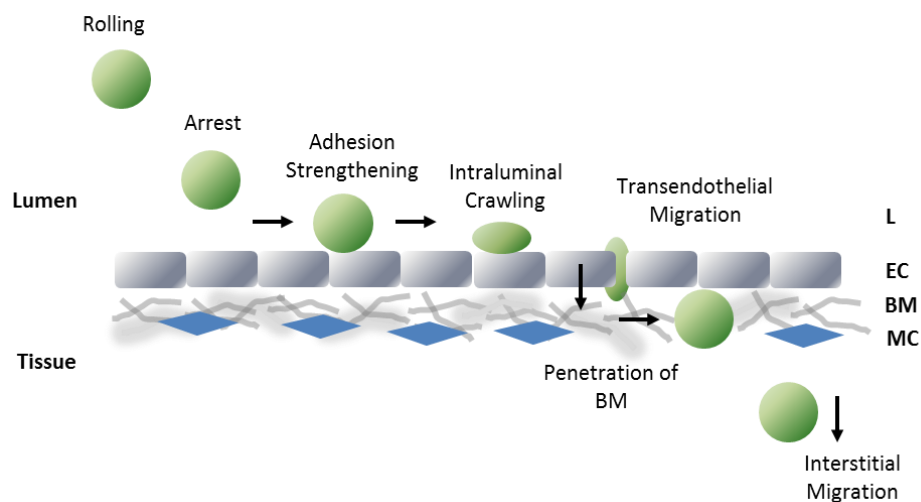


Figure 1.1: A schematic overview of the leukocyte adhesion cascade. First, leukocytes roll on the endothelial surface mediated by members of the family of selectins, until they firmly adhere *via* interactions of members of the immunoglobulin superfamily with integrins. Next, leukocytes crawl along the endothelium in order to find appropriate sites for transmigration that allow them to enter the interstitium where they can finally resolve the inflammation.

1.5 Neutrophil functions in acute inflammatory conditions

The importance of neutrophils for resolving inflammation and maintaining homeostasis (Arandjelovic & Ravichandran, 2015) also becomes evident when looking at the number of these leukocytes in the body: in humans, 50-70 % of the

circulating leukocytes are neutrophils, and up to 2×10^{11} new neutrophils are produced daily under homeostatic conditions. Under inflammatory conditions these numbers can even raise higher (Mayadas, Cullere, & Lowell, 2014). Neutrophils develop from the myeloid precursor in the bone marrow (Borregaard, 2010) and their continuous production is ensured by the granulocyte-colony stimulating factor (G-CSF) (Lieschke et al., 1994). These immune cells play a critical role in the clearance of pathogens, with their phagocytic capabilities that allow them to internalize and destroy pathogens (Kennedy & DeLeo, 2009), and by releasing reactive oxygen species or antimicrobial proteins such as cathepsins or defensins (Häger, Cowland, & Borregaard, 2010). Another prominent mechanism how pathogens are eliminated by neutrophils is through the release of neutrophil extracellular traps (NETs). These traps mainly consist of histones as well as antimicrobial proteins and enzymes, such as neutrophil elastase (NE) (Brinkmann et al., 2004). Therefore, their main function is not only to capture pathogens and keep them from spreading, it is also to eliminate those germs (Kolaczowska & Kubes, 2013). More recent findings revealed neutrophils can also take part in immunoregulatory functions: Activated neutrophils are capable of expressing and releasing cytokines, thereby influencing the recruitment of other immune cells (Cassatella, 1999).

1.6 Neutrophil functions in tumors

As described earlier, neutrophils are important for the clearance of pathogens and for the re-establishment of the body's homeostasis under acute inflammatory conditions. However, under chronic inflammatory conditions neutrophil functions

can differ a fair bit (Soehnlein, Steffens, Hidalgo, & Weber, 2017). As tumors are often described as “wounds that do not heal”, this is also the case when it comes to malignancies (Dvorak, 1986). Neutrophils have been shown to be present in various types of solid tumors and their microenvironment (Jensen et al., 2012; Rao et al., 2012; Sokratis Trelakis et al., 2011). Whereas early studies described tumor-associated neutrophils as bystanders (Uribe-Querol & Rosales, 2015), several studies linked increased neutrophil numbers in blood and tumors to a poor outcome for the patients (Gentles et al., 2015; Shen et al., 2014; S. Trelakis et al., 2011). These findings suggested a prognostic function of the neutrophil-to-lymphocyte ratio in tumors and blood (Templeton et al., 2014). Thus, it has become apparent that neutrophils must display various functions when present in tumors or their environment (**Fig. 1.2**). For instance, by releasing large amounts of reactive oxygen species (ROS) or enzymes, neutrophils can cause DNA damage within epithelial cells and thus, help initiate tumor development (Antonio et al., 2015; Knaapen, GÜngör, Schins, Borm, & Van Schooten, 2006). Moreover, neutrophils release NE. By entering tumor cells, this serine protease has the ability to downregulate the insulin receptor substrate-1 (IRS-1), a negative regulator of phosphoinositide 3-kinase (PI3K). Hence, this leads to the activation of PI3K, resulting in increased tumor cell proliferation (Houghton et al., 2010). Furthermore tumor-associated neutrophils are large sources of matrix metalloproteinase 9 (MMP9) (Coussens, Tinkle, Hanahan, & Werb, 2000), a factor well known for its role in tissue repair and regeneration (LeBert et al., 2015). A study by Bekes et al. revealed, neutrophils present within the tumor microenvironment produce MMP9, which contributes not only to angiogenesis but also tumor progression and metastasis (Bekes et al., 2011). In addition, by remodeling the extracellular matrix

(ECM), MMP9 can cause the release of vascular endothelial growth factor (VEGF). Hence, this further supports tumor angiogenesis as this factor was shown to induce endothelial cell proliferation and tubule formation *in vitro* (Bergers et al., 2000; Nozawa, Chiu, & Hanahan, 2006). As it has also been revealed that VEGF has the ability to recruit more MMP9 rich neutrophils (Christoffersson et al., 2012), this can become a vicious cycle. In addition, tumor-associated neutrophils are able to directly release their intracellularly stored VEGF upon tumor necrosis factor (TNF) stimulation (Gaudry et al., 1997).

Neutrophils can also contribute to tumor immunity by orchestrating the activity of other immune cells. For example by releasing Arginase-1 (Arg-1), neutrophils are capable of inhibiting T cell function (Dumitru, Moses, Trelakis, Lang, & Brandau, 2012). Hence, depleting neutrophils in tumor-bearing mice lead to increased CD8⁺ T cell numbers in malignant tumors and, consequently, reduced tumor growth (Fridlender et al., 2009).

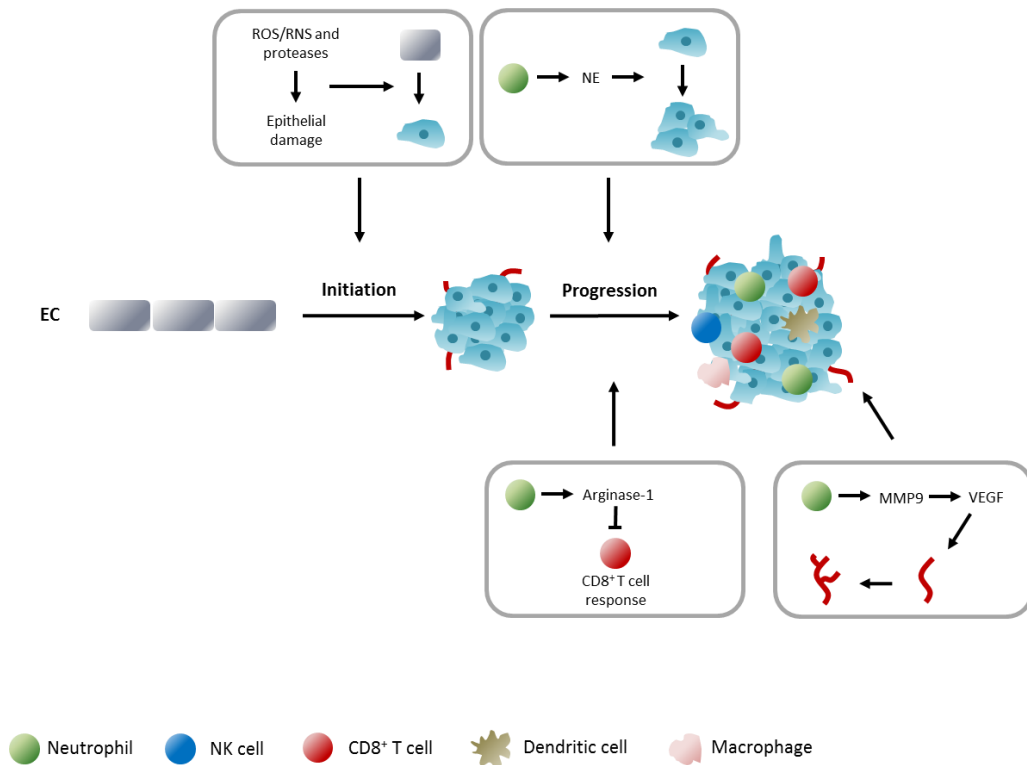


Figure 1.2: Neutrophil function within tumor development and progression. By releasing ROS or proteases neutrophils can cause damage to endothelial cells and thus, support carcinogenesis. The release of NE has been shown to enhance tumor cell proliferation. Moreover, neutrophils contain large amounts of MMP9, which can not only increase tumor progression and metastasis, but also lead to remodeling the ECM thereby causing the release of VEGF. This factor has the ability to support tumor angiogenesis. By releasing Arg-1, neutrophils can inhibit CD8⁺ T cell responses. (adapted by (Coffelt, Wellenstein, & de Visser, 2016)).

In contrast to these findings, other studies suggested neutrophils can also engage in an anti-tumor role by promoting tumor cell clearance and by activating the immune system to combat the tumor (Eruslanov et al., 2014; Mantovani, 2018). Based on these contrasting findings, a separation of tumor-associated neutrophils into two groups has been proposed: the “N1” phenotype describes anti-tumorigenic neutrophils and the “N2” phenotype refers to pro-tumorigenic

neutrophils (Fridlender et al., 2009). These phenotypes can be distinguished by their expression levels of several molecules:

N1 (anti-tumorigenic)	N2 (pro-tumorigenic)
Arg-1 ^{low}	Arg-1 ^{high}
MMP9 ^{low}	MMP9 ^{high}
VEGF ^{low}	VEGF ^{high}
C-C motif chemokines ^{low}	C-C motif chemokines ^{high}

Table 1.1: Molecules associated with the N1 and N2 phenotype of neutrophils. The expression of several molecules differs between the N1 (anti-tumorigenic) and N2 (pro-tumorigenic) phenotype of neutrophils. The N2 neutrophils show high expression levels of Arg-1, MMP9, or VEGF. In contrast, N1 neutrophils exhibit low expression levels of these molecules.

The phenomenon of cells changing phenotypes under different circumstances such as chronic inflammation or tumors is still raising a lot of questions. It has been proposed that tumor-derived factors can play a role in the phenotypic switch from protecting neutrophils under acute inflammatory conditions to tumor-supporting neutrophils (Powell & Huttenlocher, 2016). Furthermore, a recent study revealed blocking transforming growth factor-beta (TGF- β) in the tumor

microenvironment changes the pro-tumor “N2” neutrophils to the anti-tumor “N1” phenotype (Fridlender et al., 2009).

1.6.1 Recruitment of neutrophils to tumors

How neutrophils are recruited to tumors is still under debate. It is likely that the tumor and its microenvironment release cues that actively contribute to the recruitment of neutrophils (Powell & Huttenlocher, 2016). For instance, these signals can be chemokines and cytokines, such as interleukin (IL) CXCL8/IL-8 (Xie, 2001). By expressing the receptors CXCR1/IL-8RA and CXCR2/IL-8RB, neutrophils can bind these cytokines and become activated (Luan et al., 1997; McDonald et al., 2010). Recent studies also revealed that by blocking CXCR2, myeloid leukocyte recruitment into the tumor was impaired which increased the efficacy of chemotherapy in breast cancer models (Acharyya et al., 2012). This further hints that interfering with neutrophil recruitment might be a potent therapeutic approach. Moreover, targeting cytokines instead of their receptors has already been suggested as a potential treatment option (Bekes et al., 2011) as IL-8 was shown to be overexpressed in several carcinomas (Xie, 2001). However, this cytokine-receptor axis is most likely not the only pathway of neutrophil recruitment. Moreover, cytokines such as IL-1 or IL-6 are secreted and have already been implicated in supporting carcinogenesis (Ben-Neriah & Karin, 2011; Grivennikov, Greten, & Karin, 2010). It has also been proposed that tumors release DAMPs, as their high metabolism causes a lot of necrotic tissue and debris (Kreuzaler & Watson, 2012). For instance, these can be heat shock proteins, adenosine triphosphate (ATP), s100 proteins, uric acid, or mediators

such as high-mobility group box 1 (HMGB1). As mentioned earlier, these DAMPs can represent a potent trigger for sterile inflammation. Being constantly released by the tumor and its environment, this can cause a chronic state of inflammation, which has the ability to support tumor progression (Hernandez et al., 2016). By the binding of DAMPs to PRR, activation of inflammatory pathways will take place, resulting in the recruitment of inflammatory cells. It should also be mentioned that several studies revealed DAMPs are released during anti-tumor therapy (Srikrishna & Freeze, 2009), however, not leading to tumor progression, but causing a reinforcing antitumor immune response (Hernandez et al., 2016).

1.7 Aged neutrophils

Until not too long ago, neutrophils were thought to be relatively short lived cells that only remain in the circulation for a couple of hours. However, a more recent study revealed that human neutrophils can stay in the circulation for up to 5.4 days (Pillay et al., 2010). Furthermore, their expected shorter life span also led to the conclusion that neutrophils represent a homogenous cell population, once released from the bone marrow (Nicolas-Avila, Adrover, & Hidalgo, 2017). However, this view is rapidly changing over the past years as different subsets of neutrophils have now been described (Silvestre-Roig, Hidalgo, & Soehnlein, 2016). For instance, several studies revealed that neutrophils undergo phenotypic changes during their time in the circulation, a process that is referred to as the “biological ageing” of neutrophils (J. M. Adrover, Nicolas-Avila, & Hidalgo, 2016). Once neutrophils are released from the bone marrow they are known to express high levels of CXCR2, L-selectin, and Ly6G. Several *ex vivo* as well as *in vivo*

studies revealed that over time the expression levels of several molecules such as CXCR4/CD184 (Martin et al., 2003), CD11b, CD49d (J. M. Adrover et al., 2016), TLR4, ICAM-1/CD54, and CD45 (D. Zhang et al., 2015) increases, whereas expression levels of CXCR2 (Eash, Means, White, & Link, 2009), L-selectin (Casanova-Acebes et al., 2013), and Ly6G (D. Zhang et al., 2015) were shown to decrease (**Fig. 1.3**).

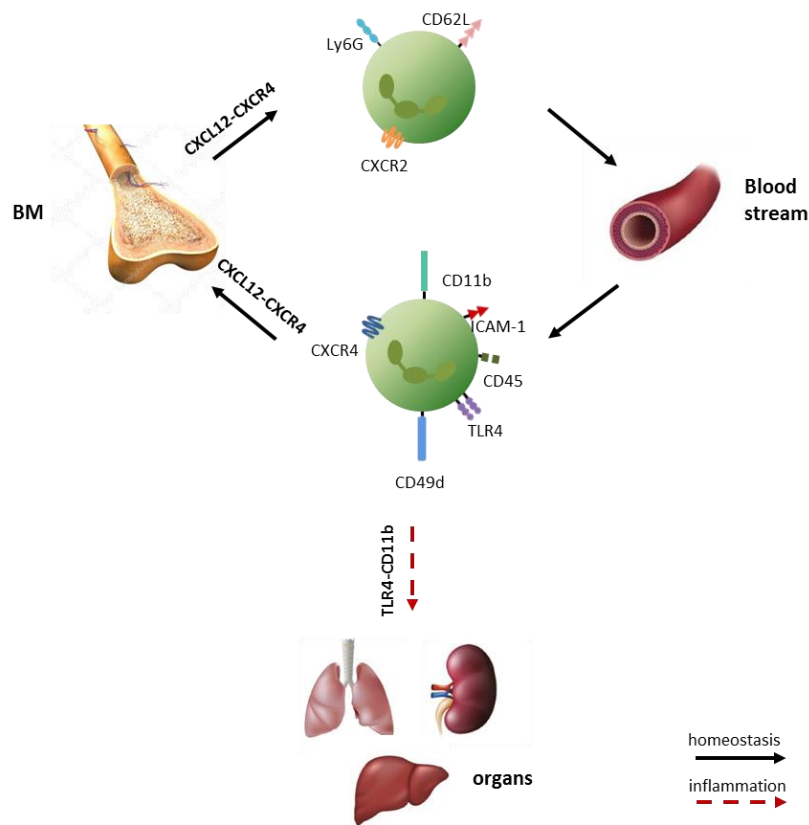


Figure 1.3: Schematic overview of the neutrophil life cycle and their fate in inflammation.

When non-aged neutrophils leave the bone marrow, they express high levels of CXCR2 and low levels of CXCR4 on their surface. However, during their time in the circulation neutrophils undergo phenotypic changes associated with an upregulation of the surface molecules CD11b, ICAM-1/CD54, TLR4, and CXCR4 while downregulating surface expression of CXCR2. This process is referred to as biological ageing. Under steady state conditions, these aged neutrophils are recruited back in the bone marrow (BM) and eliminated *via* BM macrophages. In contrast, under inflammatory conditions these immune cells are the first immune cells recruited to the site of injury or infection.

Regarding the factors that drive this biological ageing process in neutrophils, several different theories have been proposed: as this process begins once the cells are released into the circulation, it is likely to assume that a factor within the blood plasma is able to induce it. However, no specific factor could be determined just yet (J. M. Adrover et al., 2016). Moreover, a publication by Frenette's group discussed the influences of the gut microbiota on the ageing of neutrophils. Germ-free mice showed significantly reduced numbers of aged neutrophils, a phenotype that could be partly restored by administering bacteria-derived PRR agonists (D. Zhang et al., 2015). A very recent publication revealed that binding of neutrophil-released CXCL2 to CXCR2 actually facilitates the ageing process in an autocrine manner, whereas binding of the ligand CXCL12 to its receptor CXCR4 antagonizes it (J. M. Adrover et al., 2019).

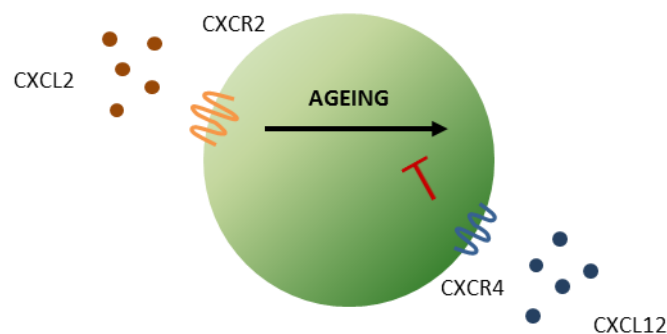


Figure 1.4: Schematic overview of factors driving the biological ageing process in neutrophils. Binding of CXCL2 to CXCR2 induces the biological ageing process; binding of CXCL12 to CXCR4 antagonizes this process (adapted from (J. M. Adrover et al., 2019)).

Studies regarding the function of aged neutrophils revealed that aged neutrophils, characterized through lower L-selectin expression, show more active $\beta 2$ integrins, release more ROS and are more likely to form NETs (Brinkmann et al., 2004).

Furthermore, another study suggested that aged neutrophils serve as first responders during acute inflammation, further hinting towards aged neutrophils being highly reactive immune cells (Uhl et al., 2016). The fact that these cells seem to be aggressive immune cells also highlights the importance of a clearing mechanism in order to protect the circulation: by upregulating CXCR4 neutrophils can home back into the bone marrow, where they are cleared by bone marrow macrophages (Martin et al., 2003). Neutrophils that already migrated into tissues usually undergo apoptosis and are phagocytosed by resident tissue macrophages. This process is known to influence neutrophil granulopoiesis *via* a negative feedback loop through IL-23 and IL-17, in order to ensure constant levels of neutrophils within the circulation (Stark et al., 2005). The role of aged neutrophils in chronic inflammatory conditions such as cancer, however, still raises a lot of questions. A very recent publication already pointed to the fact that neutrophil maturity may correlate with the complexity of neutrophil functions in cancer, and suggests targeting different stages of maturation may be a potential therapeutic approach (Mackey, Coffelt, & Carlin, 2019).

1.8 The inflammasomes

Inflammasomes represent a group of multimeric intracellular protein complexes, acting as signaling platforms upon detection of pathogenic or sterile stressors. The term “inflammasome” was first used by Tschopp and his group in 2002, describing a complex that regulated the activity of inflammatory caspases (Martinon et al., 2009). Their main components are a sensor molecule, an adaptor protein called ASC (apoptosis-associated speck-like protein containing a CARD) and the

caspase-1. Several different types of inflammasomes can be distinguished, based on their sensor molecule, e.g. absent in melanoma 2 (AIM2), NLR family pyrin domain-containing 1 (NLRP1), NLR family pyrin domain-containing 3 (NLRP3) and NLR family CARD domain-containing protein 4 (NLRC4). Whereas NLRP1, NLRP3, and NLRC4 have a NLR sensor molecule, AIM2 has a DNA binding HIN domain (Latz, Xiao, & Stutz, 2013; Ozaki, Campbell, & Doyle, 2015).

1.8.1 The NLRP3 inflammasome

The NLRP3 inflammasome is one of the best characterized types of inflammasomes. As mentioned above, it consists of a sensor molecule that belongs to the NLR family, which can be further divided into an N-terminal effector domain, a central NACHT domain and a carboxy terminal, containing LRR (Ting et al., 2008). Once a threat is present within the cell, the usually auto-repressed NACHT domain is exposed. This causes the oligomerization of NLRP3 and ASC, which contains the caspase activation and recruitment (CARD) domain. Subsequently, the pro-caspase-1 is recruited. Next, CARD brings the monomers of pro-caspase-1 into close proximity which elicits the self-cleavage of caspase-1 and creates its active form, resulting in proteolytically activating IL-1 β and IL-18 (Latz et al., 2013; Tschopp & Schroder, 2010). The release of IL-1 β leads to the recruitment of innate immune cells, whereas IL-18 is important for the release of interferon-gamma and supports the activity of natural killer cells and T cells (Dinarello, 2006; He, Hara, & Núñez, 2016).

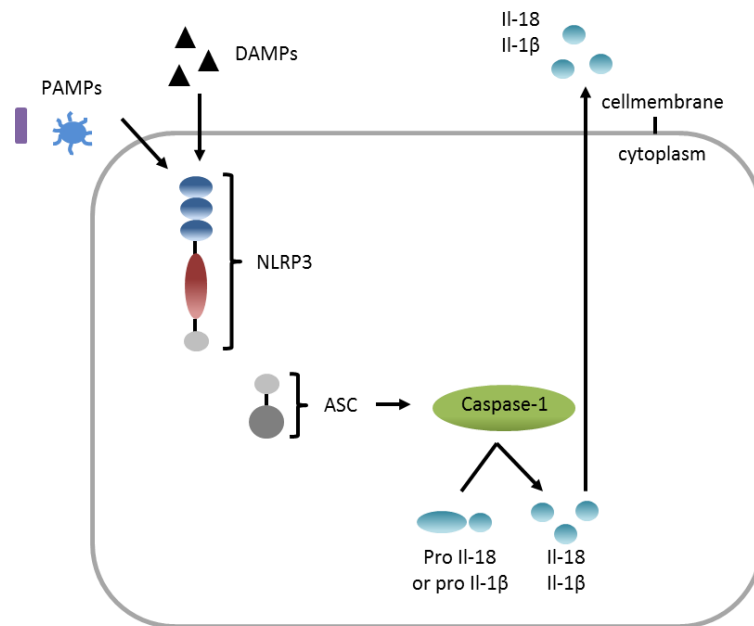


Figure 1.5: NLRP3 inflammasome complex formation. Once the cell is presented with a pathogen- or damage-associated threat, the auto-repression protecting the NLRP3 domains is removed. This leads to the oligomerization of NLRP3 and induces the recruitment of ASC, resulting in the activation of the caspase-1 and the secretion of the inflammatory cytokines IL-18 and IL-1 β (adapted from (Tschopp & Schroder, 2010)).

So far, several different types of immune cells are known to express the NLRP3 inflammasome: macrophages, dendritic cells, neutrophils in the spleen and monocytes (Jo, Kim, Shin, & Sasakawa, 2016). In order to activate the NLRP3 inflammasome, a two-step process has been proposed. The first step is a priming process, where components such as LPS bind to TLRs. This upregulates the nuclear factor 'kappa-light-chain-enhancer' of activated B-cells (NF- κ B) pathway and subsequently stimulates the transcription of NLRP3 inflammasome components (Bauernfeind et al., 2009; Franchi, Eigenbrod, & Núñez, 2009). For the second step of activation, three different possible ways have been described:

- 1) K⁺ efflux through a pore that is formed upon ATP binding to the P2X7 receptor (Ketelut-Carneiro et al., 2015; Schmid-Burgk et al., 2015)
- 2) Mitochondrial dysfunction that results in the production of ROS and the release of mitochondrial DNA into the cytosol (Lamkanfi & Dixit, 2014)
- 3) Lysosomal rupture through the phagocytosis of particles, such as silica or Alum crystals, that results in the release of lysosomal proteases and cathepsin-B (Halle et al., 2008; Hornung et al., 2008)

Activation of the NLRP3 inflammasome has been shown to be involved in many different pathologies. Therefore, deeper understanding of its mechanisms is crucial and could allow the development of novel therapeutics (Tschopp & Schroder, 2010).

1.8.2 The NLRP3 inflammasome in tumors

Persistent inflammation has been described to support carcinogenesis and tumor progression. Hence, it is not surprising that inflammasomes have been revealed to be abnormally expressed and activated in various types of tumors (H. Wang et al., 2018). Especially, activation of the NLRP3 inflammasome has been subject to many studies. Some studies point to a protective function of inflammasome activation when it comes to an immune response against the tumor (Gasparoto et al., 2014). However, most studies revealed that the NLRP3 inflammasome contributes to tumor initiation, growth, as well as metastasis (Bruchard et al., 2012; Huang et al., 2017; H. Wang et al., 2018). Moreover, it was shown that all inflammasome components, such as NLRP3, caspase-1, as well as IL-1 β and IL-18 are highly expressed in head and neck squamous cell carcinoma (HNSCC) cell

lines as well as a mouse HNSCC model (Huang et al., 2017). In breast cancer, elevated expression levels of IL-1 β have been shown to be associated with carcinogenesis (Jin et al., 1997). Overall, these findings point to the NLRP3 inflammasome being an emerging target in tumor development and progression. However, with contrasting results its role seems to be complex.

2 Objective

According to the World Health Organization, cancer is the second leading cause of death worldwide accounting for the passing of 9.6 million people in 2018 (WHO, 2018b). Until today, treatment options are still limited. Thus, it is of great importance to further uncover mechanisms tumors employ to progress, allowing the identification of future therapeutic targets. As neutrophils have been shown to play a critical role in tumor initiation and progression (see 1.2.1), and their presence has even been suggested as a prognostic value, targeting these immune cells might represent a promising strategy.

Therefore, the aim of the present studies was to unravel i) what causes the recruitment of neutrophils to the tumor, ii) what are the underlying mechanisms, and iii) what exactly is their phenotype and function, once present in the tumor and its microenvironment.

3 Material and Methods

3.1 Ethics

All following animal experiments were conducted from 2016 to 2019 at the Walter-Brendel Centre of Experimental Medicine of the LMU München (Munich, Germany), after approval by the local governmental authorities (“Regierung von Oberbayern”, 02-16-17, 02-17-68 and Reichel 14) along their guidelines to ensure animal welfare.

3.2 Animals

For the experiments different mouse strains, purchased by Charles River (Sulzfeld, Germany) at the age of 6 to 8 weeks and weighing between 15-18 g, were used. Experiments with a mouse squamous cell carcinoma cell line (SCC VII) were conducted with male C3H/HeNCrI mice. For analyses with a mouse mammary carcinoma cell line (4T1), female BALB/cJ mice were used. All remaining experiments were performed with male C57BL/6NCrI mice. Animals were housed in the Walter Brendel Centre of Experimental Medicine of LMU München under standard conditions (22 ± 2 °C, 30 – 60 % humidity, 12 h light/dark cycle, lights on at 7 am) in cages of 3, with access to food and water *ad libitum*.

3.3 Anesthesia

During all experiments and surgical procedures, mice were anesthetized using a mixture of ketamine (100 mg/kg, zoetis, Parsippany, New Jersey, USA) and

xylazine (10 mg/kg, Bayer, Leverkusen, Germany) diluted in saline (Fresenius Kabi, Bad Homburg vor der Höhe, Germany) at a ratio of 1.5:0.5:7. Anesthesia was administered *via* intraperitoneal (i.p.) injection. Constant body temperature of mice was ensured by using heating plates and heating lamps.

3.4 Cell lines

In order to investigate leukocyte trafficking to tumors, the mouse head and neck squamous cell carcinoma cell line SCC VII and the mouse mammary carcinoma cell line 4T1 were obtained from Kirsten Lauber (Department of Radiotherapy and Radiation Oncology, LMU München). Tumor cells were cultured in RPMI (Thermo Fisher Scientific, Waltham, Massachusetts, USA) media, supplemented with 10 % FBS (Biochrom, Berlin, Germany) and 1 % HEPES (PromoCell, Heidelberg, Germany) at 37 °C and 5 % CO₂. Furthermore, mouse brain endothelial cells (bEnd.3) were purchased from ATCC (Manassas, Virginia, USA) and cultured in DMEM (ATCC) supplemented with 10 % FBS at 37 °C and 5 % CO₂.

3.4.1 Thawing of cells

Cryovials (Thermo Fisher Scientific) containing the different cell lines were kept in liquid nitrogen for their long-term storage. In order to culture cells, vials were thawed and diluted in 10 ml of the appropriate medium. After transferring the suspension in cell culture flasks (Corning, Corning, New York, USA), cells were cultured at 37 °C and 5 % CO₂. Medium was changed the following day.

3.4.2 Splitting of cells

In order to split the cells, medium was removed and cells were washed with 10 ml phosphate buffered saline (PBS). Next, 2 ml of trypsin (PAN-Biotech, Aidenbach, Germany) were added to the flask and incubation at 37 °C for approximately 5 min followed, until complete detachment of all cells. After resuspending the cell suspension in 8 ml of medium, cells were collected in a Falcon tube and centrifuged. Subsequently, cells were either diluted 1:10 in a new flask or used for experiments.

3.4.3 Determination of cell numbers

In order to determine numbers of cultured cells, 50 µl of cell suspension were diluted with trypan blue solution (Sigma Aldrich, St. Louis, Missouri, USA) at a ratio of 1:1, which allows distinguishing live and dead cells. Next, the suspension was placed in a Neubauer cell counting chamber (0.1 mm depth, Laboroptik, Lancing, UK). The number of live cells was calculated by using the following equation:

Number of cells/ml = mean x dilution factor (2) x area (10^4)

3.5 Animal models

3.5.1 Orthotopic tumor models

In order to study leukocyte trafficking to solid tumors of SCC VII (floor of mouth) and 4T1 (breast) cancer cells, an orthotopic mouse model was established.

3.5.1.1 Experimental design and groups

In a first set of experiments, the different subsets of leukocytes in the tumors were characterized. In addition, neutrophils in the blood of tumor-bearing mice with a special regard to the relative age of neutrophils, were analyzed according to the following protocol:

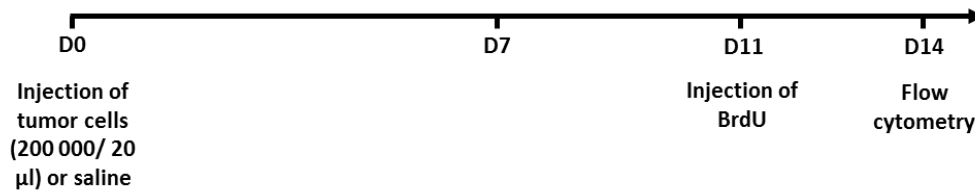


Figure 2.1: Experimental protocol to analyze leukocyte trafficking to solid tumors. First, tumor cells or saline were injected in an orthotopic manner. On day 14 (D14) tumor and blood samples were collected and analyzed by multi-channel flow cytometry. In selected experiments, the relative age of neutrophils was determined after application (i.v.) of BrdU on day 11 (D11), 72 h prior to multi-channel flow cytometry analysis.

Experiments were repeated in neutropenic mice. For this purpose, tumor-bearing mice were treated continuously for one week with a neutrophil-depleting anti-Ly6G mAb (100 μg, clone 1A8, BioXCell, Lebanon, New Hampshire, USA) *via* tail vein injections every 48 h, starting at the day of tumor cell injection:

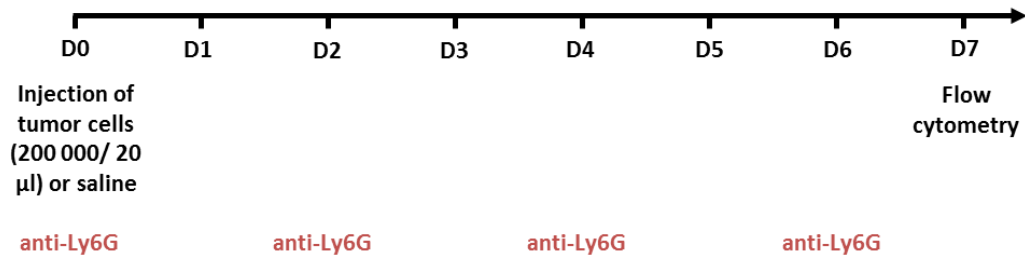


Figure 2.2: Experimental protocol to analyze leukocyte subsets present in solid tumors after neutrophil depletion. Tumor cells or saline were injected in an orthotopic manner. On day 7 (D7) after tumor cell injection, tumor and blood samples were collected and analyzed by multi-channel flow cytometry. In order to deplete neutrophils in tumor-bearing mice, i.v. injections of anti-Ly6G mAb were performed every 48 h according to previously published protocols.

In another set of experiments, the presence of aged neutrophils in tumors were analyzed after treatment with a NLRP3 inflammasome inhibitor (MCC950; 10 mg/kg, InvivoGen, San Diego, California, USA), a CXCR4 inhibitor (AMD 3100, 5 µg/kg, Tocris, Bristol, England), or a CXCR2 inhibitor (SB 225002, 5 mg/kg, Tocris) in the following manner:

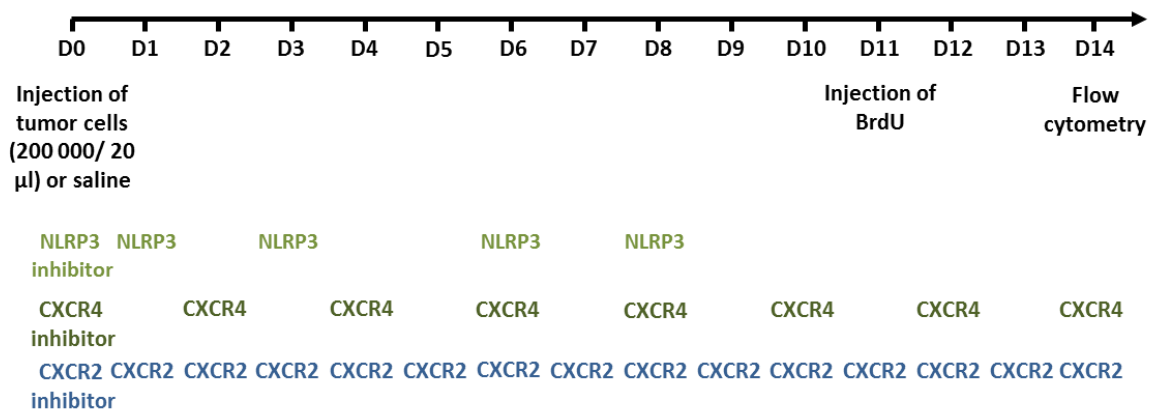


Figure 2.3: Experimental protocol to analyze leukocyte subsets in solid tumors after treatment with inhibitors or antagonists. After injecting tumor cells or saline (orthotopically), samples were collected on day 14 (D14) and analyzed by multi-channel flow cytometry. I.p. injections of a NLRP3 inflammasome inhibitor were performed on day 0 (D0), day 1 (D1), day 3 (D3), day 6 (D6), and day 8 (D8), a CXCR4 inhibitor every 48 h, and a CXCR2 inhibitor every day according to previously published protocols.

3.5.1.2 Tumor cell injection

Tumor cells (at a concentration of 2×10^5 cells/20 μ l) were injected in an orthotopic manner: SCC VII tumor cells subcutaneously into the floor of the mouth of C3H/HeNCrl mice and 4T1 tumor cells subcutaneously into the left chest of BALB/cJ mice. Control mice received saline injections.

3.5.1.3 Tissue sample preparation

Two weeks after tumor cell injection, tumor tissue and blood were harvested. Anesthetized mice were sacrificed by dislocation of the neck. Next, whole blood was taken from the *vena cava* by opening the peritoneal cavity and exposing the vessel. Using a 20 G cannula (Becton Dickinson, Franklin Lakes, New Jersey, USA), the vein was punctured and blood was carefully taken with a syringe containing 10 μ l heparin (25000 i.E, ratiopharm, Ulm, Germany). Tumors were excised and weighed, before homogenizing in 15 ml of saline. By pouring the homogenized tissue through a cell strainer (Corning, 70 μ m), a single cell suspension was obtained and collected in a 50 ml Falcon tube (Corning). After centrifugation at 1500 rpm for 5 min (Rotina 35R, Hettich, Kirchleugern, Germany) at room temperature (RT), each cell pellet from the tumor was resuspended in 500 μ l of PBS. Using 50 μ l of the samples, the overall leukocyte count was determined with the ProCyte Hematology analyzer (IDEXX, Westbrook, Maine, USA). Subsequently, 100 μ l of each anticoagulated blood and tumor sample was placed in a FACS tube (Corning) and immunostained with antibodies directed against CD45 APC-Cy7 (BD Bioscience, San Jose, California, USA), CD11b FITC (BD Bioscience), or CD11b PerCp-Cy5 (eBioscience, SanDiego, California, USA), Gr-1

PE (eBioscience), F4/80 efluor450 (eBioscience), and CXCR4 APC (Biolegend, San Diego, California, USA) for 30 min on ice. In selected experiments, T lymphocytes were identified by anti-CD8a PE-Cy7 mAb (eBioscience) and anti-CD4 AF700 mAb (eBioscience). Subsequently, erythrocytes were lysed with 1 ml of lysing solution (BD FACS Lysing solution, BD Bioscience) diluted in *Aqua inj.* (B.Braun, Melsungen, Germany) 1:10 for 10 min at RT. After washing with PBS twice, samples were resuspended in 200 µl PBS and analyzed *via* multi-channel flow cytometry.

3.5.1.3.1 Differentiation between aged and non-aged neutrophils

To determine the relative age of neutrophils, a pulse labelling technique with 5-Bromdesoxyuridin (BrdU, FITC BrdU Flow kit, BD Bioscience) was used according to previously published protocols (Uhl et al., 2016). BrdU is a thymidine analogue incorporated into DNA during its replication. By denaturing DNA, incorporated BrdU is accessible for staining and hence, for its detection. Consequently, non-aged neutrophils released from the bone marrow appear BrdU^{positive}, whereas (more) aged (circulating) neutrophils are BrdU^{negative} when analyzed by flow cytometry. Therefore, 72 h prior to the experiment mice received a single intravenous (i.v.) injection *via* the tail vein (2.5 mg/kg) in order to label neutrophil precursors in the bone marrow. Next, tissue and blood was prepared and immunostained as described previously in 3.5.1.3. Subsequently, the BrdU protocol followed according to the manufacturer description in the BrdU Flow kit. Briefly, samples were washed with 1 ml PBS (1500 rpm, 5 min, RT). Subsequently, a first fixation step followed with a 100 µl of Cytofix/Cytoperm buffer

for 15 min at RT. After washing the samples with 1 ml of the previously prepared 1 x BD Perm and wash buffer, another permeabilization step with 100 µl of the Cytoperm buffer plus followed for 10 min on ice. Next, cells were washed in 1 x BD Perm and wash buffer again, before refixation in another 100 µl of BD Cytoperm/Cytofix buffer for 5 min on ice was performed. Another washing step in 1 x BD Perm and wash buffer followed, before samples were treated with 100 µl of DNase (300 µg/ml) for 1 h at 37 °C in order to make the incorporated BrdU accessible. Next, cells were washed in 1 x BD Perm and wash buffer again and finally incubation with the antibody directed against BrdU (50 µl of the 1:50 diluted antibody) for 20 min at RT followed. After another last washing step cells were resuspended in 200 µl and measured *via* multichannel flow cytometry.

3.5.2 Heterotopic tumor models

In order to analyze neutrophil responses in the tumor and its microenvironment, a heterotopic tumor model was established in the mouse ear, enabling *in vivo* microscopy (IVM) analyses.

3.5.2.1 Experimental design and groups

In a first set of experiments, neutrophil trafficking to the tumor and its microenvironment in tumor-bearing mice was assessed according to the following protocol:

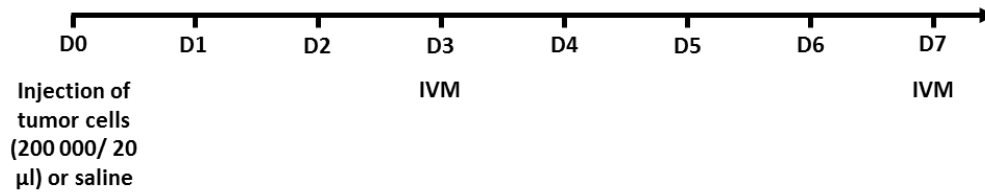


Figure 2.4: Experimental protocol for intravital imaging of the tumor and its microenvironment. Tumor cells or saline were injected into the left mouse ear. *In vivo* microscopy (IVM) was performed on day 3 (D3) and day 7 (D7).

Next, neutrophil responses in tumor-bearing mice treated with the NLRP3 inflammasome inhibitor MCC950 (10 mg/kg) were investigated.

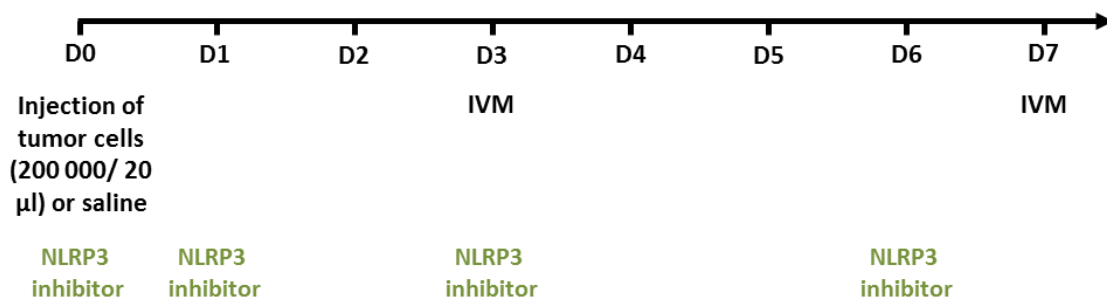


Figure 2.5: Experimental protocol for *in vivo* imaging of the tumor and its microenvironment. Tumor cells or saline were injected into the left mouse ear. *In vivo* microscopy (IVM) was performed on day 3 (D3) and day 7 (D7) directly after treatment with the NLRP3 inflammasome inhibitor *via* i.p. injections on day 0 (D0), day 1 (D1), D3 and day 6 (D6).

To directly analyze intravascular interactions of aged and non-aged neutrophils in the tumor and its microenvironment, adoptive cell transfer experiments were conducted according to previously published protocols (see 3.5.2.4) (Uhl et al., 2016).

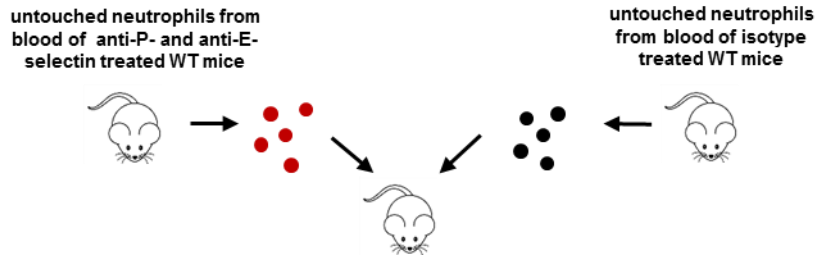


Figure 2.6: Experimental protocol for adoptive cell transfers. Neutrophils were isolated from either anti-P- and anti-E-selectin treated, or isotype control antibody-treated WT donor mice. After immunostaining the cells with anti-Ly6G mAb, neutrophils were injected i.v. into tumor-bearing mice on D7, before IVM was performed.

Moreover, the tumor imaging ear model was used to investigate angiogenesis in the tumor and its microenvironment in neutrophil-depleted tumor-bearing mice (see 3.5.1.1) and vehicle-treated tumor-bearing mice on day 7 after tumor cell/vehicle injection.

3.5.2.2 Tumor cell injection

Anesthetized mice were placed on a custom-made microscopy stage and their left outer ear was fixed onto a stack of glass slides with silicone (Kurt Obermeier GmbH & Co. KG, Bad Berleburg, Germany). In order to apply tumor cells, a polystyrene catheter (Smiths Medical, Ashford, UK) prepared with a 30 G cannula (B.Braun) was used. After disinfecting the ear (Bacilol, Hartmann, Heidenheim, Germany) the tumor cells were injected into the subcutaneous layer of the left outer ear, in a concentration of 2×10^5 cells/20 μ l. Control mice received saline injections.

3.5.2.3 *In vivo* ear imaging

Neutrophil responses in the tumor and peri-tumoral microvasculature were visualized using anti-Ly6G PE mAb (BD Bioscience). For injecting the antibody, a polystyrene catheter prepared with a 30 G cannula was used. Mice received anesthesia and were fixed onto a microscopy stage. Subsequently, the animal's tail was disinfected and the antibody was injected into the tail vein in a total volume of 100 μ l. For analyzing the vessel network in the tumor and its microenvironment, mice received an i.v. injection of FITC Dextran (150 kDa, 50 μ l, Sigma Aldrich) in the same manner.

Finally, the outer ear of mice was placed on a custom-made microscopy stage and lightly fixed with silicone gel. By adding ultrasound gel (SONOSID®, Asid Bonz, Herrenberg, Germany) on top of the ear, imaging of postcapillary venules or the architecture of the microvasculature followed.

3.5.2.4 Adoptive cell transfer experiments

To analyze intravascular interactions of aged and non-aged neutrophils in the tumor and its microenvironment, adoptive cell transfer experiments were performed. In order to obtain aged neutrophils, wildtype (WT) donor mice were treated with anti-E-selectin (50 μ g, BD Bioscience) and anti-P-selectin (50 μ g, Biolegend) mAbs i.v. 48 h and 24 h before the cell transfer experiments *via* tail vein injection. This inhibits the recruitment of aged neutrophils back to bone marrow, liver, and spleen, thus leading to the enrichment of aged neutrophils in the circulation. WT donor mice used for the transfer of non-aged neutrophils, received saline injections. Subsequently, blood was taken from the *vena cava* as

described before (see 3.5.1.3) and incubated with HetaSep (STEMCELL Technologies, Vancouver, Canada) in a ratio of 1:5 for 5 min at 37 °C. By red blood cell aggregation and sedimentation, samples were cleared from red blood cells. Next, neutrophils were stained with anti-Ly6G PE (BD Bioscience) for 20 min at RT. After washing the cells with PBS, i.v. injection into the receiving tumor-bearing mice followed, 30 min before *in vivo* ear imaging was performed.

3.5.3 *M. Cremaster* assay

The cremaster muscle represents a well-established model to investigate the different steps of leukocyte recruitment.

3.5.3.1 Experimental design and groups

This model was used to investigate the effects of NLRP3 inflammasome activation on leukocyte recruitment at different time points.

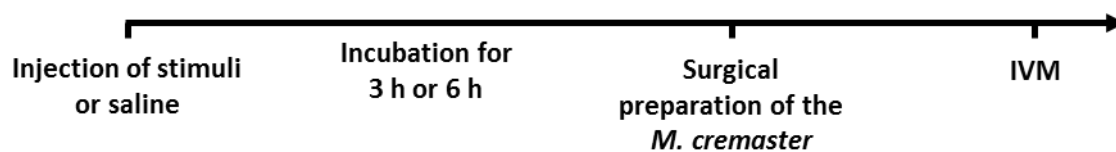


Figure 2.7: Experimental protocol for IVM of the *M. cremaster*. Alum crystals or saline were injected into the scrotum of WT mice. 3 h or 6 h later, the surgical preparation of the *M. cremaster* and *in vivo* microscopy (IVM) followed.

3.5.3.2 Intrascrotal stimulation

In order to stimulate activation of the NLRP3 inflammasome, 10 µg of Alum crystals (InvivoGen) diluted in a total volume of 350 µl saline, were injected into the scrotum of C57BL/6NCrl mice using a 30 G cannula, followed by incubation for 3 h or 6 h. Control mice received saline injections.

3.5.3.3 Surgical preparation of the intra-arterial catheter and the cremaster muscle

The preparation of the mouse cremaster muscle was performed under a surgical microscope (M651, Leica, Wetzlar, Germany) similar to the previous description by Baez (Baez, 1973), with minor adjustments. In order to allow administration of antibodies, a catheter was placed into the femoral artery in a retrograde manner. Through a ventral incision, the scrotum was opened and the right cremaster muscle was exteriorized. Connective tissue around the cremaster muscle was carefully removed. Next, the muscle was cut and opened ventrally to allow spreading over a pedestal in a plexiglas tray of a custom-made microscopy stage. To enhance visibility of the fluorescence-labeled antibodies, the pedestal contained a black coverslip. After detaching the epididymis and testicle, they were placed back into the abdominal cavity. Careful electrocautery was used to stop any bleeding along the edges of the cremaster muscle. Throughout surgical preparation and *in vivo* microscopy, the muscle was continuously superfused with warm buffered saline. In order to visualize the leukocytes of interest, cells were immunostained with anti-Gr-1 PE, anti-CD115 AF594 mAbs (Biolegend). Subsequently, IVM of postcapillary venules followed. After IVM, blood was taken

from the *vena cava* as described in 3.5.1.3 and systemic leukocyte counts were determined using a ProCyte Hematology analyzer.

3.5.4 Peritonitis assay

The peritonitis assay represents a well-established model to assess leukocyte recruitment to the peritoneal cavity after i.p. injection of various stimuli.

3.5.4.1 Experimental design and groups

In a first set of experiments, the leukocyte-recruiting properties of DAMPs such as HMGB1 (Biolegend), s100A8/A9 (Biolegend), or monosodium urate (MSU) crystals (InvivoGen) were investigated. Furthermore, the effect of the different inflammasome-activating substances on leukocyte recruitment such as poly (da:dt) (InvivoGen), flagellin (FLA-ST, InvivoGen), muramyl dipeptide (MDP, InvivoGen), or Alum crystals was assessed with the peritonitis model in the following manner:

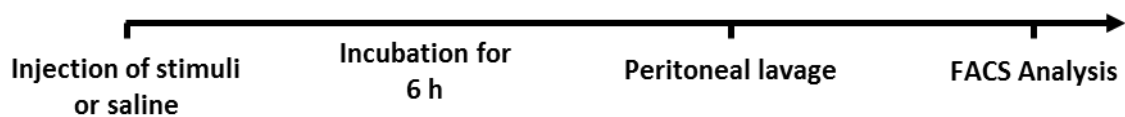


Figure 2.8: Experimental protocol for the peritonitis assay. The different stimuli or saline were injected i.p. into WT mice. 6 h later, a peritoneal lavage was performed and samples were analyzed by flow cytometry.

3.5.4.2 Induction through intraperitoneal injection

Stimuli were injected into the peritoneal cavity of WT mice using a 30 G cannula, in a total volume of 400 μ l, diluted with saline: HMGB1 in a concentration of 1 μ g/ml, s100A8/A9 in 1 μ g/ml and MSU in a concentration of 10 μ g/ml. The inflammasome-activating substances were injected in the following concentrations: poly da:dt 10 μ g/ml, FLA-ST in 10 μ g/ml, and MDP or Alum crystals in 10 μ g/ml saline. Control mice received saline injections.

3.5.4.2.1 Sample preparation

Anesthetized mice were sacrificed 6 h after i.p. injection of the stimuli, by dislocation of the neck. Using a 30 G cannula, 10 ml of cold PBS were injected into the right side of the mouse's peritoneum. Next, their peritoneal cavity was washed by inserting a butterfly cannula (14G OPTIVA®, Smiths Medical) into the left side of mouse peritoneum. In total, 10 ml of peritoneal fluid was collected in a 15 ml Falcon tube. Next, samples were centrifuged for 5 min at 1500 rpm at RT, supernatants were discarded and the pellets were resuspended in 500 μ l of PBS. Using 50 μ l of the cell suspension, the overall leukocyte count of the peritoneal lavage fluid was analyzed with a ProCytte Hematology analyzer. Of each sample, 100 μ l were placed into FACS tubes and cells were immunostained with antibodies directed against CD45 (APC-Cy7), CD11b (FITC), Gr-1 (PE), F4/80 (eFluor450) and CXCR4 (APC) for 30 min on ice. After lysing erythrocytes with 1 ml of lysing solution, followed by two washing steps with PBS, samples were resuspended in 200 μ l PBS and analyzed using a multi-channel flow cytometer.

3.5.4.2.2 Differentiation between aged and non-aged neutrophils

The relative chronological age of neutrophils recruited to the peritoneal cavity upon NLRP3 inflammasome activation was analyzed using a pulse labeling technique with 5-BrdU. First, samples were prepared as described previously (see 3.5.4.2.1), then cells were immunostained with the following antibodies: anti-CD45 APC-Cy7, anti-CD11b PerCp-Cy5, anti-Gr-1 PE, anti-F4/80 eFluor450, and anti-CXCR4 APC. Afterwards, the BrdU Flow kit protocol followed, as described in 3.5.1.3.1.

3.6 Flow cytometry

Employing multi-channel flow cytometry (Gallios, Beckman Coulter Inc, Brea, California, USA), myeloid leukocytes were identified by their expression of CD45 and CD11b. Using Gr-1 and F4/80, these cells were further distinguished into neutrophils (Gr-1^{high}, F4/80^{low}) classical monocytes (Gr-1^{high}, F4/80^{high}), and non-classical monocytes (Gr-1^{low}, F4/80^{high}). Neutrophils were further differentiated into BrdU^{positive} CXCR4^{low} (non-aged) and BrdU^{negative} CXCR4^{high} cells (aged). Lymphoid leukocytes such as T cells were identified as CD11b^{low} and CD4^{positive} or CD8a^{positive}. All results were quantified by using the FlowJo software (Treestar, Ashland, Oregon, USA).

3.7 *In vivo* microscopy

In vivo microscopy was performed using an AxioTech-Vario 100 Microscope (Zeiss MicroImaging GmbH, Goettingen, Germany), equipped with a Colibri LED light source (Zeiss MicroImaging GmbH) for fluorescence epi-illumination

microscopy. All images were taken using a 40x water immersion lens (0.5 NA, Zeiss MicroImaging GmbH). Images of the architecture of the analyzed microvasculature were obtained with a 10x water immersion lens. Microscopy videos were obtained by an AxioCam Hsm digital camera, and processed with the AxioVision 4.6 software (Zeiss MicroImaging GmbH).

Analysis of the *in vivo* microscopy videos was performed by using the imaging software Fiji (Schindelin et al., 2012). In the heterotopic tumor model, neutrophils were identified as Ly6G^{positive} cells. In the cremaster muscle assay, neutrophils were identified as Gr-1^{positive} CD115^{negative} cells, classical monocytes as Gr-1^{positive} CD115^{positive} cells, and non-classical monocytes as Gr-1^{negative} CD115^{positive} cells. Leukocytes moving slower than the associated blood flow were defined as rolling leukocytes and quantified for 60 s per venule. For firmly adherent leukocytes, a threshold for resting in the associated blood flow for >30 s, was determined and counted on the luminal surface per 100 μm vessel length. Microcirculatory parameters such as diameter and length of the vessel were determined in Fiji.

The microvascular architecture in tumor and its environment was analyzed by using the Skeleton plugin of Fiji. Briefly, the plugin is able to create skeletonized maps of the vessel network which allows determination of the number of branches per high power field, the number of junctions per high power field as well as the average branch length. The vessel density was determined as the number of branches multiplied with the average branch length and divided by the area of the high power field.

3.8 Tumorigenicity of neutrophils

To characterize the phenotype of neutrophils after NLRP3 inflammasome activation, a peritonitis assay was performed as described previously (see 3.5.4). Antibody staining, depending on the fluorescence label of each N1/N2 marker followed in the according manner:

PE - labeled marker	FITC - labeled marker	Non - labeled marker
anti-CD45 APC-Cy7	anti-CD45 APC-Cy7	anti-CD45 APC-Cy7
anti-CD11b PerCp-Cy5	anti-CD11b PerCp-Cy5	anti-CD11b PerCp-Cy5
anti-Gr-1 AF488	anti-Gr-1 PE	anti-Gr-1 PE
anti-F4/80 eFluor450	anti-F4/80 eFluor450	anti-F4/80 eFluor450
anti-CXCR4 APC	anti-CXCR4 APC	anti-CXCR4 APC

Table 2.1: Experimental protocol for immunostaining according the different surface markers.

Subsequently, further immunostaining of each sample with an antibody either directed against NE (rat, R&D Systems, Minneapolis, Minnesota, USA), MMP9 FITC (StressMarq Biosciences, Victoria, Canada), VEGF FITC (Novus Biologicals, Centennial, Colorado, USA), CCL5 PE (Biolegend), CCL3 PE (eBioscience), or Arg-1 PE (R&D Systems) was performed for 30 min on ice. For the unlabeled NE antibody, a secondary antibody (goat anti-rat AF488, Thermo Fisher Scientific) followed for 20 min at RT before continuing the regular protocol of lysing

erythrocytes and washing the samples. After resuspending the samples in 200 μ l PBS, expression levels of the molecules were measured on neutrophils *via* flow cytometry.

3.9 Activation of neutrophils

3.9.1 Analysis of integrin expression on neutrophils in the blood

As a parameter for neutrophil activation, surface expression of the integrins CD11a, CD11b, and CD49d was assessed in murine neutrophils after NLRP3 inflammasome activation by flow cytometry. To this end, whole blood was harvested from WT C57BL/6NCrl mice as described above (see 3.5.1.3). In each FACS tube, 100 μ l of anticoagulated blood sample were placed and incubated for 30 min at 37 °C either with Alum crystals (10 μ g), TNF (100 ng, R&D Systems), or PBS as negative control. After washing the samples twice with PBS, cells were labeled with antibodies directed against CD45 APC-Cy7, CD11b PerCp-Cy5, Gr-1 PE, F4/80 eFluor 450, CXCR4 APC, and CD11a (FITC, eBioscience) or CD49d (FITC, eBioscience). Erythrocytes were lysed using lysing solution as described before. Finally, after another washing step with PBS, samples were resuspended in 200 μ l PBS and integrin expression was measured by flow cytometry.

3.9.2 Analysis of ICAM-1/CD54-Fc binding properties of neutrophils

As a measure of conformational changes of β 2 integrins, binding of ICAM-1/CD54-Fc to neutrophils was assessed. For this purpose, blood was carefully taken from the *vena cava* as described previously (see 3.5.1.3). Subsequently, 50 μ l of each

anticoagulated blood sample were placed into FACS tubes and suspended in 50 μ l of Hanks balanced salt solution containing 1 mM CaCl₂ and MgCl₂ (Life Technologies, Carlsbad, California, USA). Next, incubation with the according stimuli, either phorbol-12-myristat-13-acetat (PMA, 50 ng/ml, Sigma Aldrich) as a positive control, Alum crystals (10 μ g), or PBS as a negative control followed for 30 min at 37 °C, before adding ICAM-1/CD54-Fc (10 μ g/ml, R&D Systems) and PE-conjugated anti-human IgG1 (Fc-specific, Southern Biotechnology, Birmingham, Alabama, USA). Samples were incubated for 5 min at 37 °C. After immunostaining the cells with fluorescence-labeled antibodies directed against CD45 (APC-Cy7), CD11b (FITC), F4/80 (eFluor450), Gr-1 (AF700), and CXCR4 (APC; (eBioscience), samples were washed, resuspended in 200 μ l PBS and finally, ICAM-1/CD54-Fc binding to neutrophils was measured *via* flow cytometry.

3.10 Activation of endothelial cells

To measure activation of endothelial cells, bEnd.3 microvascular endothelial cells were seeded into 12 well plates (200 000 cells/well). The following day, cells were stimulated with either Alum crystals (10 μ g/ml), TNF (100 ng/ml) as a positive control, or PBS as a negative control. After 4 h at 37 °C cells were harvested by placing 100 μ l of trypsin into each well for 5 min at 37 °C. Next, 1 ml of medium was added and the cell suspension was transferred into FACS tubes. After centrifugation at 1500 rpm for 5 min, supernatant was discarded and cells were resuspended in 100 μ l of PBS. Next, cells were labeled with antibodies directed against ICAM-1/CD54 (AF488, Biolegend), VCAM-1/CD106 (Pacific blue, Biolegend), E-selectin/CD62E (PE, BD Bioscience) and P-selectin/CD62P (APC,

Biolegend) for 30 min on ice. After fixing the cells by using lysing solution, samples were washed and resuspended in 200 µl PBS. Finally, expression levels of the target proteins were measured by flow cytometry.

The same protocol was used to assess the effects of DAMPs on endothelial cell activation. Here, cells were incubated with HMGB1 (1 µg/ml), S100A8/A9 (1 µg/ml), or MSU crystals (10 µg/ml).

3.11 Immunohistochemistry and confocal microscopy

3.11.1 Analysis of ICAM-1/CD54 and VCAM-1/CD106 expression in cremasteric venules

In order to investigate the effect of NLRP3 inflammasome activation on the expression of ICAM-1/CD54 and VCAM-1/CD106 in cremasteric postcapillary venules, mouse cremaster muscles were prepared as described previously (see 3.6.3) and subsequently detached from the mouse 6 h after intrascrotal (i.s.) injection of Alum crystals or saline. In a next step, cremaster muscles were fixed in 4 % paraformaldehyde for 10 min at RT. After washing the tissue twice in PBS, blocking and permeabilization, using 2 % bovine serum albumin (BSA) in PBS with 0.001 % Triton X-100 for 1.5 h at RT followed. Next, immunostaining of the whole mounts with anti-CD31/PECAM AF647 (1:100, Biolegend) and anti-ICAM-1/CD54 (1:100, rat, Biolegend) or anti-VCAM-1/CD106 (1:100, rat, Biolegend) in blocking solution at 4 ° C over night, was performed. After two washing steps in PBS, secondary staining with goat anti-rat AF488 antibody (Invitrogen, Carlsbad, California, USA) in 2 % BSA in PBS followed, for 2 h at RT. Subsequently, the

immunostained tissues were washed in PBS twice more before mounting them in PermaFluor (Thermo Fisher Scientific) on glass slides.

3.11.2 Visualizing neutrophils in tumor sections

Tumors were excised from tumor-bearing mice, embedded in tissue tek (Sakura, Alphen am Rhein, Netherlands) and stored at -80 °C. Subsequently, sections were cut at 20 µm using a cryostat (Thermo Fisher Scientific) and mounted onto glass slides (Thermo Fisher Scientific). After fixing the sections with 4 % formaldehyde (Microcos, Garching, Germany) for 10 min at RT, slides were washed in PBS for 10 min at RT. By incubating the slides in 2 % BSA in PBS with 0.001 % Triton-X-100 (Sigma Aldrich) for 1.5 h at RT, tumor sections were blocked and permeabilized. Next, immunostaining with anti-CD31 AF647 (1:100) and anti-Ly6G (1:50), in blocking solution at 4 °C over night, followed. After washing the slides in PBS twice, sections were mounted with PermaFluor and slides were stored at 4 °C.

3.11.2.1 Confocal microscopy and its analysis

Using a Leica SP8 confocal laser-scanning microscope (Leica) with an oil-immersion lens (Leica; 40x; NA 1.40), confocal z-stacks (z-spacing 1 µm) of postcapillary venules were acquired. In cremasteric tissue whole mounts, the fluorescence signal was analyzed using the software Fiji (Schindelin et al., 2012). Briefly, confocal microscopy images were merged and z-stacks combined. Using the ROI manager software tool, three regions of interest were placed in

postcapillary venules of interest as well as in the perivascular space to allow for background signal subtraction.

3.12 Assessment of tumor development

In order to determine the effect of neutrophil depletion on the progression of already existing tumors, C3H/HeNCrl as well as BALB/cJ mice received tumor cells in a concentration of 2×10^5 cells/20 μ l into the outer leg, which allowed easy access for continuous measurements of the tumor size on a daily basis using a caliper (Hoffmann Group, Munich, Germany). On day 7 after tumor cell injection, mice were randomly assigned into two groups. One group received treatment with the anti-Ly6G mAb (100 μ g) every 48 h, resulting in the depletion of neutrophils. The other group received vehicle treatment. After another 7 days of daily measurements, mice were sacrificed.

3.13 Cell proliferation assay

Tumor cells were seeded on a 96-well plate (5000 cells/well). The next day, medium was changed and cells were treated with either Alum crystals (10 μ g/100 μ l), a NLRP3 inflammasome inhibitor (10 μ M), a CXCR2 inhibitor, or a CXCR4 inhibitor (125 μ g/100 μ l) for 24 h at 37 °C. Subsequently, medium was replaced by serum free media and the MTT Assay was performed according to the manufacturer's protocol (Abcam, Cambridge, UK). First, MTT reagent was added for 3 h at 37 °C. In a next step, MTT solvent was also added to the wells. After placing the plate on an orbital shaker for 15 min, the absorbance was measured at

a wavelength of 590 nm in a microplate reader (Tecan, Männedorf, Switzerland). Cell proliferation was determined as the percentage of change in comparison to the negative control after background subtraction.

3.13.1 Investigating the effect of tumor-primed neutrophils on cell proliferation

Furthermore, the effect of tumor-primed neutrophils on tumor cell proliferation as well as on endothelial cell proliferation was investigated. In order to obtain tumor-primed neutrophils, tumor-bearing mice were sacrificed two weeks after tumor cell injection. Subsequently, neutrophils were isolated either from tumor-bearing mice or tumor-free WT mice with the EasySep™ Mouse Neutrophil Enrichment Kit (STEMCELL Technologies) according to the manufacturer's protocol. Briefly, whole blood was taken from the *vena cava* as described previously (see 3.5.1.3) and placed into a FACS tube, before incubating it with HetaSep at a ratio of 1:5 for 5 min at 37 °C. In a next step, 50 µl/ml of rat serum as well as 50 µl/ml of neutrophil enrichment cocktail were added to the leukocyte suspension. After incubating the samples for 15 min at 4 °C cells were washed in 1 ml PBS and centrifuged for 10 min at 300 g. After discarding the supernatant, pellets were resuspended in 500 µl of the respective media used for the cells receiving the neutrophil treatment. Next, the biotin selection cocktail was added (50 µl/ml) for another 15 min at 4 °C. After vortexing the magnetic particles for 30 s, particles were added to the samples and incubated for 10 min at 4 °C. Finally, tubes were placed into the STEMCELL magnet for 3 min at RT and the samples were poured into a new tube. After placing the isolated neutrophils into 6-well plates and

incubation at 37 °C over night, supernatants were collected and subsequently added onto the cell-cultured tumor or endothelial cells. In addition to the supernatants, some wells were also treated with a NE-inhibitor (1mg/ml). After incubation for 24 h at 37 °C, the MTT Assay was performed as described above (see 3.13).

3.14 Endothelial cell migration

In order to investigate the effect of tumor-primed neutrophils on endothelial cell migration, a scratch assay was performed. For this purpose, tumor-primed neutrophils were isolated from the peripheral blood of tumor-bearing mice using the EasySep™ Mouse Neutrophil Enrichment Kit, and placed into a 6-well plate and cultured at 37 °C over night. The same day, endothelial cells were seeded onto 6-well plates (500 000 cells/well). On the following day, a “scratch” was created in the confluent endothelial cell monolayer. After washing the cells, supernatants from cultured tumor-primed or control neutrophils (isolated from the peripheral blood of tumor-free mice) were added to the cultured endothelial cells. After 24 h the number of migrated cells into the scratch was assessed and normalized to the controls.

3.15 Multiplex immunoassays

In order to determine cytokine concentrations in SCC VII and 4T1 tumor cell supernatants, homogenized tumors, and serum samples, a Bio-Plex chemokine assay on a Bio-Plex 200 system, was performed in Kirsten Lauber’s laboratory

(Department of Radiotherapy and Radiation Oncology, LMU München) according to the manufacturer's protocol (Bio-Rad Laboratories, Munich, Germany).

3.16 ELISA

3.16.1 HMGB1

In order to measure HMGB1 concentrations in SCC VII and 4T1 cell culture supernatants, ELISA analysis was performed in Kirsten Lauber's laboratory (Department of Radiotherapy and Radiation Oncology, LMU München) according to the manufacturer's protocol (IBL International, Hamburg, Germany).

3.16.2 S100A8/A9

For the investigation of S100A8/A9 concentrations in tumor cell culture supernatants, a sandwich ELISA system, developed and performed in Thomas Vogl's laboratory (Department of Immunology, Westfälische Wilhelms-Universität Münster), was employed as described previously (Vogl et al., 2014).

3.17 MSU measurements

Concentrations of uric acid with SCC VII and 4T1 cell culture supernatants were determined by Lesca Holdt's department (Department of Laboratory Medicine, LMU München) employing a COBAS 8000 modular analyzer (Roche, Mannheim, Germany).

3.18 TLR2 and 4 activity assay

In cooperation with Kirsten Lauber's laboratory (Department of Radiotherapy and Radiation Oncology, LMU München), TLR2 and TLR4 receptor activity after stimulation with SCC VII and 4T1 cell culture supernatants was measured as described previously (Krombach et al., 2019).

3.19 Statistics

All data was analyzed using the statistical software GraphPad PRISM (GraphPad Software, San Diego, California, USA). The unpaired student's t-test was used for the comparison of two groups. For the estimation of stochastic probability of more than two groups, a one-way ANOVA followed by Dunnett's or Tukey's posthoc test was performed. All data is presented as mean \pm standard error of the mean (McKaig et al.). Statistical significance was accepted at p -Values < 0.05 .

4 Results

4.1 Cytokines in supernatants of cultured tumor cells, solid tumors, and serum samples

To explore the expression profiles of cytokines in cultured tumor cells or derived tumor tissue raised in mice, a multiplex immunoassay was performed. Our results from cell culture supernatants revealed that SCC VII cells release a larger variety of cytokines than 4T1 (**Fig. 3.1 A**). In the derived tumor tissue, however, these distinct expression patterns were no longer present, but cytokine expression patterns were in general higher (**Fig. 3.1 B**).

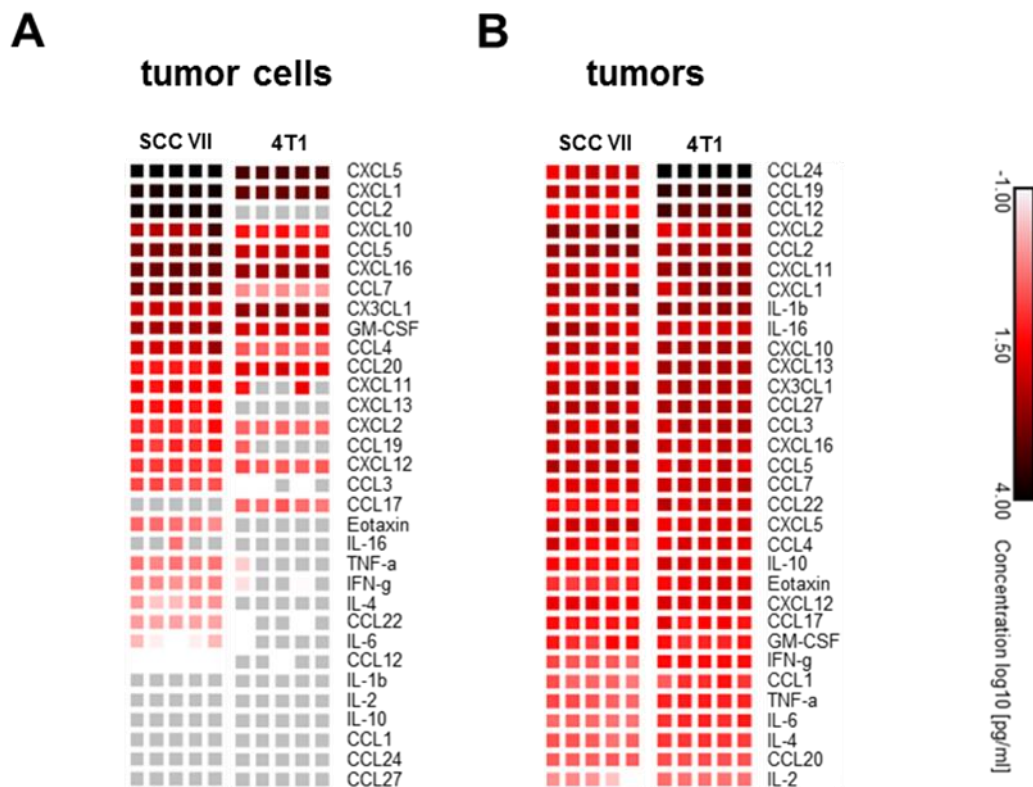


Figure 3.1: Quantification of cytokines in SCC VII and 4T1 cell culture supernatants as well as solid tumors. Data are shown as heatmaps; n=5 per group.

Moreover, we analyzed cytokine and chemokine concentrations in serum samples from healthy and tumor-bearing mice. No significant differences between these experimental groups were observed (**Fig. 3.2**).

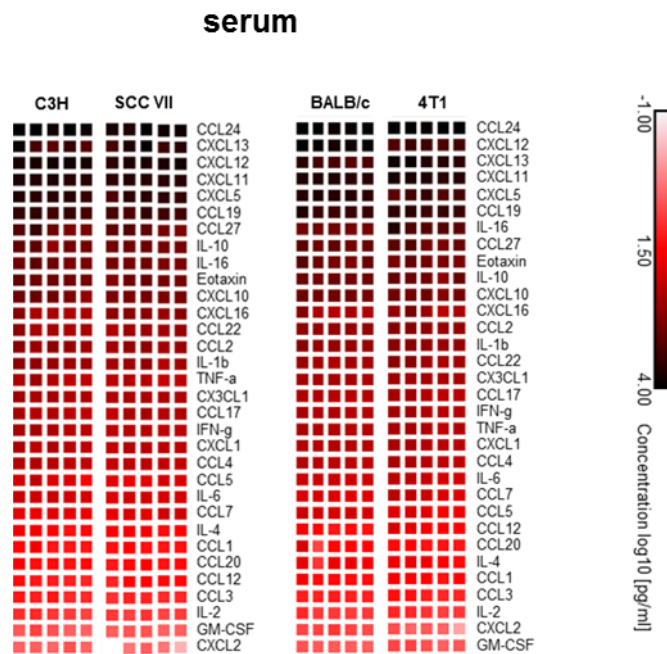


Figure 3.2: Quantification of cytokines in serum samples from SCC VII and 4T1 tumor-bearing mice and healthy controls. Data are shown as heatmaps; n=5 per group.

4.2 Neutrophils in the circulation of tumor-bearing mice

Using multi-channel flow cytometry, we aimed to investigate the number of chronologically aged and non-aged neutrophils in the circulation of healthy control and tumor-bearing mice by pulse-labeling with BrdU. In 4T1 tumor-bearing mice, a significant increase of aged (BrdU^{negative}) neutrophils and non-aged (BrdU^{positive}) neutrophils in the peripheral blood was observed as compared to healthy control mice. In contrast, SCC VII tumor-bearing mice did not show any significant changes in the number of circulating neutrophils compared to controls (**Fig. 3.3**).

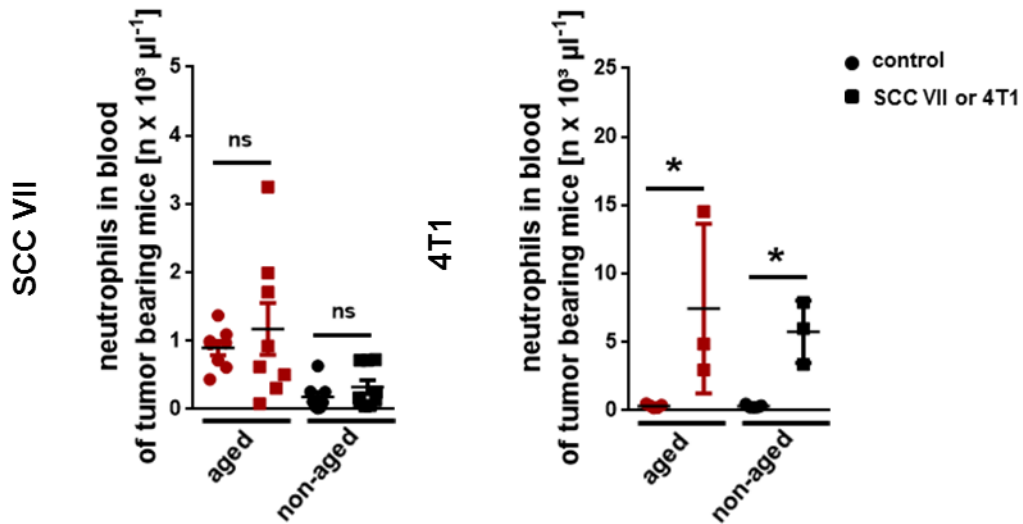


Figure 3.3: Quantitative analysis of aged and non-aged neutrophils in the circulation of healthy control and tumor-bearing mice. Data are presented as mean±SEM; n=3-9 per group; *p<0.05; n.s.=not significant.

4.3 CXCR4 expression levels on blood neutrophils in tumor-bearing mice

As a measure for neutrophil biological ageing, the expression of the chemokine receptor CXCR4 was determined on the surface of circulating neutrophils in healthy control and tumor-bearing mice by multi-channel flow cytometry. In both SCC VII and 4T1 tumor-carrying mice, neutrophils showed a significant higher expression of CXCR4 as compared to neutrophils in control mice. When continuously treating tumor-bearing mice with a CXCR2 inhibitor, this increase of CXCR4 on neutrophils was significantly reduced (**Fig. 3.4**).

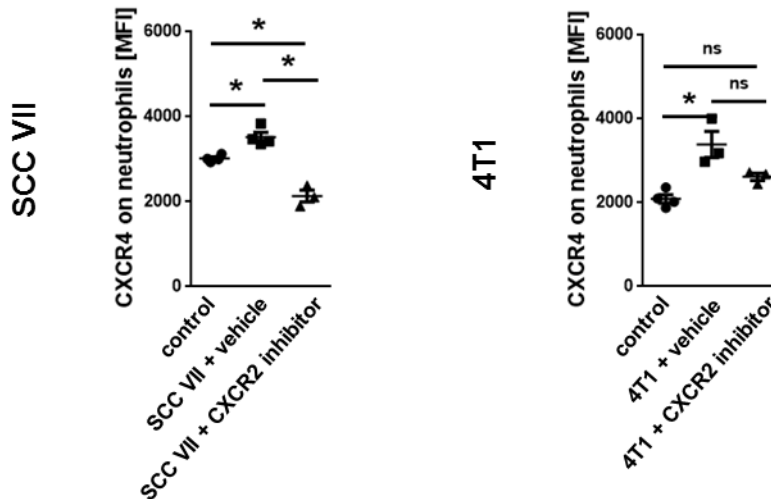


Figure 3.4: Quantification of CXCR4 expression on neutrophils in the circulation of healthy controls and tumor-bearing mice treated with a CXCR2 inhibitor or vehicle. Data are presented as mean \pm SEM; n=3-5 per group; *p<0.05; n.s.=not significant.

4.4 The fate of excessively aged neutrophils in tumor-bearing mice

4.4.1 Accumulation of aged neutrophils in the peritumoral microvasculature

In a next set of experiments, we investigated the accumulation of adoptively transferred, chronologically aged and non-aged neutrophils in the microvasculature of the tumor and of its microenvironment. In both SCC VII and 4T1 tumor-bearing mice significantly more aged neutrophils accumulated in the microvasculature of the tumor and the surrounding microenvironment than non-aged neutrophils (**Fig. 3.5**).

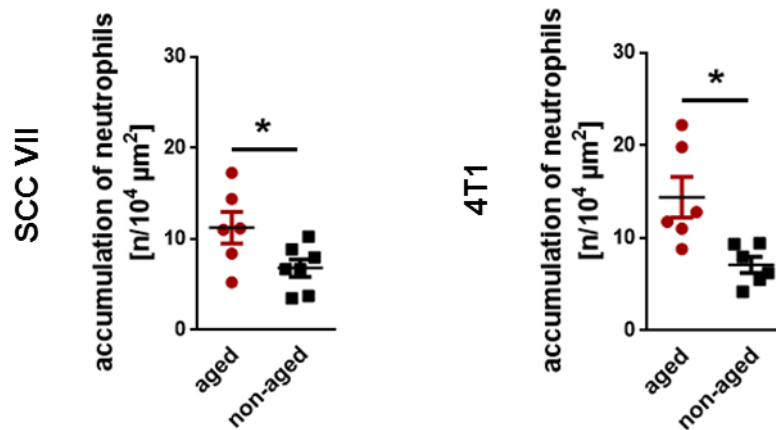


Figure 3.5: Quantification of the accumulation of adoptively transferred, chronologically aged and non-aged neutrophils in SCC VII and 4T1 tumors and their microenvironment. Data are presented as mean±SEM; n=6-7 per group; *p<0.05.

4.4.2 Leukocyte subsets in solid SCC VII and 4T1 tumors

In further experiments, the composition of different leukocyte subsets in solid SCC VII and 4T1 tumors was investigated. Employing multi-channel flow cytometry, myeloid leukocytes were identified by their expression of CD45 and CD11b. Neutrophils were subsequently characterized as Gr-1^{high} and F4/80^{negative} (**Fig. 3.6 A**). This analysis revealed that 18.90 % of all leukocytes in SCC VII tumors were myeloid leukocytes and 2.74 % were neutrophils. In the 4T1 tumors, 82.15 % were myeloid leukocytes and 13.14 % were neutrophils. Using a metabolic pulse-labeling technique with BrdU, around 80 % of the neutrophilic granulocytes present in the tumors, were BrdU^{negative} aged neutrophils, whereas only 20 % were represented by BrdU^{positive} non-aged neutrophils in both tumor entities (**Fig. 3.6 B**).

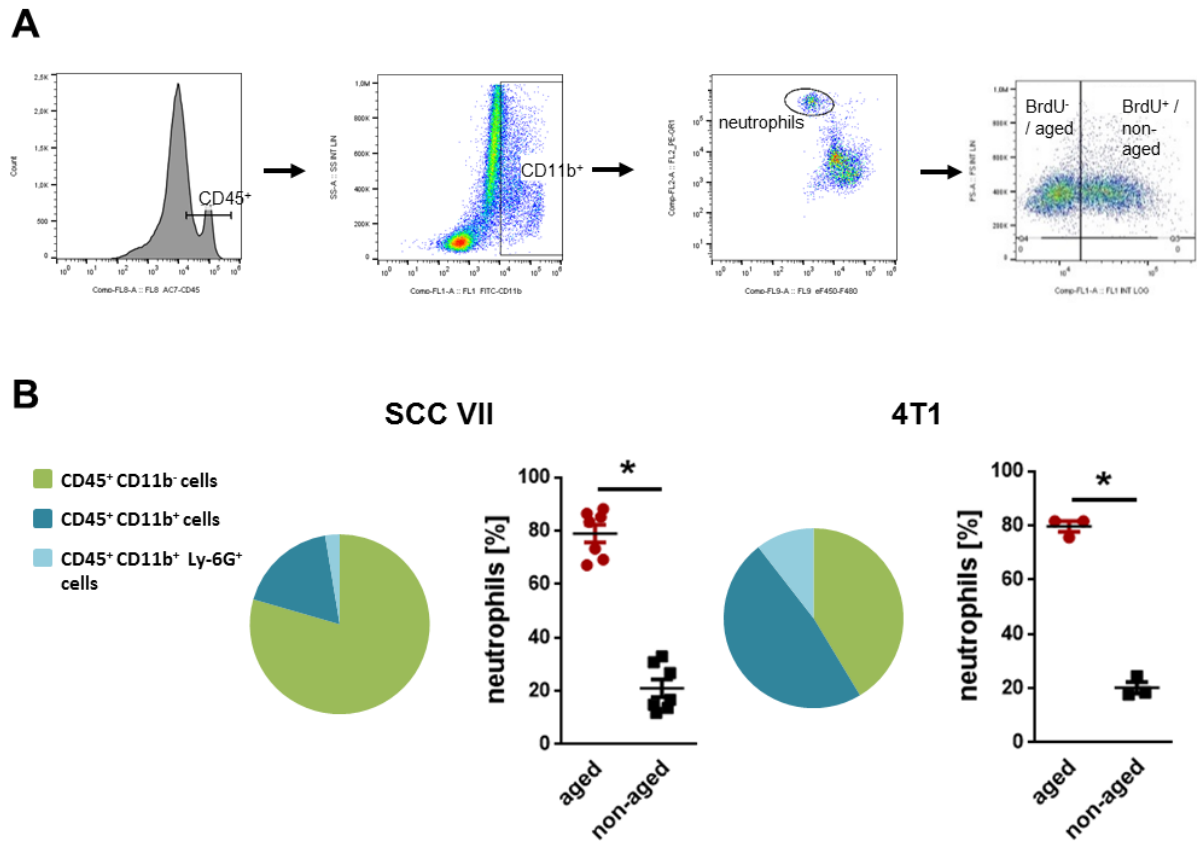


Figure 3.6: Quantitative analysis of the composition of different leukocyte subsets in solid SCC VII and 4T1 tumors. Schematic overview of the gating strategy (A). Graphical presentation of different leukocyte subsets and the percentage of aged and non-aged neutrophils in the tumors (B). Data are presented as mean±SEM; n=3-7 per group; *p<0.05.

Using immunostaining and confocal microscopy, we aimed to further characterize the presence of neutrophils within the tumors. Ly-6G^{positive} neutrophils were found in the tumor microvasculature (identified by CD31^{positive} endothelial cells) as well as in the surrounding tumor tissue (**Fig. 3.7**).

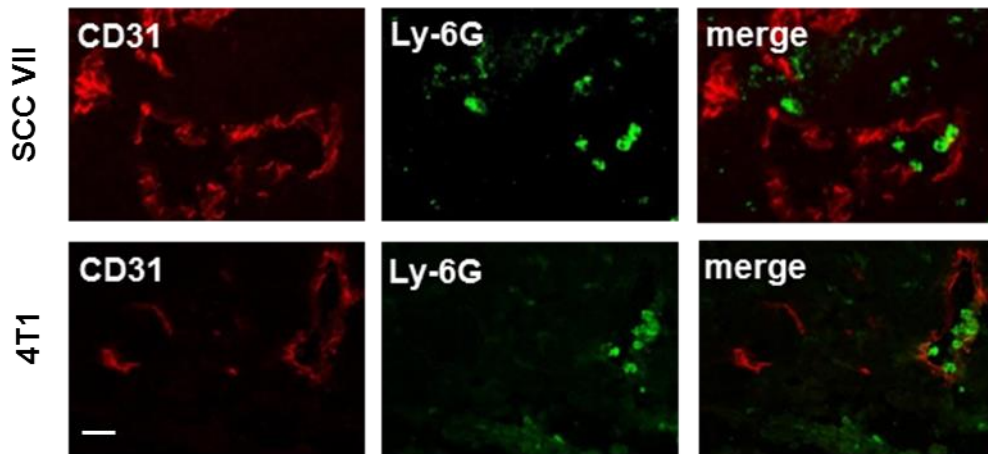


Figure 3.7: Representative confocal microscopy images of SCC VII and 4T1 tumor sections. Immunostaining with anti-CD31 and anti-Ly6G (scale bar: 25 μ m).

4.5 The recruitment of aged neutrophils

4.5.1 The release of DAMPs by tumor cells

In a next series of experiments, we performed measurements of the DAMPs uric acid, s100A8/A9, and HMGB1 known to be released by injured or dying cells. We did not detect s100A8/A9 (not shown) in SCC VII or in 4T1 tumor cell supernatants. In contrast, uric acid release from 4T1 tumor cells was three times higher than in SCC VII tumor cells (**Fig. 3.8 A**). HMGB1 concentrations were very low in SCC VII cell culture supernatants, but significantly higher in 4T1 tumor cell supernatants as compared to controls (**Fig. 3.8 B**).

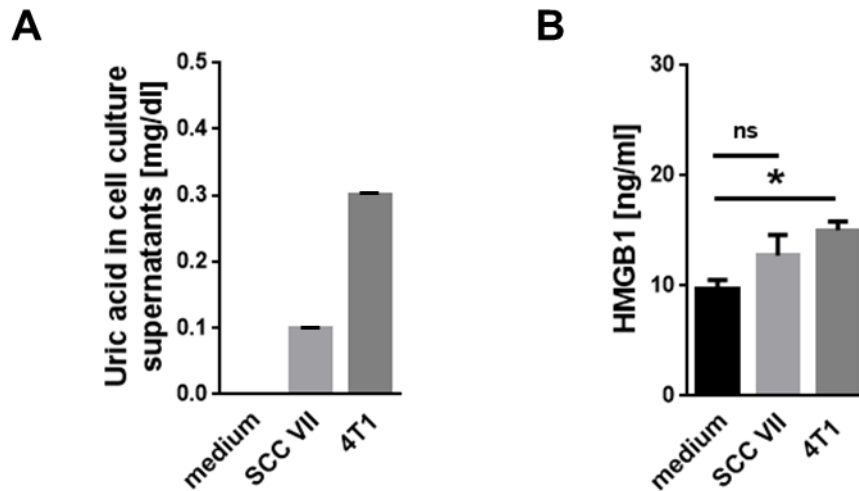


Figure 3.8: Quantitative analysis of uric acid and HMGB1 in SCC VII and 4T1 cell culture supernatants. Data are presented as mean±SEM; n=5 per group; *p<0.05; n.s.=not significant.

4.5.2 The effect of DAMPs on myeloid leukocyte recruitment

Using a peritonitis assay, we performed quantitative analysis of leukocyte subsets recruited upon stimulation with different DAMPs for 6 h. Injection of s100A8/A9 or MSU crystals led to a significantly higher extravasation of neutrophils to the peritoneal cavity, as compared to unstimulated controls. I.p. injection of HMGB1 did not reveal any effect on the recruitment of neutrophils in this model. Whereas MSU crystals also caused a significant influx of classical monocytes, s100A8/A9 led to the recruitment of these cells to a much lesser extent. Again, stimulation with HMGB1 did not show any effects on the extravasation of classical monocytes. The number of non-classical monocytes was not altered by the injection of any stimuli (**Fig. 3.9**).

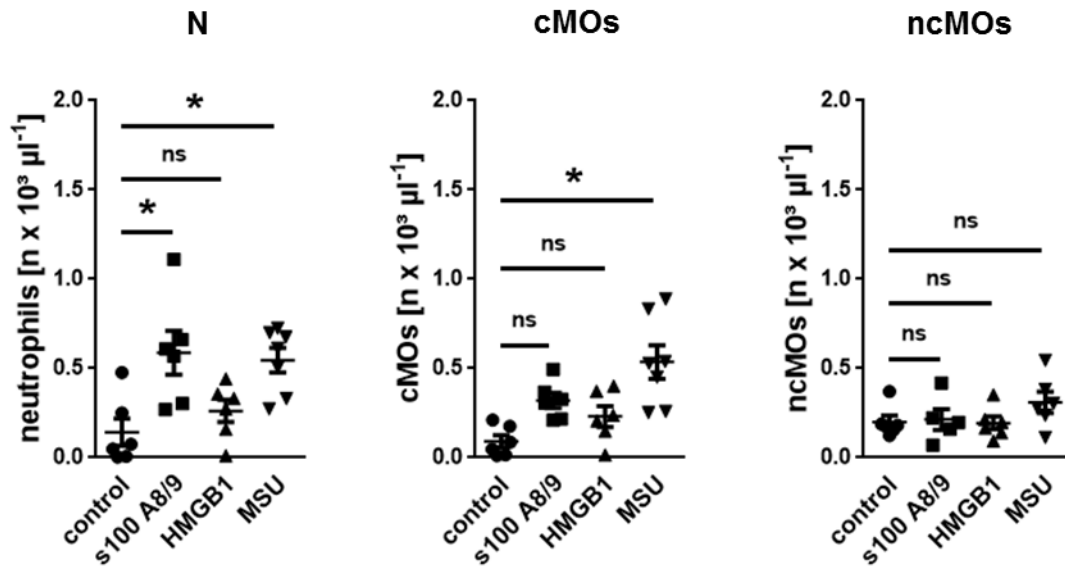


Figure 3.9: Quantification of leukocyte recruitment to the peritoneal cavity after i.p. exposure of DAMPs. Analysis of neutrophils (N), classical monocytes (cMOs), and non-classical monocytes (ncMOs) recruited to the peritoneal cavity after injection of s100A8/A9, HMGB1, and MSU. Data are presented as mean \pm SEM; n=6-7 per group; *p<0.05; n.s.=not significant.

4.5.3 The effect of tumor-released mediators on TLR2 and TLR4 activity

Using TLR2 and TLR4 reporter cells and measuring the activity of secreted alkaline phosphatase *via* a plate reader, we investigated whether SCC VII and 4T1 tumor cells secrete ligands that can potentially activate these receptors. In these experiments, treatment with supernatants from both tumor cell lines did not cause an increase in the TLR2 and TLR4 reporter activity. As a positive control, treatment with the TLR2 agonist FSL-1, a synthetic diacylated lipoprotein, or the TLR4 agonist LPS resulted in enhanced TLR2 or TLR4 activity as compared to unstimulated controls (**Fig. 3.10**).

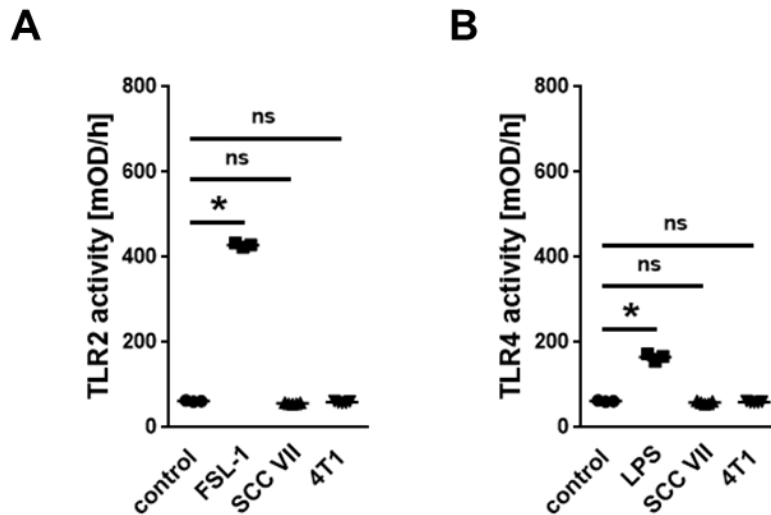


Figure 3.10: Quantitative analysis of TLR2 and TLR4 activity in reporter cells after stimulation with SCC VII and 4T1 cell culture supernatants. Data are presented as mean \pm SEM; n=5 per group; *p<0.05; n.s.=not significant.

4.5.4 The effect of MSU on inflammasome activation

As a measure of inflammasome activation, we quantified IL-1 β production after i.p. injection of MSU. 6 h after the onset of stimulation, IL-1 β levels in the peritoneal cavity were significantly increased compared to unstimulated controls (**Fig. 3.11**).

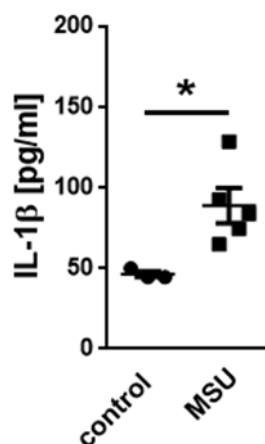


Figure 3.11: Quantification of IL-1 β in the peritoneal lavage after stimulation with MSU crystals. Data are presented as mean \pm SEM; n=5 per group; *p<0.05.

4.5.5 The effect of inflammasome activation on myeloid leukocyte recruitment

The peritonitis assay was also employed to investigate the number of extravasated neutrophils as well as classical and non-classical monocytes into the peritoneal cavity after injection of different inflammasome stimulating substances. Activating the NLRP3 inflammasome by injecting Alum crystals led to a significant increase in numbers of neutrophils in the peritoneal cavity as compared to saline injected mice. Moreover, NLRP3 inflammasome activation by Alum crystals also caused a strong recruitment of classical monocytes, however, to a much lesser degree.

Activation of the AIM2 inflammasome by injecting poly (da:dt), the NLRC4 inflammasome with FLA-ST, or stimulating the NLRP1 inflammasome with MDP did not cause extravasation of neutrophils or classical monocytes. Moreover, the number of non-classical monocytes remained unaffected by all treatments (**Fig. 3.12 A**).

Using a pulse labeling strategy with BrdU, we found that the majority (about 60 %) of neutrophils recruited upon NLRP3 inflammasome activation with Alum crystals were BrdU^{negative} aged neutrophils. Only about 40 % of the neutrophils were BrdU^{positive} non-aged neutrophils (**Fig. 3.12 B**).

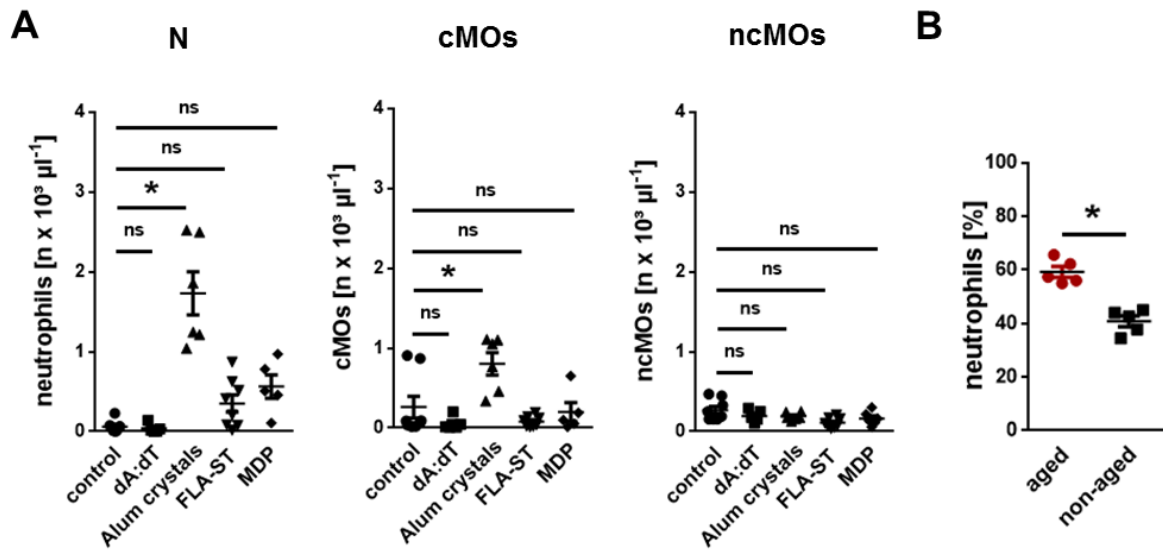


Figure 3.12: Quantification of leukocyte recruitment to the peritoneal cavity after injection of inflammasome activating substances. Analysis of neutrophils (N), classical monocytes (cMOs) and, non-classical monocytes (ncMOs) recruited to the peritoneal cavity after injection of dA:dT, Alum crystals, FLA-ST, or MDP. Data are presented as mean \pm SEM; n=5-8 per group; *p<0.05; n.s.=not significant.

4.5.6 The effect of NLRP3 inflammasome activation on neutrophils

4.5.6.1 Integrin expression

In order to analyze the activation of aged and non-aged neutrophils after exposure to NLRP3 inflammasome activating Alum crystals, integrin expression on neutrophils was measured by multi-channel flow cytometry. We found that CD11a, CD11b, and CD49d expression did not significantly differ between unstimulated aged and non-aged neutrophils harvested from the peripheral blood of WT mice. Similarly, these integrin expression levels remained unaffected by stimulating the NLRP3 inflammasome. However, activating neutrophils through TNF led to a significant increase of CD11b, but not of CD11a or CD49d in aged and non-aged neutrophils (**Fig. 3.13**).

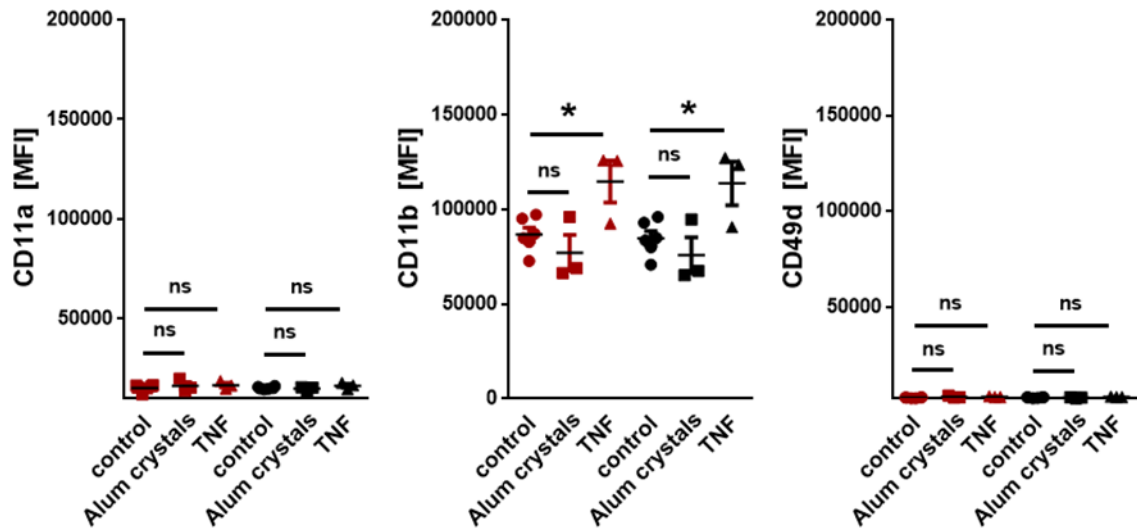


Figure 3.13: Quantification of integrin expression on aged and non-aged neutrophils. Analysis of CD11a, CD11b, and CD49d on neutrophils after stimulation with Alum crystals, TNF, or vehicle. Data are presented as mean±SEM; n=3-6 per group; *p<0.05; n.s.=not significant.

4.5.6.2 ICAM-1/CD54-Fc binding

As a measure of conformational changes of $\beta 2$ integrins, the capacity of neutrophils to bind ICAM-1/CD54-Fc was analyzed. Using multi-channel flow cytometry, we found that aged neutrophils tend to bind more ICAM-1/CD54-Fc than non-aged neutrophils. Stimulation with Alum crystals did not alter ICAM-1/CD54-Fc binding in aged or non-aged neutrophils. However, stimulation with PMA as a positive control caused a significant increase in ICAM-1/CD54-Fc binding in aged neutrophils and also, to a much lesser degree, in non-aged neutrophils (Fig. 3.14).

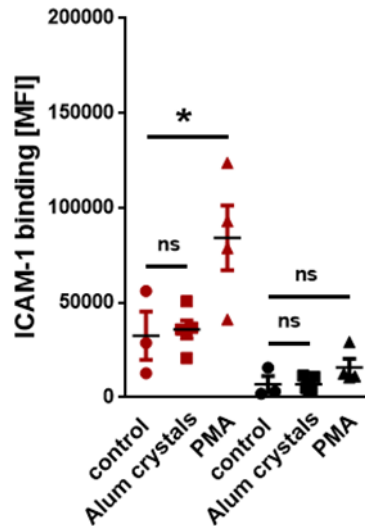


Figure 3.14: Quantitative analysis of ICAM-1/CD54-Fc binding properties of aged and non-aged neutrophils after stimulation with Alum crystals, PMA, or vehicle. Data are presented as mean±SEM; n=3-5 per group; *p<0.05; n.s.=not significant.

4.5.7 The effect of NLRP3 inflammasome activation on endothelial cells

To investigate endothelial cell activation after NLRP3 inflammasome stimulation, ICAM-1/CD54, VCAM-1/CD106, E-selectin/CD62E, and P-selectin/CD62P expression was measured using multi-channel flow cytometry. Whereas treatment with Alum crystals did not alter the expression of ICAM-1/CD54, VCAM-1/CD106, E-selectin/CD62E, or P-selectin/CD62P on cultured microvascular endothelial cells, stimulation with TNF resulted in a significantly enhanced expression of these molecules as compared to untreated controls (**Fig. 3.15**).

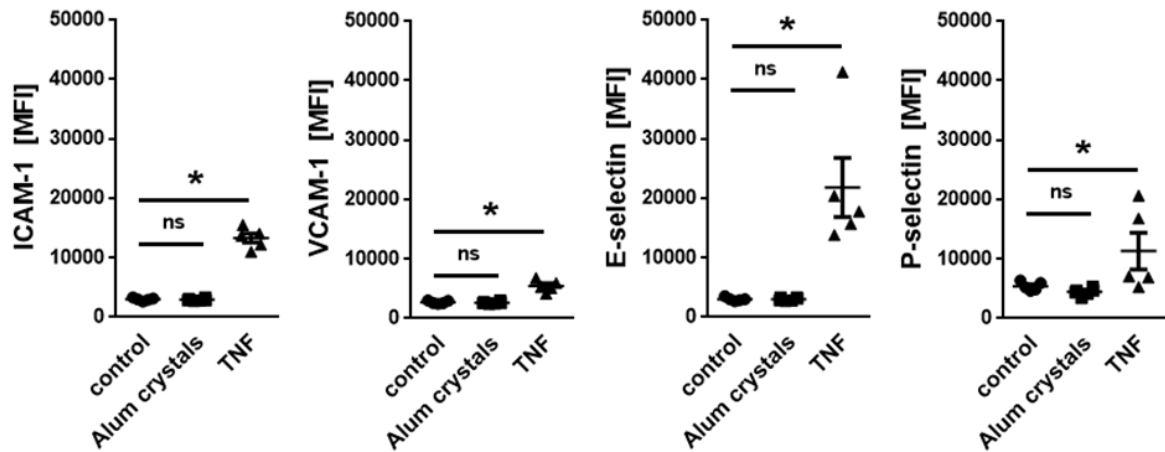


Figure 3.15: Quantification of the activation of endothelial cells after NLRP3 inflammasome stimulation. Analysis of ICAM-1/CD54, VCAM-1/CD106, E-selectin/CD62E, and P-selectin/CD62P expression levels on endothelial cells after stimulation with Alum crystals or TNF. Data are presented as mean±SEM; n=5-6; *p<0.05; n.s.=not significant.

4.5.8 The effect of DAMPs on endothelial cells

In addition, the same protocol was used to assess the potential of different DAMPs to activate endothelial cells. Stimulation with s100A8/A9, HMGB1, or MSU did not change ICAM-1/CD54, VCAM-1/CD106, E-selectin, or P-selectin expression on cultured microvascular endothelial cells as compared to untreated controls (**Fig. 3.16**).

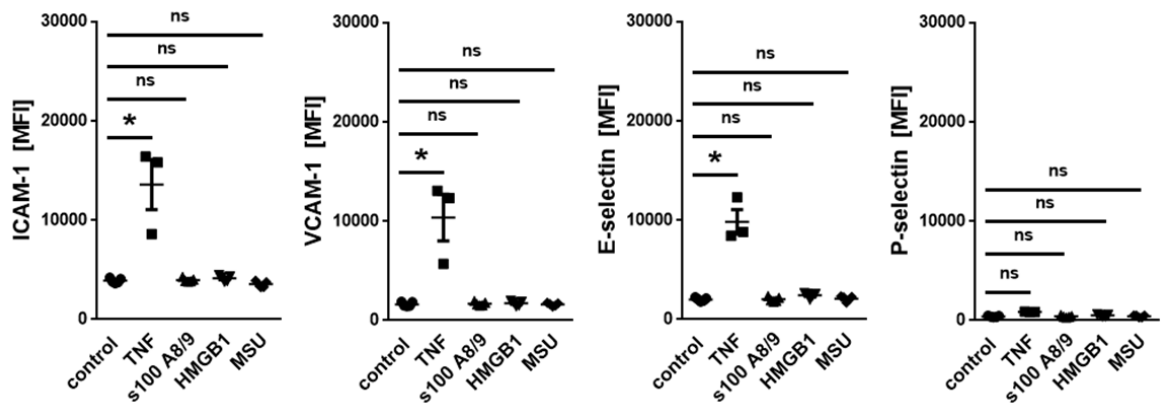


Figure 3.16: Quantification of the activation of endothelial cells after stimulation with DAMPs. Analysis of ICAM-1/CD54, VCAM-1/CD106, E-selectin/CD62E, and P-selectin/CD62P expression levels after stimulation with s100A8/A9, HMGB1, MSU, or TNF. Data are presented as mean±SEM; n=3-5 per group; *p<0.05; n.s.=not significant.

4.5.9 Cytokine release upon NLRP3 inflammasome activation

Using multiplex ELISA analysis, we also investigated the cytokine release into the peritoneal cavity upon NLRP3 inflammasome activation. In comparison to controls, stimulation with MSU led to a significant increase in IL-2, IFN γ , CXCL2, and CCL3 release (**Fig. 3.17**).

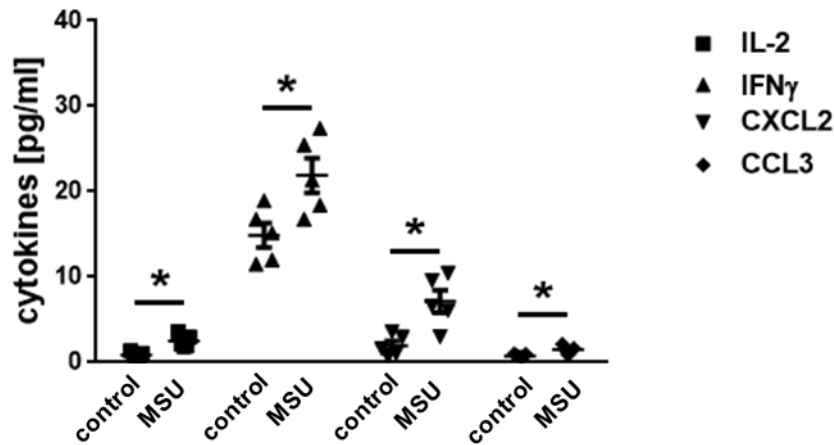


Figure 3.17: Quantification of cytokines after NLRP3 inflammasome activation. Analysis of cytokines in peritoneal lavage after injecting MSU. Data are presented as mean \pm SEM; n=5; *p<0.05.

4.5.10 ICAM-1/CD54 and VCAM-1/CD106 expression on cremasteric endothelial cells after activation of the NLRP3 inflammasome

To investigate ICAM-1/CD54 and VCAM-1/CD106 expression on cremasteric endothelial cells, we employed confocal microscopy analysis of immunohistochemically stained cremasteric tissue whole mounts (**Fig. 3.18 A**). Quantitative analysis revealed an increase in ICAM-1/CD54 expression on cremasteric endothelial cells after stimulation with Alum crystals for 6 h as compared to saline-injected controls whereas VCAM-1/CD106 expression did not change (**Fig. 3.18 B**).

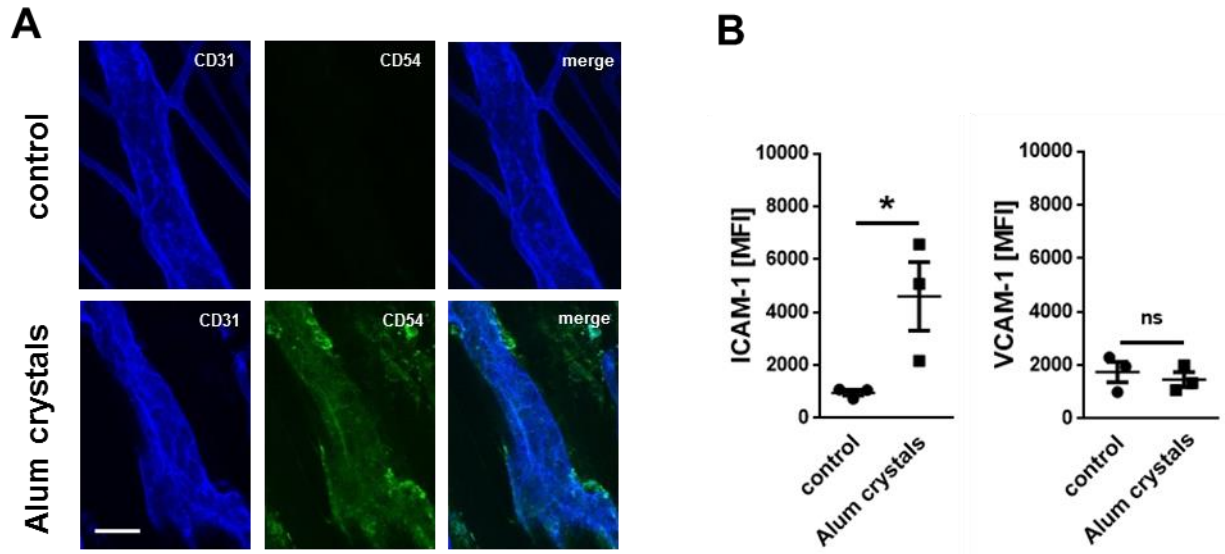


Figure 3.18: Analysis of ICAM-1/CD54 and VCAM-1/CD106 expression on cremasteric endothelial cells after NLRP3 inflammasome activation. Representative confocal images of postcapillary venules in the *M. cremaster* immunostained with anti-CD31 and anti-CD54 (scale bar: 25 μ m) (A). Quantitative analysis of ICAM-1/CD54 expression on cremasteric postcapillary venules (B). Data are presented as mean \pm SEM; n=3 per group; *p<0.05; n.s.=not significant.

4.5.11 Myeloid leukocyte trafficking in the cremaster muscle after NLRP3 inflammasome activation

4.5.11.1 Analysis after 3 h and 6 h of stimulation

Employing the *musculus cremaster* (*M. cremaster*) assay, the effect of NLRP3 inflammasome activation on the recruitment of myeloid leukocytes and their interaction with the endothelium was investigated. 3 h and 6 h after i.s. injection of Alum crystals, *in vivo* microscopy of postcapillary venules was performed in order to assess intravascular rolling and firm adherence of neutrophils and classical monocytes. The number of rolling neutrophils and classical monocytes was not altered in comparison to saline-injected control mice. Similarly, intravascular firm adherence of neutrophils and classical monocytes was not affected 3 h after

4.5.12 The effect of NLRP3 inflammasome inhibition on neutrophil trafficking in tumors

Using *in vivo* microscopy, neutrophil trafficking in the tumor and its microenvironment was observed. In SCC VII tumors, intravascular rolling was significantly increased as compared to tumor-free mice on day 3, but not on day 7 after tumor cell injection. In contrast, intravascular firm adherence of neutrophils significantly increased on day 7 after tumor cell injection as compared to healthy animals (**Fig. 3.20**). In 4T1 tumors, no significant differences were observed in numbers of intravascular rolling neutrophils on day 3 or 7 after tumor cell injection, whereas intravascular adherence of neutrophils was significantly higher on day 7 after tumor cell injection as compared to controls (**Fig. 3.20**). Treatment with an NLRP3 inflammasome inhibitor, these increased neutrophil responses in the tumor and its microenvironment were completely abolished.

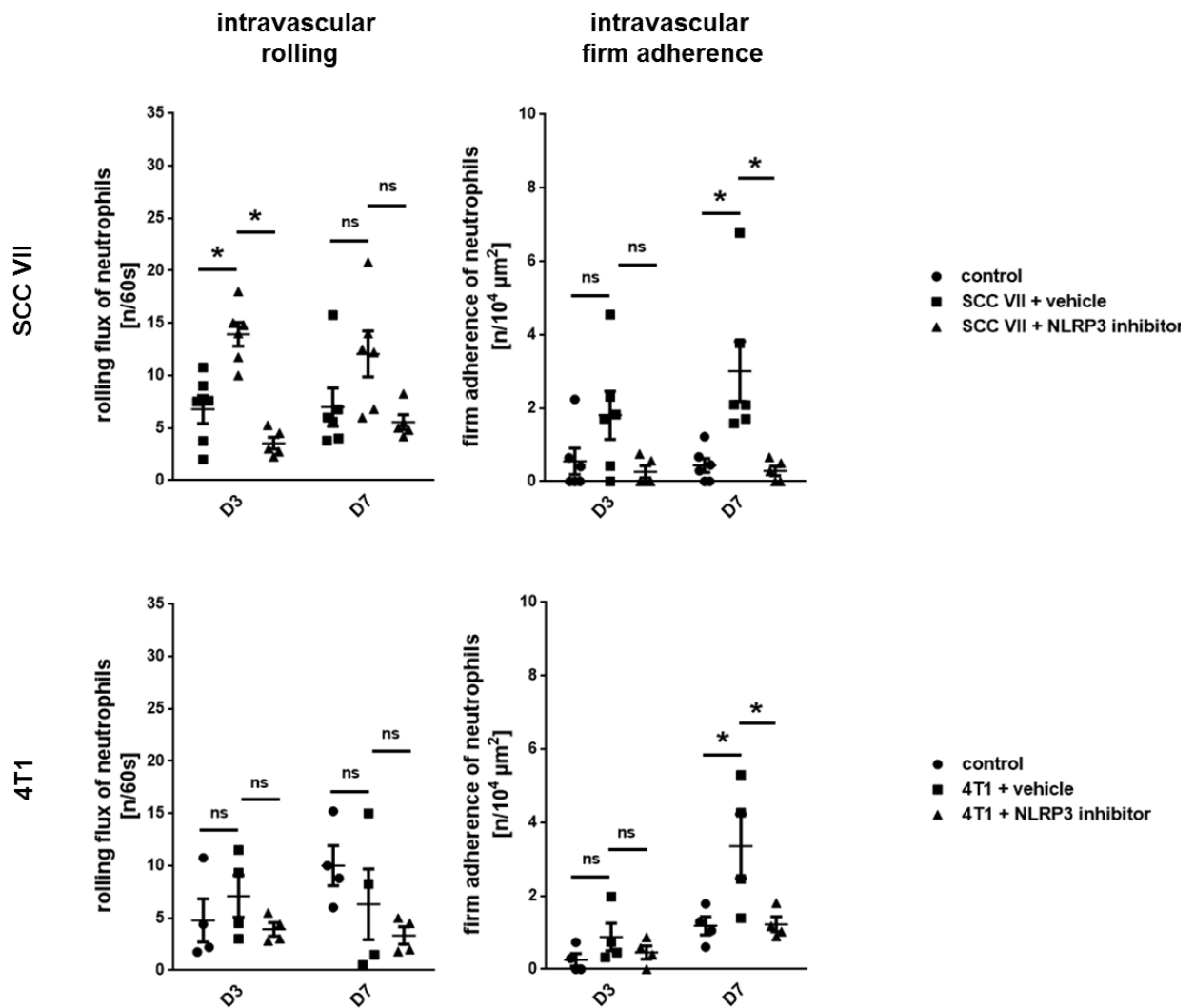


Figure 3.20: *In vivo* microscopy analysis of neutrophil trafficking in the tumor and its microenvironment. Analysis of intravascularly rolling and firmly adherent neutrophils on day 3 (D3) and day 7 (D7) after tumor cell injection in healthy control animals and vehicle- or NLRP3 inflammasome inhibitor-treated tumor-carrying mice. Data are presented as mean±SEM; n=4-6 per group; *p<0.05; n.s.=not significant.

4.6 The role of aged neutrophils in tumor progression

4.6.1 The effect of depleting neutrophils in tumor-bearing mice

In order to investigate the role of neutrophils for tumor progression in SCC VII and 4T1 carcinoma, mice were rendered neutropenic by antibody-mediated neutrophil

depletion. Multi-channel flow cytometry revealed a significantly reduced number of neutrophils in the tumors of *a priori* neutropenic mice as compared to isotype control antibody-treated tumor-carrying mice. Moreover, tumor weight was significantly lower in neutrophil-depleted tumor-bearing mice (Fig. 3.21 A). Noteworthy, delayed neutrophil depletion starting one week after the induction of tumor growth did not significantly alter the tumor size as compared to isotype control antibody-treated mice (Fig. 3.21 B).

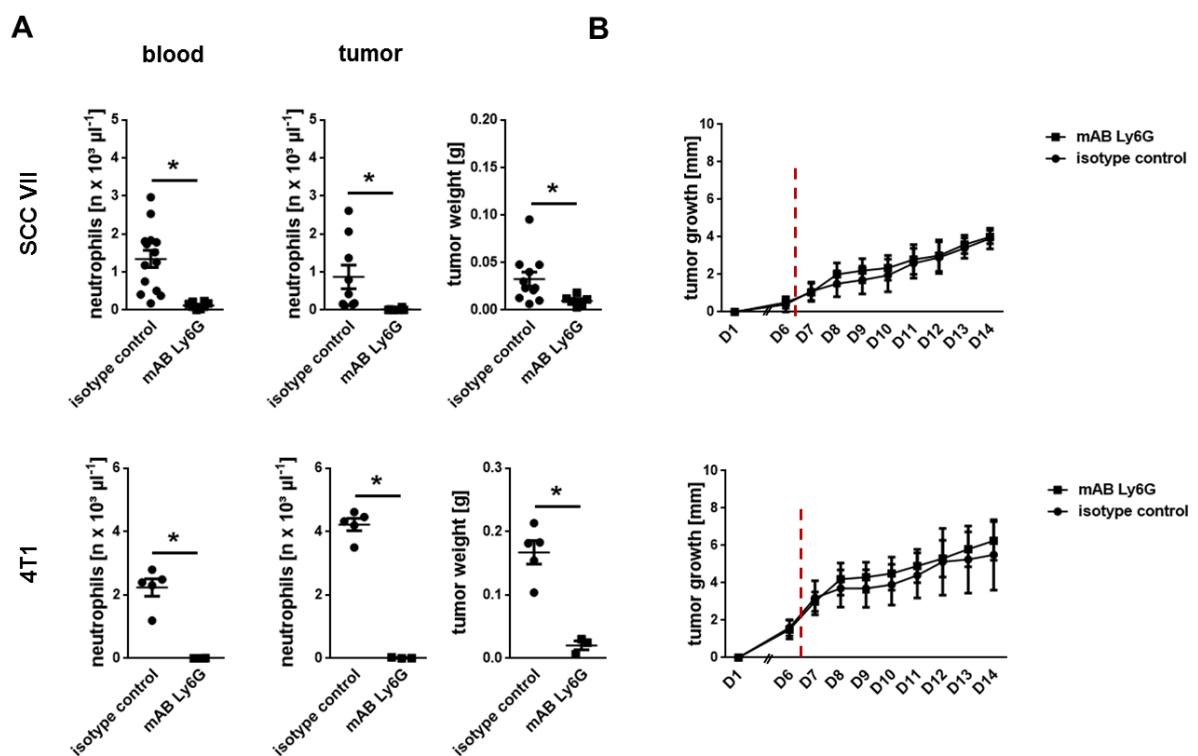


Figure 3.21: Analysis of the effects of neutrophil depletion in tumor-bearing mice. Quantification of neutrophils in peripheral blood and the tumor as well as of tumor weight in *a priori* (A) or delayed (B) neutrophil-depleted (mAb Ly6G) or isotype control antibody-treated mice. Data are presented as mean \pm SEM; n=3-11 per group; *p<0.05.

4.6.2 The effect of NLRP3, CXCR4, or CXCR2 inhibitors on tumor weight and neutrophil infiltration of tumors

To explore the role of the NLRP3 inflammasome for tumor progression, tumor weight and development rates were assessed in mice treated with the highly specific NLRP3 inflammasome inhibitor MCC950. Treatment with this inhibitor significantly decreased tumor weight and development rates in both SCC VII and 4T1 tumor-bearing mice.

To investigate the effects of directly manipulating the ageing process of circulating neutrophils, we inhibited the receptors CXCR4 and CXCR2 in tumor-injected mice. Whereas blockade of the chemokine receptor CXCR4 lead to a slight increase in the tumor weight, antagonizing the chemokine receptor CXCR2 resulted in a significant decrease in tumor weight. The tumor development rate however, was not significantly altered by these interventions (**Fig. 3.22**).

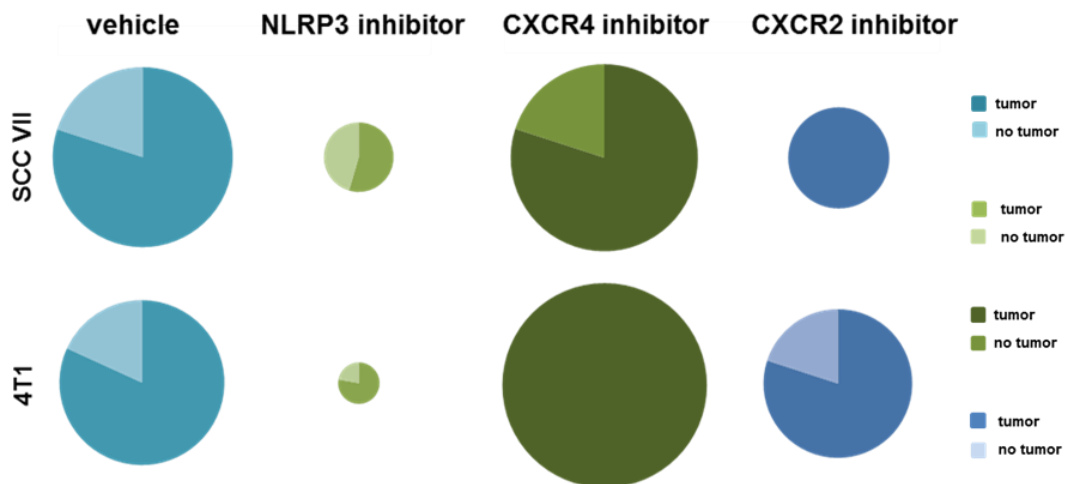


Figure 3.22: Quantitative analysis of tumor weight and tumor development after blocking the NLRP3 inflammasome, CXCR2, or CXCR4 in tumor-bearing mice. Graphical presentation of the tumor development rate and the average tumor weight, depicted by the size of the circle. Tumor-bearing mice were either treated with vehicle, an NLRP3 inhibitor, a CXCR4 inhibitor or a CXCR2 inhibitor. Data are presented as mean; n=3-15 per group.

In addition, tumor infiltration of aged and non-aged neutrophils was measured in these experiments. Blockade of the NLRP3 inflammasome in SCC VII or 4T1 tumor-bearing mice, led to a significant reduction in the number of neutrophils in the tumor (**Fig. 3.23 A**). In contrast, treatment with inhibitors of CXCR4 or CXCR2, however, did not significantly alter the number of neutrophils in the tumors (**Fig. 3.23 B**).

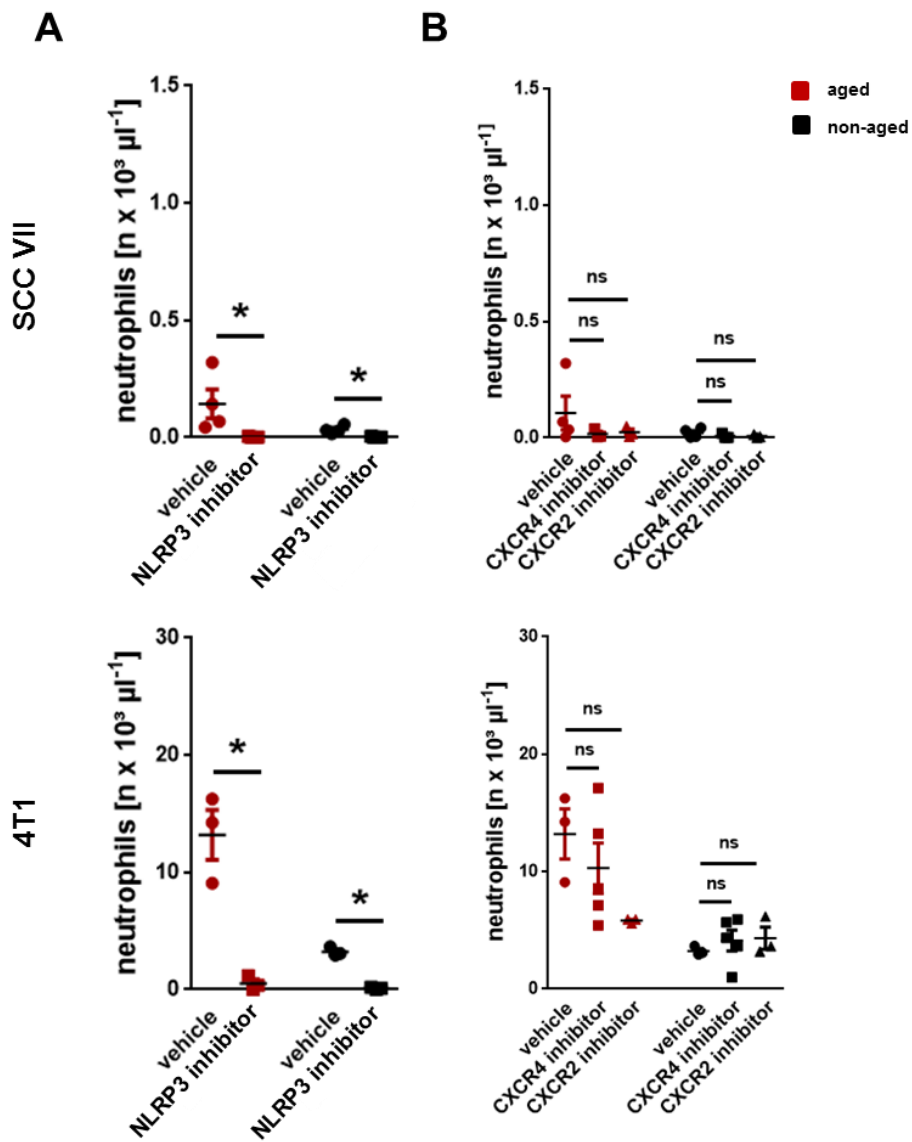


Figure 3.23: Quantitative analysis of neutrophil infiltration into tumors after blocking the NLRP3 inflammasome, CXCR2 and CXCR4 in tumor-bearing mice. Quantitative analysis of aged and non-aged neutrophils in tumors of mice treated with a NLRP3 inhibitor (**A**), a CXCR2 inhibitor, or a CXCR4 inhibitor (**B**). Data are presented as mean±SEM; n=3-5 per group; *p<0.05; n.s.=not significant.

4.6.3 Direct effects on tumor cell proliferation

Employing a MTT assay, we sought to analyze the role of the NLRP3 inflammasome for SCC VII or 4T1 tumor cell proliferation. In our experiments, neither activating the NLRP3 inflammasome by Alum crystals, nor inhibiting its activation by MCC950, led to any significant changes in SCC VII or 4T1 tumor cell proliferation as compared to controls. Similarly, blockade of the chemokine receptors CXCR2 or CXCR4 did not affect the proliferation of SCC VII or 4T1 cells (Fig. 3.24 A+B).

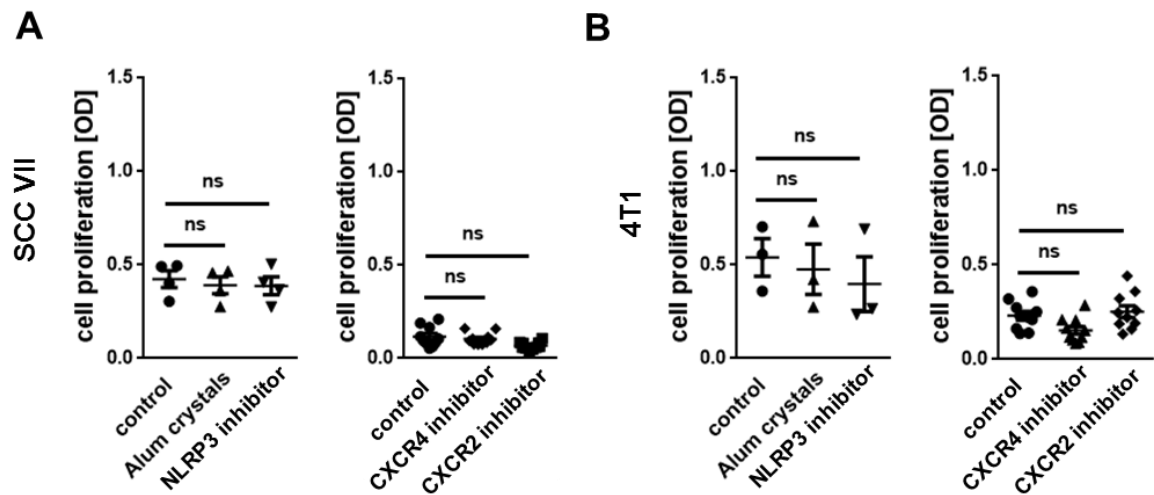


Figure 3.24: Quantification of tumor cell proliferation after treatment with Alum crystals, a NLRP3 inhibitor, a CXCR4 inhibitor, or a CXCR2 inhibitor. Data are presented as mean \pm SEM; n=3-10 per group; n.s.=not significant.

4.7 The mechanisms underlying tumor growth mediated by aged neutrophils

4.7.1 Expression of N1 and N2 phenotype-associated molecular markers in neutrophils recruited by NLRP3 inflammasome activation

To further investigate the phenotype of neutrophils recruited to the peritoneal cavity after NLRP3 inflammasome activation, several surface markers associated with a N1 or N2 phenotype of these immune cells were analyzed by multi-channel flow cytometry. Aged neutrophils recruited upon NLRP3 inflammasome activation showed higher expression levels of NE, MMP9, CCL5, VEGF, CCL3, and Arg-1 on their surface as compared to non-aged neutrophils (**Fig. 3.25**).

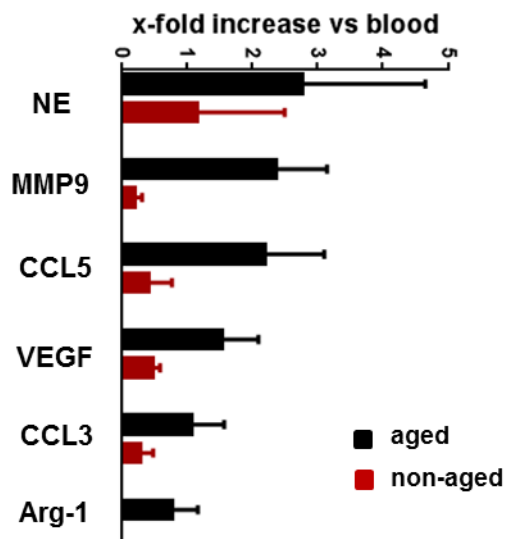


Figure 3.25: Quantitative analysis of the expression of N1 and N2 phenotype-associated molecules on aged and non-aged neutrophils. Data are presented as mean \pm SEM; n=3-11 per group.

4.7.2 The effect of tumor-primed neutrophils on tumor cell proliferation

The effect of neutrophils isolated from the peripheral blood of tumor-bearing mice on tumor cell proliferation was investigated by a MTT assay. Both SCC VII and 4T1 tumor cells showed a significant increase in their proliferation upon incubation with supernatants from tumor-primed neutrophils, either isolated from the blood of tumor-bearing C3H/HeNCrI mice (SCC VII tumors) or BALB/cJ mice (4T1 tumors) as compared to supernatants from neutrophils isolated from tumor-free control animals. This increase in tumor cell proliferation was significantly attenuated upon administration of a NE inhibitor (**Fig. 3.26**).

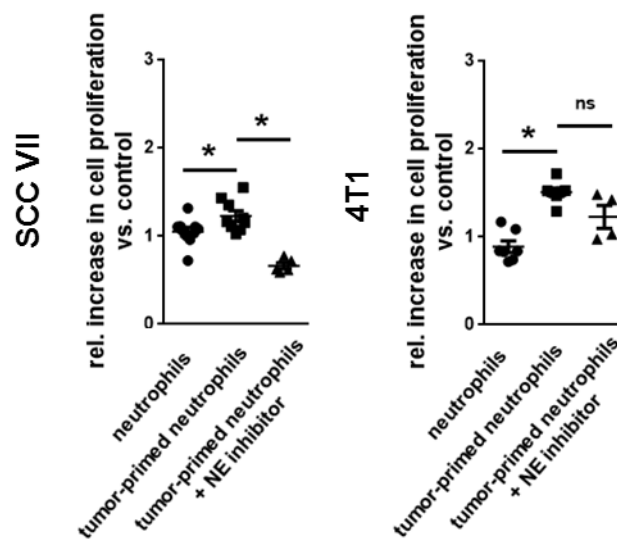


Figure 3.26: Quantification of tumor cell proliferation after treatment with supernatants from tumor-primed neutrophils. Data are presented as mean \pm SEM; n=4-10 per group; *p<0.05; n.s.=not significant.

4.7.3 The effect of tumor-primed neutrophils on microvascular endothelial cell proliferation

In a next set of experiments, we sought to characterize the effect of tumor-primed neutrophils on the proliferation of microvascular endothelial cells. Incubation of bEnd.3 microvascular endothelial cells with supernatants from tumor-primed neutrophils did not significantly alter their proliferation as compared to supernatants from control neutrophils harvested from tumor-free mice (**Fig. 3.27**).

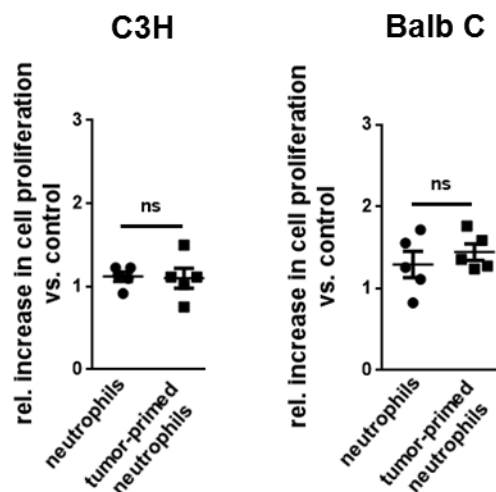


Figure 3.27: Quantification of microvascular endothelial cell proliferation after treatment with supernatants from tumor-primed neutrophils. Data are presented as mean \pm SEM; n=5 per group; n.s.=not significant.

4.7.4 The effect of tumor-primed on the migration of microvascular endothelial cells

To evaluate the effect of tumor-primed neutrophils on the migration of microvascular endothelial cells, a scratch assay was performed. Incubation with supernatants from neutrophils isolated from tumor-bearing mice did not significantly change the number of microvascular endothelial cells migrating into

the scratch as compared to supernatants from control neutrophils harvested from tumor-free mice (**Fig. 3.28**).

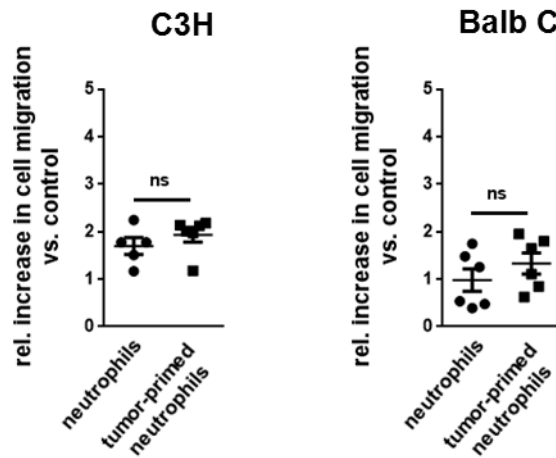


Figure 3.28: Quantification of microvascular endothelial cell migration after treatment with supernatants from tumor-primed neutrophils. Data are presented as mean±SEM; n=5-6 per group; n.s.=not significant.

4.7.5 The effect of neutrophil depletion on the microvascular network of tumors

Moreover, we sought to investigate the effect of neutrophils on the architecture of the microvasculature of the tumor and its microenvironment. No alterations in the overall vessel density as well as in the number of vessel branches or junctions were observed in neutrophil-depleted mice, as compared to isotype control antibody-treated mice (**Fig. 3.29**).

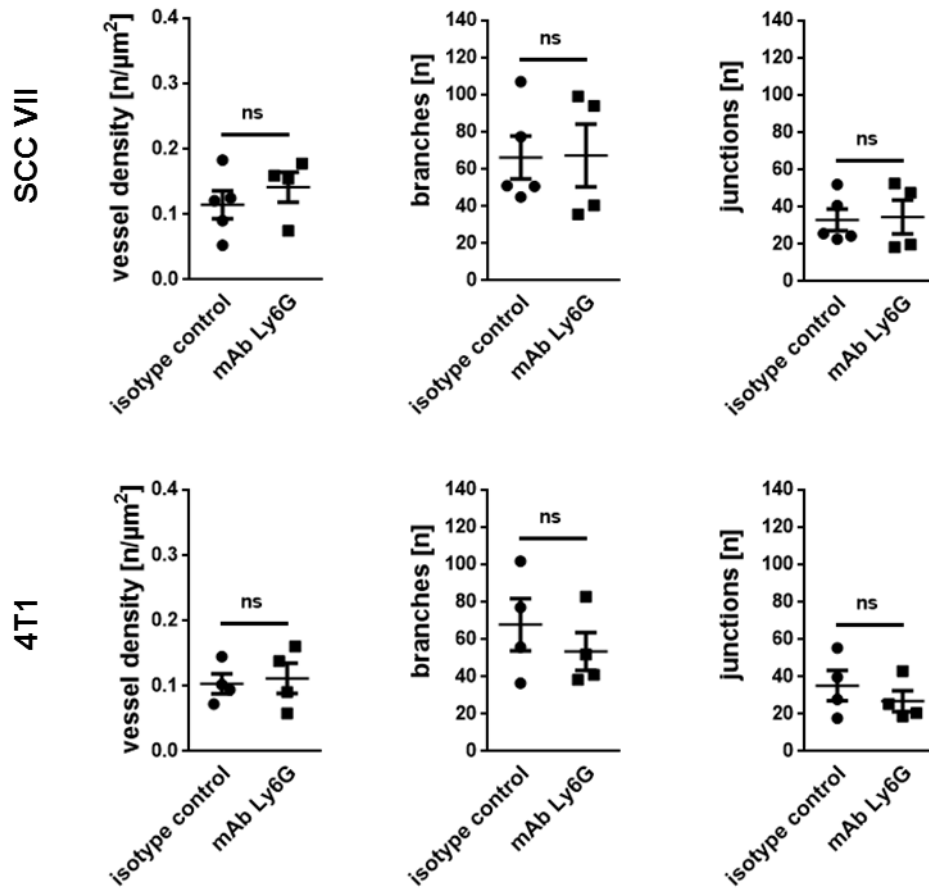


Figure 3.29: Quantitative analysis of the vessel density, the number of branches, and the number of junctions in neutrophil-depleted tumor-bearing mice (mAb Ly6G). Data are presented as mean±SEM; n=4-5 per group; n.s.=not significant.

4.7.6 The effect of depleting neutrophils on T cell infiltration into tumors

Finally, we aimed to investigate the effect of neutrophils on the infiltration of CD4⁺ and CD8⁺ T cells into tumors. Using antibody-mediated depletion of neutrophils in SCC VII or 4T1 tumor-bearing mice, no effect on numbers of CD8⁺ and CD4⁺ T cells present in tumors were observed as compared to isotype control antibody-treated mice (**Fig. 3.30**).

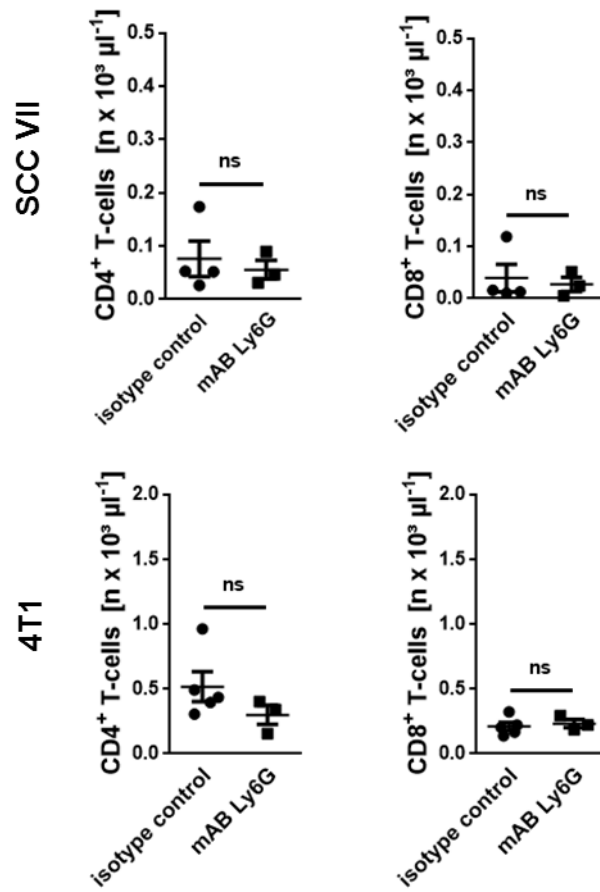


Figure 3.30: Quantitative analysis of CD4⁺ or CD8⁺ T cells in the tumors of neutrophils-depleted mice (mAb Ly6G). Data are presented as mean \pm SEM; n=3-5 per group; n.s.=not significant.

5 Discussion

5.1 Material and Methods

In order to validate our findings, we chose to perform the studies in two different types of tumors, the SCC VII head and neck cancer and the 4T1 breast cancer. These tumors strongly differ in their immunomodulatory properties. Whereas the 4T1 has previously been described as a highly immunogenic tumor, the SCC VII is considered as poorly immunogenic (Lechner et al., 2013). Hence, mechanisms found to be relevant for tumor progression in both types of tumors, have greater potential of becoming therapeutic targets.

The model organism we decided to employ for our investigations was the mouse, as the mouse immune system is relatively well characterized. Due to our selection of tumors, and the origin of our tumor cells, experiments were performed with two different mouse strains: C3H/HeNCrl mice for the investigation of SCC VII tumors and BALB/cJ mice for analyzing 4T1 tumors. Both models are syngeneic or allograft models, meaning we inject tumor cells that were derived from the same genetic background as our mouse strain. Other mouse models that are often used to investigate potential cancer therapeutics are xenograft models where human cancer cells are transplanted into immunocompromised mice. Altering the immune system assures that mice do not reject human cell transplants. The syngeneic model, however, does not require these alterations in the immune system. Hence, when investigating the influence of the immune system on tumorigenesis or examining potential immunotherapies the syngeneic model holds clear advantages over the xenograft model.

In order to investigate tumor progression we decided to not only employ one mouse model, but two.

We incorporated an orthotopic mouse model, in which we injected tumor cells in their usual growth site – the floor of the mouth in case of SCC VII or the chest in case of 4T1 cells. This approach enables the investigation of tumor progression with the influence of a rather natural tumor microenvironment. In addition, the orthotopic model allows the growth of tumors that are easy to dissect. Thereby, single cell suspensions for the use of multi-channel flow cytometry analysis could be obtained.

Multi-channel flow cytometry is a widely used laser-based method to analyze the expression of cell surface and intracellular molecules and characterize cell types within a heterogeneous cell population. The method not only measures size and volume of the cells, but also the fluorescence intensity by fluorescent-labeled antibodies bound to specific cell-associated molecules. However, depending on the type of flow cytometer, and the number of lasers and detectors it is equipped with, only a specific number of fluorescent labels can be detected, thus limiting the amount of molecules one could measure.

We also used flow cytometry analysis of orthotopically-grown tumors, from mice rendered neutropenic. These analyses gave direct insight on the potential impact of neutrophils for tumor progression and the recruitment of immune cells to the tumor. Moreover, we were able to investigate the effect of different inhibitors or antagonists on tumor development, by using this approach. By employing a pulse-labeling technique with BrdU, we also had the opportunity to gain insight on the relative chronological age of neutrophils that were present in the tumor. BrdU is a

thymidine analogue, thus enabling the incorporation into DNA during its replication. It is a very well-established approach to detect all proliferating cells from time of introduction to tissue fixation (Salic & Mitchison, 2008). Hence, BrdU^{positive} cells are non-aged neutrophils and BrdU^{negative} cells are aged neutrophils. To be able to detect the BrdU, a harsh and long treatment of the samples is necessary in order to denature DNA and provide access to BrdU. These different steps can possibly interfere with expression levels of other surface molecules, thereby making appropriate negative controls of great importance to avoid false results. However, with BrdU allowing the direct detection of cell proliferation, it is a very reliable method, creating stable results.

The second tumor model we employed is a heterotopic model, in which we injected tumor cells into the ear. This approach offers a great opportunity of consecutive, non-invasive live imaging of leukocyte-tumor interactions. We used this model for *in vivo* imaging of neutrophil-tumor interactions on various days after tumor cell injection under baseline conditions, but also after treating tumor-carrying mice with different inhibitors or antagonists. Moreover, we also employed this model for adoptive cell transfer experiments which allowed the direct comparison between interactions of chronologically aged vs chronologically non-aged neutrophils in the tumor and its microenvironment. The heterotopic model also enabled us to examine the microvascular architecture in tumor-bearing mice and in tumor-bearing mice that were rendered neutropenic, thereby analyzing the effect of neutrophils on tumor angiogenesis.

Furthermore, we combined our tumor models with two additional mouse models: the *M. cremaster* assay and the peritonitis assay. By adding these two models, we

were able to investigate molecules of interest from the investigated pathways outside of the tumor and its microenvironment. The *M. cremaster* assay is a very well established model for live imaging of leukocyte-endothelial interactions after the administration of inflammatory stimuli. Due to the thin nature of the muscle, imaging the different steps of the leukocyte adhesion cascade is possible. By combining this approach with the use of fluorescence-labeled antibodies, we were also able to distinguish distinct immune cell populations and even phenotypes. With the use of the peritonitis assay, the recruitment of different leukocyte subsets to the peritoneal cavity after administering various stimuli could be investigated. By employing multi-channel flow cytometry, we were able to quantify these recruited immune cells. However, this should only be considered a “screening assay” as there is no possibility to distinguish between the interactions of certain immune cells that may have contributed to their infiltration into the peritoneal cavity.

We also employed multi-channel flow cytometry to quantify leukocyte subsets within the tumor, characterize the phenotype of neutrophils, and analyze the activation status of neutrophils and endothelial cells. When measuring these activity states of cells, one disadvantage of this method is that only stronger shifts or upregulations of molecules are detectable. Moreover, as some of these experiments were performed *ex vivo* in blood, or *in vitro* in cell culture experiments, one has to be cautious not to activate the immune cells by the process of taking the blood or simply pipetting not carefully enough. In addition, as cell culture is an isolated approach, the results do not give any indication on the influences from other cells. Hence, we also employed immunohistochemistry of cremasteric whole mounts as another way of measuring the activation of

endothelial cells, for instance. By combining these methods, it is possible to get a more comprehensive understanding.

To gain more detailed insight on the underlying mechanisms of neutrophils in tumor progression, we also employed several other *in vitro* experiments such as a cell proliferation assay or a cell migration assay. The MTT cell proliferation assay is a commonly used method to investigate the number of viable cells, based on the transformation of yellow MTT((3-(4,5-Dimethylthiazol-2-yl)-2,5-Diphenyltetrazolium Bromide) into blue formazan *via* mitochondrial enzymes (Sylvester, 2011). Thus, we were able to examine the influence of different stimuli and specific molecular factors on cell proliferation. In order to explore cell migration we employed a scratch assay. By creating a scratch in the monolayer of confluent cells, and comparing the cell migration rate into this scratch, the effect of different stimuli could be observed. However, it should be noted that *in vitro* experiments display isolated events as there is no environmental influence. Hence, it is best to combine these with other *in vivo* approaches. For instance, a possible approach might be to target the molecular factors found in these experiments, in tumor-bearing mice and measure tumor progression.

In cooperation with other laboratories, we also employed multiplex analysis and ELISA measurements. These methods, especially the multiplex, offer a great screening assay for a large variety of cytokines in many different samples.

5.2 Results

Previous studies demonstrated that tumors release a variety of signals that are able to influence the tumor microenvironment as well as to manipulate the host's immune response (Coffelt, Wellenstein, & de Visser, 2016; Coussens et al., 2000). It has also become apparent that even in earlier stages, cancer is a systemic disease rather than a local threat. The potential of tumor-released signals to modulate the immune system however, is still not well understood.

To compare our poorly immunogenic tumor, the SCC VII and the highly immunogenic 4T1 tumor, we performed multiplex analysis. Thereby, we investigated which signals can be found within cell culture supernatants, solid tumors and are released into the systemic circulation. Our data revealed that in cell culture supernatants, SCC VII cells release a larger variety of cytokines in comparison to 4T1 tumor cells. In contrast, in solid tumors raised from these cells in mice, these differences were no longer present. However, 4T1 tumors produced higher amounts of cytokines than SCC VII tumors. This might be contributing to the higher immunomodulatory properties of 4T1 tumors as compared to SCC VII tumors (Lechner et al., 2013). Interestingly, we did not observe any differences regarding the concentrations of cytokines in the serum of tumor-bearing mice as compared to healthy mice. However, circulating neutrophils might encounter higher concentrations of these tumor-derived chemokines only when making their way through the tumor and its microenvironment. Moreover, it is possible that the tumor-released cytokines are taken up by erythrocytes (Karsten, Breen, & Herbert, 2018) and presented to circulating neutrophils. Hence, SCC VII and 4T1 tumor exhibit common and distinct cytokine expression profiles.

To evaluate the numbers of neutrophils present in the systemic circulation of tumor-bearing mice, we employed multi-channel flow cytometry. In these experiments, we were able to reveal that tumor-bearing mice showed a slight (in case of SCC VII) or a strong increase (in case of 4T1) in the number of blood neutrophils. This neutrophilia is a previously described phenomenon in various types of tumors and has often been described to be associated with a poor clinical outcome (Atzpodien & Reitz, 2008; Bellocq et al., 1998; Schmidt et al., 2005).

A recent publication demonstrated that CXCL2, another ligand for CXCR2, initiates the process of neutrophil biological ageing in an autocrine manner (J. M. Adrover et al., 2019). Noteworthy, data from the multiplex analysis also revealed that concentrations of ligands for CXCR2 were high in tumor cell supernatants as well as in tumors itself. We therefore hypothesized that elevated tumor levels of CXCR2 ligands in tumor-bearing mice cause circulating neutrophils to age much faster than under homeostatic conditions.

Neutrophils have been shown to acquire higher expression levels of the chemokine receptor CXCR4, during their time in the circulation, making CXCR4 an ideal marker for aged neutrophils (Eash et al., 2009; Uhl et al., 2016). We found that CXCR4 expression was significantly increased on circulating neutrophils in tumor-bearing mice as compared to neutrophils in tumor-free control mice. Blockade of the ageing-promoting chemokine receptor CXCR2 in tumor-bearing mice significantly reduced the expression of CXCR4 on blood neutrophils, suggesting that neutrophils in tumor-bearing mice exhibit an excessively aged phenotype which is mediated through ligands of CXCR2. Neutrophils in tumor patients have been shown to display an extended half-life due to cues released by

the tumor microenvironment (Cheretakis, Leung, Sun, Dror, & Glogauer, 2006; Sawanobori et al., 2008). With neutrophils spending more time in the circulation, this might potentially further support neutrophil ageing.

5.2.1 The fate of excessively ageing neutrophils in cancer

The time neutrophils spend in the circulation was shown to have a large impact on their molecular repertoire, and hence, their function. Ageing neutrophils represent highly reactive immune cells that are among the first line of defense when battling infections (Uhl et al., 2016). At the same time, this highly reactive phenotype of neutrophils can also represent a threat for vascular health under certain conditions by promoting microvascular thrombosis (J. M. Adrover et al., 2019). Considering that thrombosis has been described as a common complication in tumor patients (Sallah, Wan, & Nguyen, 2002), excessively ageing neutrophils in cancer might particularly contribute to this phenomenon. The fate of excessively ageing neutrophils in cancer, however, is still unclear.

Employing immunostaining and confocal microscopy on tumor sections, we detected neutrophils in SCC VII and 4T1 tumors as well as in the tumor microvasculature. The presence of neutrophils in these solid tumors was confirmed by multi-channel flow cytometry tumor homogenates. In particular, 18.90 % of the tumor leukocytes in SCC VII were CD11b^{positive} myeloid leukocytes, and 2.74 % were Ly6G^{positive} neutrophils. With 82.15 % of CD11b^{positive} myeloid leukocytes, and 13.14 % Ly6G^{positive} neutrophils, levels of these cells in 4T1 tumors were a lot higher. Using a pulse labeling technique with BrdU, we further identified

that the majority (about 80 %) of neutrophils present in tumors were aged neutrophils.

To confirm these findings, we performed adoptive cell transfer experiments and used *in vivo* microscopy to image interactions between aged and non-aged neutrophils in the tumor and its microenvironment. Our data indicate that particularly aged neutrophils (isolated from mice exhibiting > 80 % aged neutrophils in their circulation upon treatment with blocking anti-P- and E-selectin antibodies) accumulate in the microvasculature of the tumor and of its microenvironment as compared to non-aged neutrophils isolated from WT mice treated with isotype control antibodies (exhibiting < 20 % aged neutrophils). This might be explained by previous studies demonstrating increased surface levels of integrins such as CD11a, CD11b and CD49d (J. M. Adrover et al., 2016; Uhl et al., 2016) on aged neutrophils which enable these highly reactive immune cells to migrate to sites of inflammation faster. Thus, excessively ageing neutrophils preferentially infiltrate malignant tumors.

5.2.2 The recruitment of excessively ageing neutrophils to tumors

Neutrophil recruitment can be evoked through a variety of stimuli, for instance DAMPs released by necrotic or damaged tissue. Previous studies already described the release of DAMPs, such as s100A8/A9, HMGB1, or MSU in various types of tumors (Hernandez et al., 2016). Thus, we aimed to analyze the amount of HMGB1, s100A8/A9, and uric acid in our tumor cells. HMGB1 as well as s100A8/A9 concentrations in supernatants from cell-cultured tumor cells were

measured using ELISA, whereas uric acid measurements were obtained using a COBAS 8000 modular analyzer.

S100A8/A9 was not detected in the supernatants from our tumor cells, whereas HMGB1 was found to be secreted by 4T1 tumor cells and – in very low concentrations – by SCC VII tumor cells. Uric acid was detected in supernatants from both cell lines. Interestingly, in 4T1 tumor cell supernatants a higher amount of uric acid was measured than in SCC VII. Considering that many studies have already shown that s100A8/A9 is found in various types of cancer and that it might play an important role in tumor progression, (Gebhardt, Németh, Angel, & Hess, 2006; Salama, Malone, Mihaimed, & Jones, 2008), our findings seem to be surprising at a first glance. However, many positive results of s100A8/A9 might originate from phagocytes in tumors, rather from tumor cells themselves, as these immune cells have been shown to be a prominent source for s100A8/A9 (Foell, Wittkowski, Vogl, & Roth, 2007). In the context of 4T1 tumor cells releasing HMGB1 into the supernatant, but not of SCC VII tumor cells, this finding might be another hint towards 4T1 being a more immunogenic tumor that displays more immunomodulatory potential than SCC VII, through the release of a larger variety of DAMPs. Both types of tumors secreting MSU, might contribute to both of the tumors immunomodulatory properties, as uric acid is known to be a potent trigger for inflammation and immune activation, for instance in active gout (Shi, Mucsi, & Ng, 2010). Next, we employed a peritonitis assay in order to investigate the potential of DAMPs to induce leukocyte recruitment. Whereas s100A8/A9 as well as MSU crystals caused a significant influx of neutrophils and to a lesser degree of monocytes, into the peritoneal cavity, HMGB1 did not cause any leukocyte recruitment in this assay. In the past, HMGB1 was already thought to be

implicated in leukocyte recruitment, however, recent studies revealed pure recombinant HMGB1 does not display proinflammatory activity (Bianchi, 2009), and that its oxidation status strongly regulates its activity (H. Yang et al., 2012).

In addition, we also investigated whether the released DAMPs we identified in our tumor cell supernatants, have the ability to activate TLR2 or TLR4, the principal receptors for HMGB1. Interestingly, treatment with SCC VII and 4T1 cell supernatants did not activate either of the receptors, indicating that HMGB1 may not be released by our tumor cells in concentrations that result in TLR2 or TLR4 activation (Yu et al., 2006). This further led us into the conclusion that particularly MSU might mediate neutrophil recruitment to tumors.

DAMPs such as MSU promote inflammatory responses *via* the activation of inflammasomes, an intracellular protein complex facilitating the production of inflammatory mediators including IL-1 β (Martinon, Pétrilli, Mayor, Tardivel, & Tschopp, 2006). Consequently, we hypothesized that activation of inflammasomes might regulate the trafficking of excessively ageing neutrophils in cancer to malignant tumors. Confirming this hypothesis, administration of MSU crystals led to the release of IL-1 β in the peritoneal cavity, indicating inflammasome activity. Employing a peritonitis assay, we found that activation of the NLRP3 inflammasome with Alum crystals, but not of the AIM2 inflammasome with poly (da:dt), the NLRC4 inflammasome with FLA-ST, or the NLRP1 inflammasome with MDP, led to a significant recruitment of neutrophils and – to a lesser degree of classical monocytes to the peritoneal cavity. The majority of neutrophils recruited upon NLRP3 inflammasome activation was represented by aged neutrophils as indicated by BrdU pulse labeling.

To investigate whether activation of the NLRP3 inflammasome causes direct effects on neutrophils, integrin expression was analyzed on neutrophils isolated from the peripheral blood of WT mice *via* flow cytometry. No effect of stimulation with Alum crystals on the expression levels of CD11a, CD11b, or CD49d on neutrophils was observed. Moreover, the ability to bind ICAM-1/CD54-Fc is another parameter indicative of conformational changes in β 2 integrins, hence, neutrophil activation. However, we also did not detect any changes after stimulation with Alum crystals. Furthermore, we also aimed to analyze the effects of NLRP3 inflammasome activation on endothelial cells by measuring the expression levels of ICAM-1/CD54, VCAM-1/CD106, E-selectin, and P-selectin. However, stimulation with Alum crystals did not lead to any upregulation of these molecules on the surface of cultured microvascular endothelial cells. A recent study described that DAMPs do have the potential to activate endothelial cells. In this study, however, endothelial cells were not treated by DAMPs directly, but with supernatants from tumor cells after radiation (Krombach et al., 2019).

On the contrary, when we looked at the effect of NLRP3 stimulation with MSU crystals on the release of cytokines in an *in vivo* setting, the peritoneal cavity, we detected increased levels of cytokines, likely released from macrophages, such as IL-2, IFN γ , CXCL2 and CCL3. These findings suggest that it is actually the NLRP3 inflammasome in macrophages that becomes activated and then facilitates neutrophil recruitment by releasing cytokines. This is in line with previous findings showing that crystals were phagocytosed by macrophages, incorporated into the phagolysosome, and finally lead to lysosomal rupture resulting in activating an immune response through releasing cytokines (Hornung et al., 2008). Another aspect further confirming this hypothesis is, after injecting Alum crystals into the *M.*

cremaster, cremasteric endothelial cells did show an increase in ICAM-1/CD54, whereas cell-cultured microvascular endothelial cells did not show an upregulation of this molecule after direct stimulation. In this context, we observed that activation of the NLRP3 inflammasome particularly promote intravascular adherence and (subsequent) transmigration of neutrophils and – to a lesser degree – of monocyte to the perivascular tissue as elicited by *in vivo* microscopy on the mouse cremaster muscle. Hence, in an *in vivo* setting where macrophages are present, endothelial cells become activated through the cytokines released by macrophages which in turn facilitates neutrophil recruitment.

With inflammasomes being such a potent trigger of inflammatory responses, it is not too surprising that the involvement of these signaling platforms in various pathologies is currently subject to many discussions. Especially, the NLRP3 inflammasome has been implicated to play a role in tumor progression, however, results have been rather contrasting so far. On the one hand, inflammasome loss of function has been reported to be associated with enhanced rate and size in induced skin carcinogenesis (Gasparoto et al., 2014). On the other hand, expression of NLRP3 components and the cytokine IL-1 β has been detected in oral squamous cell carcinoma tissues, and downregulation of the NLRP3 expression in oral squamous cell carcinoma tumor cells significantly reduced the tumor growth *in vivo* (H. Wang et al., 2018).

It should be noted that IL-1 β has recently been shown to stimulate the IL-17-G-CSF axis (Ueda, Cain, Kuraoka, Kondo, & Kelsoe, 2009), meaning inflammasome activation can further support neutrophilia, which in turn is known to support tumor progression. Consequently, we aimed to investigate the effect of the NLRP3

inflammasome in neutrophil trafficking to malignant tumors. In order to investigate this, we established an *in vivo* ear model that enabled us to continuously image neutrophil responses, in the tumor. The number of rolling neutrophils was increased in SCC VII but not in 4T1 tumor-bearing mice, whereas significantly more neutrophils were adherent in mice injected with both types of tumors. Interestingly these increased neutrophil responses were completely abolished when we treated tumor-bearing mice with the NLRP3 inflammasome inhibitor MCC950. Hence, these data suggest that the NLRP3 inflammasome controls neutrophil trafficking to malignant tumors.

5.2.3 The role of excessively ageing neutrophils in tumor progression

After identifying that excessively ageing neutrophils are recruited to the tumor and its microenvironment *via* the NLRP3 inflammasome, we sought to evaluate the role of excessively ageing neutrophils in tumor progression. Consequently, we depleted neutrophils in tumor-bearing mice, starting the same day as tumor cell injection to ensure the tumor does not have any neutrophils to support tumor growth. As expected neutrophils in the blood of tumor-bearing mice as well as in malignant tumors were nearly absent. Interestingly, also the tumor weight was significantly lower in neutrophil-depleted animals as compared to isotype-treated controls. This is in line with previous studies that revealed neutrophil depletion results in reduced tumor growth (Jablonska et al., 2010; Jamieson et al., 2012). Together with other experimental studies also reporting tumor-supporting properties of neutrophils (L. Yang et al., 2004), and the fact that chemotherapy-induced neutropenia was described to be beneficial for the patient (Di Maio et al.,

2005), it becomes more and more evident that neutrophils are key players in tumor progression. In contrast, when neutrophils were depleted one week after tumor cell injection, tumor weight was not affected. Hence, these data suggest that neutrophils are in fact important for tumor progression; however, their presence seems to be of utter importance for the tumor, especially in the beginning. A recent publication revealed that neutrophils from mice with early-stage cancer displayed enhanced migratory behavior and showed elevated metabolic activity, in comparison to control neutrophils (Patel et al., 2018). This further points towards the importance of neutrophils in early tumor disease.

In order to investigate possible ways to interfere with tumor growth, we employed two approaches: we treated tumor-bearing mice with an NLRP3 inhibitor to impair neutrophil trafficking or with CXCR4 or CXCR2 inhibitors in order to interfere with the neutrophil ageing process. Consequently, tumor weight as well as the tumor development rate was assessed. To get a more comprehensive overview, we also investigated tumor infiltration of neutrophils, after mice received these different treatments by using a flow cytometer.

Especially inhibiting the NLRP3 inflammasome resulted in a strong decrease in the tumor weight and slightly diminished the tumor development rate. Data from the multi-channel flow cytometry illustrated that inhibiting the NLRP3 inflammasome lead to a significant reduction of neutrophils in the tumor, thus interfering with the recruitment of neutrophils. Both of these findings further confirmed that the NLRP3 inflammasome is a potential therapeutic target with its involvement in neutrophil trafficking.

Inhibiting CXCR2 also slightly decreased tumor weight, whereas the tumor weight in animals treated with a CXCR4 antagonist was slightly increased. Inhibiting CXCR2 or CXCR4 however, did not cause any significant alteration in neutrophil infiltration into the SCC VII or the 4T1 tumors.

Since we have shown that CXCR2 binding enhanced the aged phenotype of neutrophils, we hypothesized that by inhibiting CXCR2 in tumor-bearing mice, this ageing process is interfered with and thereby less reactive tumor-supporting neutrophils are generated. As binding of CXCR4 was shown to antagonize the ageing process of neutrophils, blocking this receptor leads to a lack of inhibition, thereby creating excessively aged, over-reactive neutrophils (J. M. Adrover et al., 2019). In addition, blocking CXCR4 also inhibits the recruitment of aged neutrophils back to the bone marrow, liver, and spleen (Furze & Rankin, 2008), hence, leading to an increase of aged neutrophils in the circulation. Thus, the tumor has more an even bigger repertoire of excessively ageing neutrophils to support its progression. So overall, we conclude that while the NLRP3 inflammasome is a key regulator in the recruitment of neutrophils, CXCR2 and CXCR4 rather regulates the ageing status of neutrophils than the recruitment of these immune cells itself.

CXCR2 has already gotten a lot of attention in the field of cancer therapeutics. In contrast to our findings, studies have shown to block neutrophil recruitment *via* antagonizing CXCR2 (Jamieson et al., 2012; G. Wang et al., 2016), although one publication demonstrated this recruitment was only transiently reduced and rebounded at later time points (Sody et al., 2019). However, other studies also confirmed that even though reduction in tumor growth was observed in CXCR2^{-/-}

mice, no difference in neutrophil infiltration was observed (Keane, Belperio, Xue, Burdick, & Strieter, 2004), thus, further supporting our findings. Hence, the chemokine receptor seems to play an important part in shaping the phenotype of neutrophils. Accordingly, CXCR2 already is a promising therapeutic target as first clinical trial reported positive results in breast cancer patients (Schott et al., 2017).

5.2.4 The mechanisms excessively ageing neutrophils employ to mediate tumor growth

In the final set of experiments, we sought to gain a deeper understanding how excessively ageing neutrophils support tumor progression and what mechanisms they employ in this context. To this end, expression levels of N1 and N2 phenotype associated molecules were measured *via* multi-channel flow cytometry on neutrophils recruited by the NLRP3 inflammasome to the peritoneal cavity of WT mice. We found that aged neutrophils show higher surface expression levels of molecules that were associated with a pro tumorigenic (N2) phenotype of neutrophils (Liang & Ferrara, 2016; Powell & Huttenlocher, 2016) including the surface expression of NE, MMP-9, VEGF, CCL3, CCL5, and Arg-1 than non-aged neutrophils. This is in line with recent observations demonstrating that neutrophils progressively degranulate and release their protein content (e.g., NE, MMP-9) during ageing in the circulation *via* a CXCR2-dependent mechanism before being ultimately cleared from the bloodstream as ‘exhausted’ neutrophils at the end of their life (Adrover et al., 2020).

By releasing all of these different markers, neutrophils can potentially exhibit various functional properties. In our experiments, SCC VII or 4T1 tumor cells

exposed to supernatants from tumor-primed, excessively ageing neutrophils, tumor cell proliferation was significantly higher as compared to tumor cells exposed to supernatants from neutrophils isolated from healthy mice. We also added a NE inhibitor when we treated the tumor cells with supernatants from tumor-primed neutrophils. This completely diminished the increase in cell proliferation. Several studies have already indicated that this cell proliferation might be enhanced by secreting NE through downregulating IRS-1, a key regulator of PI3K (Houghton et al., 2010). Hence our results confirm the findings from previous studies, and clarifying that excessively ageing neutrophils in cancer support tumor progression through stimulating tumor cell proliferation by NE.

Previously, it has been shown that tumor-associated neutrophils have the ability to support processes such as angiogenesis (Christoffersson et al., 2012; Massena et al., 2015). To this end, we first sought to investigate the effect of tumor-primed neutrophils on endothelial cell proliferation and migration. In our experiments, we did not observe any effects on endothelial cell proliferation or migration in response to supernatants from tumor-primed neutrophils as compared to supernatants from control neutrophils. In addition, we also depleted neutrophils in tumor-bearing mice and analyzed the microvascular architecture of the tumors. We did not observe any differences in the vessel density, the number of branches or the number of junctions between neutrophil-depleted and isotype-control antibody-treated animals, collectively suggesting that in our models, neutrophils do not support tumor angiogenesis. Thus, excessively ageing neutrophils in cancer might be a different subpopulation of neutrophils as compared to the previously described CD49^{high} VEGFR1^{high} CXCR4^{high} neutrophils that were identified to support vascularization of non-vascularized hypoxic tissue (Christoffersson et al.,

2012; Massena et al., 2015) or the MMP9^{high} VEGF^{high} CXCR4^{high} neutrophils that promote angiogenesis in experimental melanoma or fibrosarcoma (Jablonska et al., 2010).

Furthermore, we examined the effect of neutrophils on the presence of T cells in tumors, as previous studies have shown that by releasing Arg-1, neutrophils have the ability to suppress CD8⁺ T cell recruitment (Rodriguez et al., 2004; Rotondo et al., 2009). However, no difference in the numbers of T cells in the tumor, were observed when comparing neutrophil-depleted and isotype-treated tumor mice. Thus, in our model neutrophils do not show any effect on T cell recruitment. A potential reason for this observation might be that the tumors have other pathways substituting for the depleted neutrophils, thereby suppressing CD8⁺ T cell infiltration. For instance, also macrophages have been shown to be sources for Arg-1 and to be implicated in interfering with T cell function (Rodriguez et al., 2003).

6 Conclusion

In conclusion, our data unraveled a previously unknown self-sustaining mechanism of malignant tumors that promotes excessive biological ageing of circulating neutrophils. To this end, tumor-released ligands of the chemokine receptor CXCR2 induce a highly reactive, pro-tumorigenic phenotype in these immune cells. Concomitantly, tumor-released uric acid activates the NLRP3 inflammasome in peritumoral macrophages which, in turn, produce inflammatory mediators attracting excessively ageing neutrophils to the neoplastic lesions. Here, these immune cells stimulate the proliferation of malignant cells by liberating neutrophil elastase, which ultimately promotes tumor growth. Counteracting excessive neutrophil ageing in cancer (by CXCR2 inhibitors) and/or trafficking to malignant tumors (by NLRP3 inflammasome inhibitors) effectively interfered with tumor progression and might therefore provide a promising, already feasible strategy in cancer therapy.

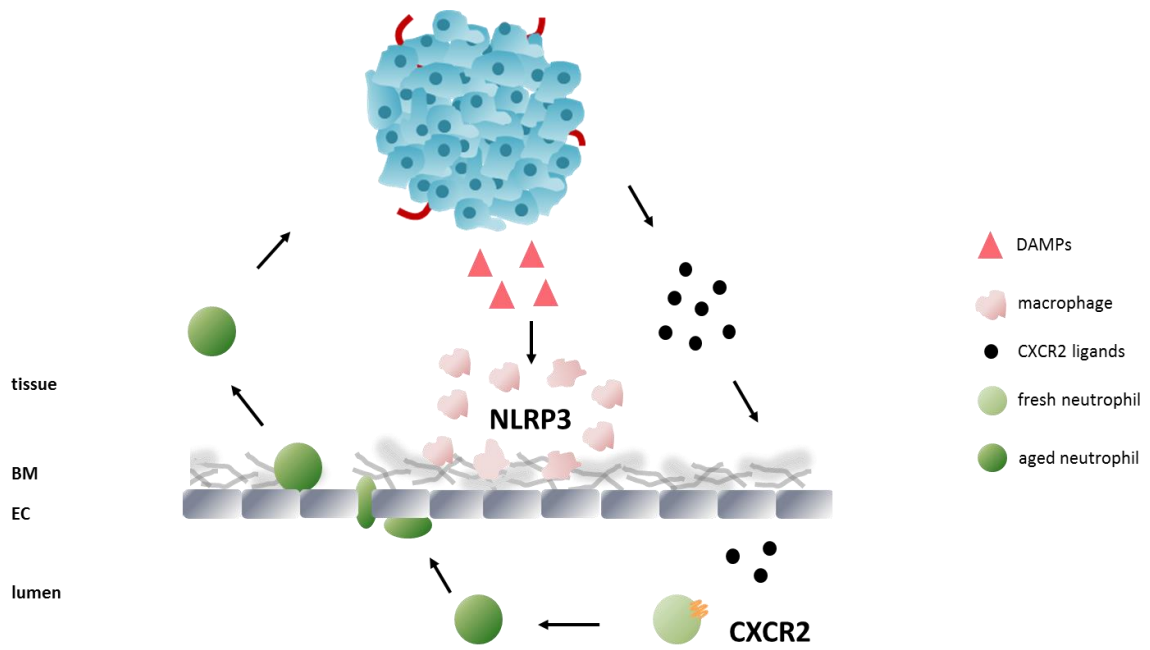


Figure 4.1: Graphical synopsis. A schematic overview on the here identified mechanisms underlying neutrophil trafficking in cancer is shown.

7 Table of figures and tables

Figure 1.1: A schematic overview of the leukocyte adhesion cascade.

Figure 1.2: Neutrophil function within tumor development and progression.

Figure 1.3: Schematic overview of the neutrophil life cycle and their fate in inflammation.

Figure 1.4: Schematic overview of factors driving the biological ageing process in neutrophils.

Figure 1.5: NLRP3 inflammasome complex formation.

Figure 2.1: Experimental protocol to analyze leukocyte trafficking to solid tumors.

Figure 2.2: Experimental protocol to analyze leukocyte subsets present in solid tumors after neutrophil depletion.

Figure 2.3: Experimental protocol to analyze leukocyte subsets in solid tumors after treatment with inhibitors or antagonists.

Figure 2.4: Experimental protocol for intravital imaging of the tumor and its microenvironment.

Figure 2.5: Experimental protocol for *in vivo* imaging of the tumor and its microenvironment.

Figure 2.6: Experimental protocol for adoptive cell transfers.

Figure 2.7: Experimental protocol for IVM of the *M. cremaster*.

Figure 2.8: Experimental protocol for the peritonitis assay.

Figure 3.1: Quantification of cytokines in SCC VII and 4T1 cell culture supernatants as well as solid tumors.

Figure 3.2: Quantification of cytokines in serum samples from SCC VII and 4T1 tumor-bearing mice and healthy controls.

Figure 3.3: Quantitative analysis of aged and non-aged neutrophils in the circulation of healthy control and tumor-bearing mice.

Figure 3.4: Quantification of CXCR4 expression on neutrophils in the circulation of healthy controls and tumor-bearing mice treated with a CXCR2 inhibitor or vehicle.

Figure 3.5: Quantification of the accumulation of adoptively transferred, chronologically aged and non-aged neutrophils in SCC VII and 4T1 tumors and their microenvironment.

Figure 3.6: Quantitative analysis of the composition of different leukocyte subsets in solid SCC VII and 4T1 tumors.

Figure 3.7: Representative confocal microscopy images of SCC VII and 4T1 tumor sections.

Figure 3.8: Quantitative analysis of uric acid and HMGB1 in SCC VII and 4T1 cell culture supernatants.

Figure 3.9: Quantification of leukocyte recruitment to the peritoneal cavity after i.p. exposure of DAMPs.

Figure 3.10: Quantitative analysis of TLR2 and TLR4 activity in reporter cells after stimulation with SCC VII and 4T1 cell culture supernatants.

Figure 3.11: Quantification of IL-1 β in the peritoneal lavage after stimulation with MSU crystals.

Figure 3.12: Quantification of leukocyte recruitment to the peritoneal cavity after injection of inflammasome activating substances.

Figure 3.13: Quantification of integrin expression on aged and non-aged neutrophils.

Figure 3.14: Quantitative analysis of ICAM-1/CD54-Fc binding properties of aged and non-aged neutrophils after stimulation with Alum crystals, PMA, or vehicle.

Figure 3.15: Quantification of the activation of endothelial cells after NLRP3 inflammasome stimulation.

Figure 3.16: Quantification of the activation of endothelial cells after stimulation with DAMPs.

Figure 3.17: Quantification of cytokines after NLRP3 inflammasome activation.

Figure 3.18: Analysis of ICAM-1/CD54 and VCAM-1/CD106 expression on cremasteric endothelial cells after NLRP3 inflammasome activation.

Figure 3.19: Analysis of IVM on the cremaster muscle after 3 h and 6 h of stimulation with Alum crystals.

Figure 3.20: *In vivo* microscopy analysis of neutrophil trafficking in the tumor and its microenvironment.

Figure 3.21: Analysis of the effects of neutrophil depletion in tumor-bearing mice.

Figure 3.22: Quantitative analysis of tumor weight and tumor development after blocking the NLRP3 inflammasome, CXCR2, or CXCR4 in tumor-bearing mice.

Figure 3.23: Quantitative analysis of neutrophil infiltration into tumors after blocking the NLRP3 inflammasome, CXCR2 and CXCR4 in tumor-bearing mice.

Figure 3.24: Quantification of tumor cell proliferation after treatment with Alum crystals, a NLRP3 inhibitor, a CXCR4 inhibitor, or a CXCR2 inhibitor.

Figure 3.25: Quantitative analysis of the expression of N1 and N2 phenotype-associated molecules on aged and non-aged neutrophils.

Figure 3.26: Quantification of tumor cell proliferation after treatment with supernatants from tumor-primed neutrophils.

Figure 3.27: Quantification of microvascular endothelial cell proliferation after treatment with supernatants from tumor-primed neutrophils.

Figure 3.28: Quantification of microvascular endothelial cell migration after treatment with supernatants from tumor-primed neutrophils.

Figure 3.29: Quantitative analysis of the vessel density, the number of branches, and the number of junctions in neutrophil-depleted tumor-bearing mice.

Figure 3.30: Quantitative analysis of CD4⁺ or CD8⁺ T cells in the tumors of neutrophils-depleted mice.

Figure 4.1: Graphical synopsis.

Table 1.1: Molecules associated with the N1 and N2 phenotype of neutrophils.

Table 2.1: Experimental protocol for immunostaining according the different surface markers.

8 References

- A. Baudino, T. (2015). Targeted Cancer Therapy: The Next Generation of Cancer Treatment. *Current Drug Discovery Technologies*, 12(1), 3-20.
- Acharyya, S., Oskarsson, T., Vanharanta, S., Malladi, S., Kim, J., Morris, P. G., Massagué, J. (2012). A CXCL1 paracrine network links cancer chemoresistance and metastasis. *Cell*, 150(1), 165-178.
- Adrover, J. M., Aroca-Crevillén, A., Crainiciuc, G., Ostos, F., Rojas-Vega, Y., Rubio-Ponce, A., Hidalgo, A. (2020). Programmed 'disarming' of the neutrophil proteome reduces the magnitude of inflammation. *Nature Immunology*.
- Adrover, J. M., Del Fresno, C., Crainiciuc, G., Cuartero, M. I., Casanova-Acebes, M., Weiss, L. A., Hidalgo, A. (2019). A Neutrophil Timer Coordinates Immune Defense and Vascular Protection. *Immunity*, 50(2), 390-402 e310.
- Adrover, J. M., Nicolas-Avila, J. A., & Hidalgo, A. (2016). Aging: A Temporal Dimension for Neutrophils. *Trends Immunol*, 37(5), 334-345.
- Almåsbak, H., Aarvak, T., & Vemuri, M. C. (2016). CAR T Cell Therapy: A Game Changer in Cancer Treatment. *Journal of immunology research*, 2016, 5474602-5474602.
- Antonio, N., Bønnelykke-Behrndtz, M. L., Ward, L. C., Collin, J., Christensen, I. J., Steiniche, T., Martin, P. (2015). The wound inflammatory response exacerbates growth of pre-neoplastic cells and progression to cancer. *The EMBO Journal*, 34(17), 2219-2236.
- Arandjelovic, S., & Ravichandran, K. S. (2015). Phagocytosis of apoptotic cells in homeostasis. *Nature Immunology*, 16, 907.
- Arnaout, M. A., Mahalingam, B., & Xiong, J. P. (2005). Integrin structure, allostery, and bidirectional signaling. *Annual Review of Cell and Developmental Biology*, 21(1), 381-410.
- Atzpodien, J., & Reitz, M. (2008). Peripheral Blood Neutrophils as Independent Immunologic Predictor of Response and Long-Term Survival upon

- Immunotherapy in Metastatic Renal-Cell Carcinoma. *Cancer Biotherapy and Radiopharmaceuticals*, 23(1), 129-134.
- Baez, S. (1973). An open cremaster muscle preparation for the study of blood vessels by in vivo microscopy. *Microvascular Research*, 5(3), 384-394.
- Bauernfeind, F. G., Horvath, G., Stutz, A., Alnemri, E. S., MacDonald, K., Speert, D., Latz, E. (2009). Cutting edge: NF-kappaB activating pattern recognition and cytokine receptors license NLRP3 inflammasome activation by regulating NLRP3 expression. *Journal of immunology (Baltimore, Md. : 1950)*, 183(2), 787-791.
- Bekes, E. M., Schweighofer, B., Kupriyanova, T. A., Zajac, E., Ardi, V. C., Quigley, J. P., & Deryugina, E. I. (2011). Tumor-recruited neutrophils and neutrophil TIMP-free MMP-9 regulate coordinately the levels of tumor angiogenesis and efficiency of malignant cell intravasation. *The American journal of pathology*, 179(3), 1455-1470.
- Bellocq, A., Antoine, M., Flahault, A., Philippe, C., Crestani, B., Bernaudin, J. F., Cadranel, J. (1998). Neutrophil alveolitis in bronchioloalveolar carcinoma: induction by tumor-derived interleukin-8 and relation to clinical outcome. *The American journal of pathology*, 152(1), 83-92.
- Ben-Neriah, Y., & Karin, M. (2011). Inflammation meets cancer, with NF- κ B as the matchmaker. *Nature Immunology*, 12, 715.
- Benson, J. R., Jatoi, I., Keisch, M., Esteva, F. J., Makris, A., & Jordan, V. C. (2009). Early breast cancer. *The Lancet*, 373(9673), 1463-1479.
- Bergers, G., Brekken, R., McMahon, G., Vu, T. H., Itoh, T., Tamaki, K., Hanahan, D. (2000). Matrix metalloproteinase-9 triggers the angiogenic switch during carcinogenesis. *Nature cell biology*, 2(10), 737-744.
- Bernier, J., Hall, E. J., & Giaccia, A. (2004). Radiation oncology: a century of achievements. *Nature Reviews Cancer*, 4(9), 737-747.
- Bianchi, M. E. (2007). DAMPs, PAMPs and alarmins: all we need to know about danger. *Journal of Leukocyte Biology*, 81(1), 1-5.
- Bianchi, M. E. (2009). HMGB1 loves company. *Journal of Leukocyte Biology*, 86(3), 573-576.

- Bixel, M. G., Li, H., Petri, B., Khandoga, A. G., Khandoga, A., Zarbock, A., Vestweber, D. (2010). CD99 and CD99L2 act at the same site as, but independently of, PECAM-1 during leukocyte diapedesis. *Blood*, 116(7), 1172-1184.
- Bonilla, F. A., & Oettgen, H. C. (2010). Adaptive immunity. *Journal of Allergy and Clinical Immunology*, 125(2), S33-S40.
- Borregaard, N. (2010). Neutrophils, from Marrow to Microbes. *Immunity*, 33(5), 657-670.
- Bosch, F. X., Manos, M. M., Muñoz, N., Sherman, M., Jansen, A. M., Peto, J., .International Biological Study on Cervical Cancer Study, G. (1995). Prevalence of Human Papillomavirus in Cervical Cancer: a Worldwide Perspective. *JNCI: Journal of the National Cancer Institute*, 87(11), 796-802.
- Bottazzi, B., Doni, A., Garlanda, C., & Mantovani, A. (2010). An Integrated View of Humoral Innate Immunity: Pentraxins as a Paradigm. *Annual Review of Immunology*, 28(1), 157-183.
- Brinkmann, V., Reichard, U., Goosmann, C., Fauler, B., Uhlemann, Y., Weiss, D. S., Zychlinsky, A. (2004). Neutrophil Extracellular Traps Kill Bacteria. *Science*, 303(5663), 1532-1535.
- Bruchard, M., Mignot, G., Derangère, V., Chalmin, F., Chevriaux, A., Végran, F., Ghiringhelli, F. (2012). Chemotherapy-triggered cathepsin B release in myeloid-derived suppressor cells activates the Nlrp3 inflammasome and promotes tumor growth. *Nature Medicine*, 19, 57.
- Burstein, H. J., Lacchetti, C., Anderson, H., Buchholz, T. A., Davidson, N. E., Gelmon, K. A., Griggs, J. J. (2018). Adjuvant Endocrine Therapy for Women With Hormone Receptor–Positive Breast Cancer: ASCO Clinical Practice Guideline Focused Update. *Journal of Clinical Oncology*, 37(5), 423-438.
- Campbell, J. J., Qin, S., Bacon, K. B., Mackay, C. R., & Butcher, E. C. (1996). Biology of chemokine and classical chemoattractant receptors: differential

- requirements for adhesion-triggering versus chemotactic responses in lymphoid cells. *The Journal of cell biology*, 134(1), 255-266.
- Casanova-Acebes, M., Pitaval, C., Weiss, L. A., Nombela-Arrieta, C., Chèvre, R., A-González, N., Hidalgo, A. (2013). Rhythmic modulation of the hematopoietic niche through neutrophil clearance. *Cell*, 153(5), 1025-1035.
- Cassatella, M. A. (1999). Neutrophil-Derived Proteins: Selling Cytokines by the Pound. In F. J. Dixon (Ed.), *Advances in Immunology* (Vol. 73, pp. 369-509): Academic Press.
- Chaplin, D. D. (2010). Overview of the immune response. *J Allergy Clin Immunol*, 125(2 Suppl 2), S3-23.
- Chavez, J. C., Bachmeier, C., & Kharfan-Dabaja, M. A. (2019). CAR T-cell therapy for B-cell lymphomas: clinical trial results of available products. *Therapeutic advances in hematology*, 10, 2040620719841581-2040620719841581.
- Cheretakis, C., Leung, R., Sun, C. X., Dror, Y., & Glogauer, M. (2006). Timing of neutrophil tissue repopulation predicts restoration of innate immune protection in a murine bone marrow transplantation model. *Blood*, 108(8), 2821-2826.
- Christoffersson, G., Vagesjo, E., Vandooren, J., Liden, M., Massena, S., Reinert, R. B., Phillipson, M. (2012). VEGF-A recruits a proangiogenic MMP-9-delivering neutrophil subset that induces angiogenesis in transplanted hypoxic tissue. *Blood*, 120(23), 4653-4662.
- Circelli, L., Tornesello, M., Buonaguro, F. M., & Buonaguro, L. (2017). Use of adjuvants for immunotherapy. *Human vaccines & immunotherapeutics*, 13(8), 1774-1777.
- Coffelt, S. B., Wellenstein, M. D., & de Visser, K. E. (2016). Neutrophils in cancer: neutral no more. *Nat Rev Cancer*, 16(7), 431-446.
- Cooper, M. D., & Alder, M. N. (2006). The Evolution of Adaptive Immune Systems. *Cell*, 124(4), 815-822.
- Coussens, L. M., Tinkle, C. L., Hanahan, D., & Werb, Z. (2000). MMP-9 supplied by bone marrow-derived cells contributes to skin carcinogenesis. *Cell*, 103(3), 481-490.

- Di Maio, M., Gridelli, C., Gallo, C., Shepherd, F., Piantedosi, F. V., Cigolari, S., Perrone, F. (2005). Chemotherapy-induced neutropenia and treatment efficacy in advanced non-small-cell lung cancer: a pooled analysis of three randomised trials. *The Lancet Oncology*, 6(9), 669-677.
- Dinarello, C. A. (2006). Interleukin 1 and interleukin 18 as mediators of inflammation and the aging process. *The American Journal of Clinical Nutrition*, 83(2), 447S-455S.
- Dumitru, C. A., Moses, K., Trellakis, S., Lang, S., & Brandau, S. (2012). Neutrophils and granulocytic myeloid-derived suppressor cells: immunophenotyping, cell biology and clinical relevance in human oncology. *Cancer Immunology, Immunotherapy*, 61(8), 1155-1167.
- Dvorak. (1986). Tumors: wounds that do not heal.
- Eash, K. J., Means, J. M., White, D. W., & Link, D. C. (2009). CXCR4 is a key regulator of neutrophil release from the bone marrow under basal and stress granulopoiesis conditions. *Blood*, 113(19), 4711-4719.
- Egeblad, M., Nakasone, E. S., & Werb, Z. (2010). Tumors as organs: complex tissues that interface with the entire organism. *Developmental cell*, 18(6), 884-901.
- Eruslanov, E. B., Bhojnarwala, P. S., Quatromoni, J. G., Stephen, T. L., Ranganathan, A., Deshpande, C., Singhal, S. (2014). Tumor-associated neutrophils stimulate T cell responses in early-stage human lung cancer. *The Journal of clinical investigation*, 124(12), 5466-5480.
- Fabian, C. J. (2007). The what, why and how of aromatase inhibitors: hormonal agents for treatment and prevention of breast cancer. *International journal of clinical practice*, 61(12), 2051-2063.
- Farkona, S., Diamandis, E. P., & Blasutig, I. M. (2016). Cancer immunotherapy: the beginning of the end of cancer? *BMC Medicine*, 14(1), 73.
- Foell, D., Wittkowski, H., Vogl, T., & Roth, J. (2007). S100 proteins expressed in phagocytes: a novel group of damage-associated molecular pattern molecules. *Journal of Leukocyte Biology*, 81(1), 28-37.

- Ford, D., Easton, D. F., Stratton, M., Narod, S., Goldgar, D., Devilee, P., Zelada-Hedman, M. (1998). Genetic Heterogeneity and Penetrance Analysis of the BRCA1 and BRCA2 Genes in Breast Cancer Families. *The American Journal of Human Genetics*, 62(3), 676-689.
- Forthal, D. N. (2014). Functions of Antibodies. *Microbiology spectrum*, 2(4), 1-17.
- Franchi, L., Eigenbrod, T., & Núñez, G. (2009). Cutting edge: TNF-alpha mediates sensitization to ATP and silica via the NLRP3 inflammasome in the absence of microbial stimulation. *Journal of immunology (Baltimore, Md. : 1950)*, 183(2), 792-796.
- Fridlender, Z. G., Sun, J., Kim, S., Kapoor, V., Cheng, G., Ling, L., Albelda, S. M. (2009). Polarization of tumor-associated neutrophil phenotype by TGF-beta: "N1" versus "N2" TAN. *Cancer Cell*, 16(3), 183-194.
- Furze, R. C., & Rankin, S. M. (2008). Neutrophil mobilization and clearance in the bone marrow. *Immunology*, 125(3), 281-288.
- Gallucci, S., & Matzinger, P. (2001). Danger signals: SOS to the immune system. *Current Opinion in Immunology*, 13(1), 114-119.
- Gasparoto, T. H., de Oliveira, C. E., de Freitas, L. T., Pinheiro, C. R., Hori, J. I., Garlet, G. P., Campanelli, A. P. (2014). Inflammasome activation is critical to the protective immune response during chemically induced squamous cell carcinoma. *PLoS One*, 9(9), e107170.
- Gaudry, M., Brégerie, O., Andrieu, V., El Benna, J., Pocard, M.-A., & Hakim, J. (1997). Intracellular Pool of Vascular Endothelial Growth Factor in Human Neutrophils. *Blood*, 90(10), 4153-4161.
- Gebhardt, C., Németh, J., Angel, P., & Hess, J. (2006). S100A8 and S100A9 in inflammation and cancer. *Biochemical Pharmacology*, 72(11), 1622-1631.
- Geering, B., Stoeckle, C., Conus, S., & Simon, H.-U. (2013). Living and dying for inflammation: neutrophils, eosinophils, basophils. *Trends in Immunology*, 34(8), 398-409.
- Gentles, A. J., Newman, A. M., Liu, C. L., Bratman, S. V., Feng, W., Kim, D., Alizadeh, A. A. (2015). The prognostic landscape of genes and infiltrating immune cells across human cancers. *Nat Med*, 21(8), 938-945.

- Ghoncheh, M., Pournamdar, Z., & Salehiniya, H. (2016). Incidence and Mortality and Epidemiology of Breast Cancer in the World. *Asian Pacific Journal of Cancer Prevention*, 17(S3), 43-46.
- Gillison, M. L., Broutian, T., Pickard, R. K. L., Tong, Z.-y., Xiao, W., Kahle, L., Chaturvedi, A. K. (2012). Prevalence of oral HPV infection in the United States, 2009-2010. *JAMA*, 307(7), 693-703.
- Grivennikov, S. I., Greten, F. R., & Karin, M. (2010). Immunity, inflammation, and cancer. *Cell*, 140(6), 883-899.
- Häger, M., Cowland, J. B., & Borregaard, N. (2010). Neutrophil granules in health and disease. *Journal of Internal Medicine*, 268(1), 25-34.
- Halle, A., Hornung, V., Petzold, G. C., Stewart, C. R., Monks, B. G., Reinheckel, T., Golenbock, D. T. (2008). The NALP3 inflammasome is involved in the innate immune response to amyloid-beta. *Nature Immunology*, 9(8), 857-865.
- Hanahan, D., & Weinberg, R. A. (2000). The Hallmarks of Cancer. *Cell*, 100(1), 57-70.
- Hanahan, D., & Weinberg, Robert A. (2011). Hallmarks of Cancer: The Next Generation. *Cell*, 144(5), 646-674.
- Harding, J., Burtness, B. (2005). Cetuximab: An epidermal growth factor receptor chimeric human-murine monoclonal antibody. *Drugs Today*, 41(2), 1.
- He, Y., Hara, H., & Núñez, G. (2016). Mechanism and Regulation of NLRP3 Inflammasome Activation. *Trends in biochemical sciences*, 41(12), 1012-1021.
- Hernandez, C., Huebener, P., & Schwabe, R. F. (2016). Damage-associated molecular patterns in cancer: a double-edged sword. *Oncogene*, 35(46), 5931-5941.
- Hidalgo, A., Peired, A. J., Wild, M., Vestweber, D., & Frenette, P. S. (2007). Complete identification of E-selectin ligands on neutrophils reveals distinct functions of PSGL-1, ESL-1, and CD44. *Immunity*, 26(4), 477-489.

- Hodi, F. S., O'Day, S. J., McDermott, D. F., Weber, R. W., Sosman, J. A., Haanen, J. B., Urban, W. J. (2010). Improved survival with ipilimumab in patients with metastatic melanoma. *The New England journal of medicine*, 363(8), 711-723.
- Hornung, V., Bauernfeind, F., Halle, A., Samstad, E. O., Kono, H., Rock, K. L., Latz, E. (2008). Silica crystals and aluminum salts activate the NALP3 inflammasome through phagosomal destabilization. *Nat Immunol*, 9(8), 847-856.
- Houghton, A. M., Rzymkiewicz, D. M., Ji, H., Gregory, A. D., Egea, E. E., Metz, H. E., Shapiro, S. D. (2010). Neutrophil elastase-mediated degradation of IRS-1 accelerates lung tumor growth. *Nat Med*, 16(2), 219-223.
- Huang, C. F., Chen, L., Li, Y. C., Wu, L., Yu, G. T., Zhang, W. F., & Sun, Z. J. (2017). NLRP3 inflammasome activation promotes inflammation-induced carcinogenesis in head and neck squamous cell carcinoma. *J Exp Clin Cancer Res*, 36(1), 116.
- Ishida, Y., Agata, Y., Shibahara, K., & Honjo, T. (1992). Induced expression of PD-1, a novel member of the immunoglobulin gene superfamily, upon programmed cell death. *The EMBO journal*, 11(11), 3887-3895.
- Iwasaki, A., & Medzhitov, R. (2004). Toll-like receptor control of the adaptive immune responses. *Nature Immunology*, 5, 987.
- Iwasaki, A., & Medzhitov, R. (2010). Regulation of adaptive immunity by the innate immune system. *Science*, 327(5963), 291-295.
- Jablonska, J., Leschner, S., Westphal, K., Lienenklaus, S., & Weiss, S. (2010). Neutrophils responsive to endogenous IFN- β regulate tumor angiogenesis and growth in a mouse tumor model. *The Journal of clinical investigation*, 120(4), 1151-1164.
- Jamieson, T., Clarke, M., Steele, C. W., Samuel, M. S., Neumann, J., Jung, A., Sansom, O. J. (2012). Inhibition of CXCR2 profoundly suppresses inflammation-driven and spontaneous tumorigenesis. *The Journal of clinical investigation*, 122(9), 3127-3144.

- Jensen, T. O., Schmidt, H., Møller, H. J., Donskov, F., Høyer, M., Sjoegren, P., Steiniche, T. (2012). Intratumoral neutrophils and plasmacytoid dendritic cells indicate poor prognosis and are associated with pSTAT3 expression in AJCC stage I/II melanoma. *Cancer*, 118(9), 2476-2485.
- Jin, L., Yuan, R. Q., Fuchs, A., Yao, Y., Joseph, A., Schwall, R., Rosen, E. M. (1997). Expression of interleukin-1 β in human breast carcinoma. *Cancer*, 80(3), 421-434.
- Jo, E. K., Kim, J. K., Shin, D. M., & Sasakawa, C. (2016). Molecular mechanisms regulating NLRP3 inflammasome activation. *Cell Mol Immunol*, 13(2), 148-159.
- Kanneganti, T.-D., Lamkanfi, M., & Núñez, G. (2007). Intracellular NOD-like Receptors in Host Defense and Disease. *Immunity*, 27(4), 549-559.
- Kansas, G. (1996). Selectins and their ligands: current concepts and controversies. *Blood*, 88(9), 3259-3287.
- Karsten, E., Breen, E., & Herbert, B. R. (2018). Red blood cells are dynamic reservoirs of cytokines. *Scientific reports*, 8(1), 3101-3101.
- Keane, M. P., Belperio, J. A., Xue, Y. Y., Burdick, M. D., & Strieter, R. M. (2004). Depletion of CXCR2 Inhibits Tumor Growth and Angiogenesis in a Murine Model of Lung Cancer. *The Journal of Immunology*, 172(5), 2853.
- Keir, M. E., Butte, M. J., Freeman, G. J., & Sharpe, A. H. (2008). PD-1 and Its Ligands in Tolerance and Immunity. *Annual Review of Immunology*, 26(1), 677-704.
- Kennedy, A. D., & DeLeo, F. R. (2009). Neutrophil apoptosis and the resolution of infection. *Immunol Res*, 43(1-3), 25-61.
- Ketelut-Carneiro, N., Silva, G. K., Rocha, F. A., Milanezi, C. M., Cavalcanti-Neto, F. F., Zamboni, D. S., & Silva, J. S. (2015). IL-18 Triggered by the Nlrp3 Inflammasome Induces Host Innate Resistance in a Pulmonary Model of Fungal Infection. *The Journal of Immunology*, 194(9), 4507-4517.
- Key, T. J., Verkasalo, P. K., & Banks, E. (2001). Epidemiology of breast cancer. *The Lancet Oncology*, 2(3), 133-140.

- King, M.-C., Marks, J. H., & Mandell, J. B. (2003). Breast and Ovarian Cancer Risks Due to Inherited Mutations in *BRCA1* and *BRCA2*. *Science*, 302(5645), 643.
- Knaapen, A. M., Güngör, N., Schins, R. P. F., Borm, P. J. A., & Van Schooten, F. J. (2006). Neutrophils and respiratory tract DNA damage and mutagenesis: a review. *Mutagenesis*, 21(4), 225-236.
- Kolaczowska, E., & Kubes, P. (2013). Neutrophil recruitment and function in health and inflammation. *Nature reviews. Immunology*, 13(3), 159-175.
- Kreuzaler, P., & Watson, C. J. (2012). Killing a cancer: what are the alternatives? *Nature Reviews Cancer*, 12, 411.
- Krombach, J., Hennel, R., Brix, N., Orth, M., Schoetz, U., Ernst, A., Lauber, K. (2019). Priming anti-tumor immunity by radiotherapy: Dying tumor cell-derived DAMPs trigger endothelial cell activation and recruitment of myeloid cells. *Oncoimmunology*, 8(1), e1523097.
- Lamkanfi, M., & Dixit, Vishva M. (2014). Mechanisms and Functions of Inflammasomes. *Cell*, 157(5), 1013-1022.
- Latz, E., Xiao, T. S., & Stutz, A. (2013). Activation and regulation of the inflammasomes. *Nature reviews. Immunology*, 13(6), 397-411.
- Lawrence, M. B., Kansas, G. S., Kunkel, E. J., & Ley, K. (1997). Threshold levels of fluid shear promote leukocyte adhesion through selectins (CD62L,P,E). *The Journal of cell biology*, 136(3), 717-727.
- Leach, D. R., Krummel, M. F., & Allison, J. P. (1996). Enhancement of Antitumor Immunity by CTLA-4 Blockade. *Science*, 271(5256), 1734.
- LeBert, D. C., Squirrell, J. M., Rindy, J., Broadbridge, E., Lui, Y., Zakrzewska, A., Huttenlocher, A. (2015). Matrix metalloproteinase 9 modulates collagen matrices and wound repair. *Development (Cambridge, England)*, 142(12), 2136-2146.
- LeBien, T. W., & Tedder, T. F. (2008). B lymphocytes: how they develop and function. *Blood*, 112(5), 1570-1580.

- Lechner, M. G., Karimi, S. S., Barry-Holson, K., Angell, T. E., Murphy, K. A., Church, C. H., Epstein, A. L. (2013). Immunogenicity of murine solid tumor models as a defining feature of in vivo behavior and response to immunotherapy. *Journal of immunotherapy (Hagerstown, Md. : 1997)*, 36(9), 477-489.
- Ley, K., Laudanna, C., Cybulsky, M. I., & Nourshargh, S. (2007). Getting to the site of inflammation: the leukocyte adhesion cascade updated. *Nature reviews. Immunology*, 7(9), 678-689.
- Liang, W., & Ferrara, N. (2016). The Complex Role of Neutrophils in Tumor Angiogenesis and Metastasis. *Cancer Immunol Res*, 4(2), 83-91.
- Lieschke, G. J., Grail, D., Hodgson, G., Metcalf, D., Stanley, E., Cheers, C., Dunn, A. R. (1994). Mice lacking granulocyte colony-stimulating factor have chronic neutropenia, granulocyte and macrophage progenitor cell deficiency, and impaired neutrophil mobilization. *Blood*, 84(6), 1737.
- Ljunggren, H.-G., & Kärre, K. (1990). In search of the 'missing self': MHC molecules and NK cell recognition. *Immunology Today*, 11, 237-244.
- Luan, J., Shattuck-Brandt, R., Haghnegahdar, H., Owen, J. D., Strieter, R., Burdick, M., Richmond, A. (1997). Mechanism and biological significance of constitutive expression of MGSA/GRO chemokines in malignant melanoma tumor progression. *Journal of Leukocyte Biology*, 62(5), 588-597.
- Maas, S. L., Soehnlein, O., & Viola, J. R. (2018). Organ-Specific Mechanisms of Transendothelial Neutrophil Migration in the Lung, Liver, Kidney, and Aorta. *Frontiers in Immunology*, 9(2739).
- Mackey, J. B. G., Coffelt, S. B., & Carlin, L. M. (2019). Neutrophil Maturity in Cancer. *Frontiers in Immunology*, 10(1912).
- Makki, J. (2015). Diversity of Breast Carcinoma: Histological Subtypes and Clinical Relevance. *Clinical medicine insights. Pathology*, 8, 23-31.
- Mantovani, A. (2018). The inflammation – cancer connection. *The FEBS Journal*, 285(4), 638-640.
- Martin, C., Burdon, P. C. E., Bridger, G., Gutierrez-Ramos, J.-C., Williams, T. J., & Rankin, S. M. (2003). Chemokines Acting via CXCR2 and CXCR4 Control

- the Release of Neutrophils from the Bone Marrow and Their Return following Senescence. *Immunity*, 19(4), 583-593.
- Martinon, F., Mayor, A., & Tschopp, J. (2009). The Inflammasomes: Guardians of the Body. *Annual Review of Immunology*, 27(1), 229-265.
- Martinon, F., Pétrilli, V., Mayor, A., Tardivel, A., & Tschopp, J. (2006). Gout-associated uric acid crystals activate the NALP3 inflammasome. *Nature*, 440(7081), 237-241.
- Marur, S., & Forastiere, A. A. (2008). Head and Neck Cancer: Changing Epidemiology, Diagnosis, and Treatment. *Mayo Clinic Proceedings*, 83(4), 489-501.
- Massena, S., Christoffersson, G., Vågesjö, E., Seignez, C., Gustafsson, K., Binet, F., Phillipson, M. (2015). Identification and characterization of VEGF-A-responsive neutrophils expressing CD49d, VEGFR1, and CXCR4 in mice and humans. *Blood*, 126(17), 2016-2026.
- Matzinger, P. (2002). The Danger Model: A Renewed Sense of Self. *Science*, 296(5566), 301-305.
- Mayadas, T. N., Cullere, X., & Lowell, C. A. (2014). The Multifaceted Functions of Neutrophils. *Annual Review of Pathology: Mechanisms of Disease*, 9(1), 181-218.
- McDonald, B., Pittman, K., Menezes, G. B., Hirota, S. A., Slaba, I., Waterhouse, C. C. M., Kubes, P. (2010). Intravascular Danger Signals Guide Neutrophils to Sites of Sterile Inflammation. *Science*, 330(6002), 362-366.
- McEver, R. P., & Cummings, R. D. (1997). Perspectives series: cell adhesion in vascular biology. Role of PSGL-1 binding to selectins in leukocyte recruitment. *The Journal of clinical investigation*, 100(3), 485-491.
- McKaig, R. G., Baric, R. S., & Olshan, A. F. (1998). Human Papillomavirus and head and neck cancer: Epidemiology and molecular biology. *Head & Neck*, 20(3), 250-265.
- McPherson, K., Steel, C. M., & Dixon, J. M. (2000). Breast cancer—epidemiology, risk factors, and genetics. *BMJ*, 321(7261), 624.

- Medzhitov, R., & Janeway, C. (2000). Innate Immunity. *New England Journal of Medicine*, 343(5), 338-344.
- Medzhitov, R., & Janeway, C. A. (2002). Decoding the Patterns of Self and Nonself by the Innate Immune System. *Science*, 296(5566), 298-300.
- Mócsai, A., Ruland, J., & Tybulewicz, V. L. J. (2010). The SYK tyrosine kinase: a crucial player in diverse biological functions. *Nature reviews. Immunology*, 10(6), 387-402.
- Mogensen, T. H. (2009). Pathogen recognition and inflammatory signaling in innate immune defenses. *Clin Microbiol Rev*, 22(2), 240-273, Table of Contents.
- Muller, W. A., Weigl, S. A., Deng, X., & Phillips, D. M. (1993). PECAM-1 is required for transendothelial migration of leukocytes. *The Journal of experimental medicine*, 178(2), 449-460.
- Nicolas-Avila, J. A., Adrover, J. M., & Hidalgo, A. (2017). Neutrophils in Homeostasis, Immunity, and Cancer. *Immunity*, 46(1), 15-28.
- Nourshargh, S., & Alon, R. (2014). Leukocyte migration into inflamed tissues. *Immunity*, 41(5), 694-707.
- Nourshargh, S., Hordijk, P. L., & Sixt, M. (2010). Breaching multiple barriers: leukocyte motility through venular walls and the interstitium. *Nat Rev Mol Cell Biol*, 11(5), 366-378.
- Nourshargh, S., Krombach, F., & Dejana, E. (2006). The role of JAM-A and PECAM-1 in modulating leukocyte infiltration in inflamed and ischemic tissues. *Journal of Leukocyte Biology*, 80(4), 714-718.
- Nozawa, H., Chiu, C., & Hanahan, D. (2006). Infiltrating neutrophils mediate the initial angiogenic switch in a mouse model of multistage carcinogenesis. *Proceedings of the National Academy of Sciences*, 103(33), 12493-12498.
- Ozaki, E., Campbell, M., & Doyle, S. L. (2015). Targeting the NLRP3 inflammasome in chronic inflammatory diseases: current perspectives. *Journal of inflammation research*, 8, 15-27.

- Pardoll, D. M., & Topalian, S. L. (1998). The role of CD4+ T cell responses in antitumor immunity. *Current Opinion in Immunology*, 10(5), 588-594.
- Parkin, J., & Cohen, B. (2001). An overview of the immune system. *The Lancet*, 357(9270), 1777-1789.
- Patel, S., Fu, S., Mastio, J., Dominguez, G. A., Purohit, A., Kossenkov, A., Gabrilovich, D. I. (2018). Unique pattern of neutrophil migration and function during tumor progression. *Nature Immunology*, 19(11), 1236-1247.
- Phillipson, M., Heit, B., Colarusso, P., Liu, L., Ballantyne, C. M., & Kubes, P. (2006). Intraluminal crawling of neutrophils to emigration sites: a molecularly distinct process from adhesion in the recruitment cascade. *The Journal of experimental medicine*, 203(12), 2569-2575.
- Pichlmair, A., & Reis e Sousa, C. (2007). Innate Recognition of Viruses. *Immunity*, 27(3), 370-383.
- Pieper, K., Grimbacher, B., & Eibel, H. (2013). B-cell biology and development. *Journal of Allergy and Clinical Immunology*, 131(4), 959-971.
- Pillay, J., den Braber, I., Vrisekoop, N., Kwast, L. M., de Boer, R. J., Borghans, J. A. M., Koenderman, L. (2010). In vivo labeling with H2O2 reveals a human neutrophil lifespan of 5.4 days. *Blood*, 116(4), 625-627.
- Plosker, G. L., & Keam, S. J. (2006). Trastuzumab. *Drugs*, 66(4), 449-475.
- Powell, D. R., & Huttenlocher, A. (2016). Neutrophils in the Tumor Microenvironment. *Trends Immunol*, 37(1), 41-52.
- Rao, H.-L., Chen, J.-W., Li, M., Xiao, Y.-B., Fu, J., Zeng, Y.-X., Xie, D. (2012). Increased intratumoral neutrophil in colorectal carcinomas correlates closely with malignant phenotype and predicts patients' adverse prognosis. *PloS one*, 7(1), e30806-e30806.
- Ribas, A., Shin, D. S., Zaretsky, J., Frederiksen, J., Cornish, A., Avramis, E., Comin-Anduix, B. (2016). PD-1 Blockade Expands Intratumoral Memory T Cells. *Cancer Immunol Res*, 4(3), 194-203.
- Rodriguez, P. C., Quiceno, D. G., Zabaleta, J., Ortiz, B., Zea, A. H., Piazuelo, M. B., Ochoa, A. C. (2004). Arginase I Production in the Tumor

- Microenvironment by Mature Myeloid Cells Inhibits T-Cell Receptor Expression and Antigen-Specific T-Cell Responses. *Cancer Research*, 64(16), 5839.
- Rodriguez, P. C., Zea, A. H., DeSalvo, J., Culotta, K. S., Zabaleta, J., Quiceno, D. G., Ochoa, A. C. (2003). Arginine Consumption by Macrophages Modulates the Expression of CD3 ζ Chain in T Lymphocytes. *The Journal of Immunology*, 171(3), 1232-1239.
- Rotondo, R., Barisione, G., Mastracci, L., Grossi, F., Orengo, A. M., Costa, R., Barbieri, O. (2009). IL-8 induces exocytosis of arginase 1 by neutrophil polymorphonuclears in nonsmall cell lung cancer. *International Journal of Cancer*, 125(4), 887-893.
- Sakuishi, K., Apetoh, L., Sullivan, J. M., Blazar, B. R., Kuchroo, V. K., & Anderson, A. C. (2010). Targeting Tim-3 and PD-1 pathways to reverse T cell exhaustion and restore anti-tumor immunity. *The Journal of experimental medicine*, 207(10), 2187-2194.
- Salama, I., Malone, P. S., Mihaimed, F., & Jones, J. L. (2008). A review of the S100 proteins in cancer. *European Journal of Surgical Oncology*, 34(4), 357-364.
- Salic, A., & Mitchison, T. J. (2008). A chemical method for fast and sensitive detection of DNA synthesis in vivo. *Proceedings of the National Academy of Sciences of the United States of America*, 105(7), 2415-2420.
- Sallah, S., Wan, J. Y., & Nguyen, N. P. (2002). Venous Thrombosis in Patients with Solid Tumors: Determination of Frequency and Characteristics. *Thromb Haemost*, 87(04), 575-579.
- Sawanobori, Y., Ueha, S., Kurachi, M., Shimaoka, T., Talmadge, J. E., Abe, J., Matsushima, K. (2008). Chemokine-mediated rapid turnover of myeloid-derived suppressor cells in tumor-bearing mice. *Blood*, 111(12), 5457-5466.
- Schindelin, J., Arganda-Carreras, I., Frise, E., Kaynig, V., Longair, M., Pietzsch, T., Cardona, A. (2012). Fiji: an open-source platform for biological-image analysis. *Nature Methods*, 9, 676.

- Schmid-Burgk, J. L., Gaidt, M. M., Schmidt, T., Ebert, T. S., Bartok, E., & Hornung, V. (2015). Caspase-4 mediates non-canonical activation of the NLRP3 inflammasome in human myeloid cells. *European Journal of Immunology*, *45*(10), 2911-2917.
- Schmidt, H., Bastholt, L., Geertsen, P., Christensen, I. J., Larsen, S., Gehl, J., & von der Maase, H. (2005). Elevated neutrophil and monocyte counts in peripheral blood are associated with poor survival in patients with metastatic melanoma: a prognostic model. *British journal of cancer*, *93*(3), 273-278.
- Schott, A. F., Goldstein, L. J., Cristofanilli, M., Ruffini, P. A., McCanna, S., Reuben, J. M., Wicha, M. (2017). Phase Ib Pilot Study to Evaluate Reparixin in Combination with Weekly Paclitaxel in Patients with HER-2–Negative Metastatic Breast Cancer. *Clinical Cancer Research*, *23*(18), 5358-5365.
- Schymeinsky, J., Then, C., & Walzog, B. (2005). The non-receptor tyrosine kinase Syk regulates lamellipodium formation and site-directed migration of human leukocytes. *Journal of Cellular Physiology*, *204*(2), 614-622.
- Shen, M., Hu, P., Donskov, F., Wang, G., Liu, Q., & Du, J. (2014). Tumor-associated neutrophils as a new prognostic factor in cancer: a systematic review and meta-analysis. *PloS one*, *9*(6), e98259-e98259.
- Shewach, D. S., & Kuchta, R. D. (2009). Introduction to Cancer Chemotherapeutics. *Chemical Reviews*, *109*(7), 2859-2861.
- Shi, Y., Mucsi, A. D., & Ng, G. (2010). Monosodium urate crystals in inflammation and immunity. *Immunological Reviews*, *233*(1), 203-217.
- Silvestre-Roig, C., Hidalgo, A., & Soehnlein, O. (2016). Neutrophil heterogeneity: implications for homeostasis and pathogenesis. *Blood*, *127*(18), 2173-2181.
- Sody, S., Uddin, M., Grüneboom, A., Görgens, A., Giebel, B., Gunzer, M., & Brandau, S. (2019). Distinct Spatio-Temporal Dynamics of Tumor-Associated Neutrophils in Small Tumor Lesions. *Frontiers in Immunology*, *10*(1419).

- Soehnlein, O., Steffens, S., Hidalgo, A., & Weber, C. (2017). Neutrophils as protagonists and targets in chronic inflammation. *Nature reviews. Immunology*, 17(4), 248-261.
- Sperandio, M. (2006). Selectins and glycosyltransferases in leukocyte rolling in vivo. *The FEBS Journal*, 273(19), 4377-4389.
- Sperandio, M., Smith, M. L., Forlow, S. B., Olson, T. S., Xia, L., McEver, R. P., & Ley, K. (2003). P-selectin glycoprotein ligand-1 mediates L-selectin-dependent leukocyte rolling in venules. *The Journal of experimental medicine*, 197(10), 1355-1363.
- Srikrishna, G., & Freeze, H. H. (2009). Endogenous damage-associated molecular pattern molecules at the crossroads of inflammation and cancer. *Neoplasia (New York, N.Y.)*, 11(7), 615-628.
- Stark, M. A., Huo, Y., Burcin, T. L., Morris, M. A., Olson, T. S., & Ley, K. (2005). Phagocytosis of apoptotic neutrophils regulates granulopoiesis via IL-23 and IL-17. *Immunity*, 22(3), 285-294.
- Sturgis, E. M., & Cinciripini, P. M. (2007). Trends in head and neck cancer incidence in relation to smoking prevalence. *Cancer*, 110(7), 1429-1435.
- Sylvester, P. W. (2011). Optimization of the Tetrazolium Dye (MTT) Colorimetric Assay for Cellular Growth and Viability. In S. D. Satyanarayanajois (Ed.), *Drug Design and Discovery: Methods and Protocols* (pp. 157-168). Totowa, NJ: Humana Press.
- Takeda, K., & Akira, S. (2005). Toll-like receptors in innate immunity. *International Immunology*, 17(1), 1-14.
- Templeton, A. J., McNamara, M. G., Seruga, B., Vera-Badillo, F. E., Aneja, P., Ocana, A., Amir, E. (2014). Prognostic role of neutrophil-to-lymphocyte ratio in solid tumors: a systematic review and meta-analysis. *J Natl Cancer Inst*, 106(6), dju124.
- Ting, J. P. Y., Lovering, R. C., Alnemri, E. S., Bertin, J., Boss, J. M., Davis, B. K., Ward, P. A. (2008). The NLR gene family: a standard nomenclature. *Immunity*, 28(3), 285-287.

- Topalian, S. L., Hodi, F. S., Brahmer, J. R., Gettinger, S. N., Smith, D. C., McDermott, D. F., Sznol, M. (2012). Safety, activity, and immune correlates of anti-PD-1 antibody in cancer. *The New England journal of medicine*, 366(26), 2443-2454.
- Trellakis, S., Bruderek, K., Dumitru, C. A., Gholaman, H., Gu, X., Bankfalvi, A., . . . Brandau, S. (2011). Polymorphonuclear granulocytes in human head and neck cancer: enhanced inflammatory activity, modulation by cancer cells and expansion in advanced disease. *Int J Cancer*, 129(9), 2183-2193.
- Trellakis, S., Bruderek, K., Dumitru, C. A., Gholaman, H., Gu, X., Bankfalvi, A., Brandau, S. (2011). Polymorphonuclear granulocytes in human head and neck cancer: Enhanced inflammatory activity, modulation by cancer cells and expansion in advanced disease. *International Journal of Cancer*, 129(9), 2183-2193.
- Triebel, F., Jitsukawa, S., Baixeras, E., Roman-Roman, S., Genevee, C., Viegas-Pequignot, E., & Hercend, T. (1990). LAG-3, a novel lymphocyte activation gene closely related to CD4. *The Journal of experimental medicine*, 171(5), 1393-1405.
- Tschopp, J., & Schroder, K. (2010). NLRP3 inflammasome activation: The convergence of multiple signalling pathways on ROS production? *Nature reviews. Immunology*, 10(3), 210-215.
- Ueda, Y., Cain, D. W., Kuraoka, M., Kondo, M., & Kelsoe, G. (2009). IL-1R type I-dependent hemopoietic stem cell proliferation is necessary for inflammatory granulopoiesis and reactive neutrophilia. *Journal of immunology (Baltimore, Md. : 1950)*, 182(10), 6477-6484.
- Uhl, B., Vadlau, Y., Zuchtriegel, G., Nekolla, K., Sharaf, K., Gaertner, F., Reichel, C. A. (2016). Aged neutrophils contribute to the first line of defense in the acute inflammatory response. *Blood*, 128(19), 2327-2337.
- Uribe-Querol, E., & Rosales, C. (2015). Neutrophils in Cancer: Two Sides of the Same Coin. *Journal of immunology research*, 2015, 983698.

- Urruticoechea, A., Alemany, R., Balart, J., Villanueva, A., Vinals, F., & Capella, G. (2010). Recent Advances in Cancer Therapy: An Overview. *Current Pharmaceutical Design*, 16(1), 3-10.
- Vigneswaran, N., & Williams, M. D. (2014). Epidemiologic trends in head and neck cancer and aids in diagnosis. *Oral and maxillofacial surgery clinics of North America*, 26(2), 123-141.
- Vogl, T., Eisenblätter, M., Völler, T., Zenker, S., Hermann, S., van Lent, P., Roth, J. (2014). Alarmin S100A8/S100A9 as a biomarker for molecular imaging of local inflammatory activity. *Nature communications*, 5, 4593-4593.
- Wang, G., Lu, X., Dey, P., Deng, P., Wu, C. C., Jiang, S., DePinho, R. A. (2016). Targeting YAP-Dependent MDSC Infiltration Impairs Tumor Progression. *Cancer discovery*, 6(1), 80-95.
- Wang, H., Luo, Q., Feng, X., Zhang, R., Li, J., & Chen, F. (2018). NLRP3 promotes tumor growth and metastasis in human oral squamous cell carcinoma. *BMC Cancer*, 18(1), 500.
- Weiner, L. M., Surana, R., & Wang, S. (2010). Monoclonal antibodies: versatile platforms for cancer immunotherapy. *Nature reviews. Immunology*, 10(5), 317-327.
- WHO. (2018a). Retrieved from <https://www.who.int/cancer/prevention/diagnosis-screening/breast-cancer/en/>
- WHO. (2018b, 12.09.2018). Fact sheet on Cancer.
- Woodfin, A., Reichel, C. A., Khandoga, A., Corada, M., Voisin, M.-B., Scheiermann, C., Nourshargh, S. (2007). JAM-A mediates neutrophil transmigration in a stimulus-specific manner in vivo: evidence for sequential roles for JAM-A and PECAM-1 in neutrophil transmigration. *Blood*, 110(6), 1848-1856.
- Woodfin, A., Voisin, M.-B., Beyrau, M., Colom, B., Caille, D., Diapouli, F.-M., Nourshargh, S. (2011). The junctional adhesion molecule JAM-C regulates polarized transendothelial migration of neutrophils in vivo. *Nature Immunology*, 12(8), 761-769.

- Xie, K. (2001). Interleukin-8 and human cancer biology. *Cytokine & Growth Factor Reviews*, 12(4), 375-391.
- Yaddanapudi, K., Mitchell, R. A., & Eaton, J. W. (2013). Cancer vaccines: Looking to the future. *Oncoimmunology*, 2(3), e23403-e23403.
- Yang, H., Lundbäck, P., Ottosson, L., Erlandsson-Harris, H., Venereau, E., Bianchi, M. E., Antoine, D. J. (2012). Redox modification of cysteine residues regulates the cytokine activity of high mobility group box-1 (HMGB1). *Molecular medicine (Cambridge, Mass.)*, 18(1), 250-259.
- Yang, L., DeBusk, L. M., Fukuda, K., Fingleton, B., Green-Jarvis, B., Shyr, Y., Lin, P. C. (2004). Expansion of myeloid immune suppressor Gr⁺CD11b⁺ cells in tumor-bearing host directly promotes tumor angiogenesis. *Cancer Cell*, 6(4), 409-421.
- Yu, M., Wang, H., Ding, A., Golenbock, D. T., Latz, E., Czura, C. J., .Yang, H. (2006). HMGB1 SIGNALS THROUGH TOLL-LIKE RECEPTOR (TLR) 4 AND TLR2. *Shock*, 26(2), 174-179.
- Zarbock, A., & Ley, K. (2009). Neutrophil adhesion and activation under flow. *Microcirculation (New York, N.Y. 1994)*, 16(1), 31-42.
- Zhang, D., Chen, G., Manwani, D., Mortha, A., Xu, C., Faith, J. J., Frenette, P. S. (2015). Neutrophil ageing is regulated by the microbiome. *Nature*, 525(7570), 528-532.
- Zhang, X., & Mosser, D. M. (2008). Macrophage activation by endogenous danger signals. *J Pathol*, 214(2), 161-178.
- Zuchtriegel, G., Uhl, B., Hessenauer, M. E., Kurz, A. R., Rehberg, M., Lauber, K., Reichel, C. A. (2015). Spatiotemporal expression dynamics of selectins govern the sequential extravasation of neutrophils and monocytes in the acute inflammatory response. *Arterioscler Thromb Vasc Biol*, 35(4), 899-910.

9 Acknowledgements

First of all, I would like to thank my supervisor Prof. Dr. med. Christoph Reichel for giving me the opportunity to investigate this fascinating project. I am very grateful for all the scientific discussions, his supervision, enthusiasm and support during my PhD thesis.

Second, want to thank my thesis advisory committee, Prof. Dr. rer. nat. Kirsten Lauber and Prof. Dr. med. Christian Schulz, for the discussions and their helpful feedback.

I also would like to acknowledge the SFB914 for funding my project and the associated IRTG for all the excellent lectures, method courses and soft skill courses that I got to attend. A special “thank you” goes to Dr. rer. nat. Verena Kochan, for helping whenever necessary and for making the “job” of a student speaker very easy!

Thank you to all group members in our lab, especially to Gabi and Bernd, for always sharing their expertise, to Johanna for the support and good atmosphere and Claudia for excellent technical assistance in the cell culture, all the help with experiments and more!

Many thanks also to my friends and my family for their constant support!

10 Publications and scientific presentations

Publications

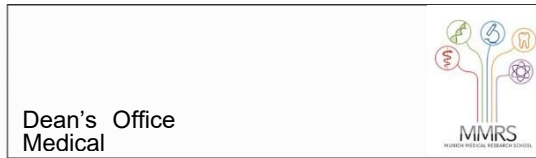
- 1) **Mittmann, L. A.**, Schaubaecher, J., Hennel, R., Holdt, L., Lauber, K., Uhl, B., Reichel, C. A. (2020). Excessive ageing of neutrophils in cancer accelerates tumor progression. (under revision)
- 2) Gryksa, K., **Mittmann, L. A.**, Bauer, A., Peterlik, D., Flor, P.J., Uschold-Schmidt, N., Bosch, O.J. (2020). Metabotropic glutamate receptor subtype 7 controls maternal care, maternal motivation and maternal aggression in mice. *Genes, Brain and Behavior*.19:e12627.
- 3) Puhr-Westerheide, D., Schink, S., Fabritius, M., **Mittmann, L. A.**, Hessenauer, M., Pircher, J., Zuchtriegel, G., Uhl,B., Holzer, M., Massberg, S., Krombach, F. (2019). Neutrophils promote venular thrombosis by shaping the rheological environment for platelet aggregation. *Scientific Reports*. 9, 15932.
- 4) Bromberger, T., Klapproth, S., Rohwedder, I., Zhu, L., **Mittmann, L. A.**, Reichel, C. A., Sperandio, M., Moser, M. (2018). Direct Rap1/Talin1 interaction regulates platelet and neutrophil integrin activity in mice. *Blood*, 132(26), 2754-2762.
- 5) Praetner, M., Zuchtriegel, G., Holzer, M., Uhl, B., Schaubächer, J., **Mittmann, L. A.**, Fabritius, M., Fürst, R., Zahler, S., Funken, D., Lerchenberger, M., Khandoga, A., Kanse, S., Lauber, K., Krombach, F., Reichel, C. A. (2018). Plasminogen Activator Inhibitor-1 Promotes Neutrophil Infiltration and Tissue Injury on Ischemia–Reperfusion. *Arteriosclerosis, Thrombosis, and Vascular Biology*, 38(4), 829-842.

- 6) Zuchtriegel, G., **Mittmann, L. A.**, Sandip, K., Uhl, B., Sperandio, M., Krombach, F., Reichel, C. A. (2020). Vitronectin stabilizes intravascular adhesion of neutrophils by coordinating beta2 integrin clustering. (under revision)
- 7) Uhl, B., **Mittmann, L. A.**, Schaubächer, J., Dominik, J., Braun, C., Pick, R., Canis, M., Lauber, K., Sperandio, M., Krombach, F., Reichel, C. A. (2020). Heteromerization of uPA and PAI-1 promotes advanced stages of breast cancer by programming macrophages to attract pro-tumorigenic neutrophils. (in preparation)
- 8) Sharaf, K., **Mittmann, L.A.**, Nekolla, K., Rehberg, M., Krombach, F., Uhl, B., Zuchtriegel, G., Reichel, C. A. (2020). Distinct interstitial migration patterns of neutrophils and monocytes contribute to effective pathogen clearance. (in preparation)

Scientific presentations

05/2017	1 st TAC Meeting	oral presentation
09/2017	Scientific Retreat of IRTG914 Villa Vigoni, Italy	oral presentation
08/2018	2 nd TAC Meeting	oral presentation
11/2018	Scientific Retreat of IRTG914 Günzburg, Germany	oral presentation
11/2018	Joint Dutch German Vascular Biology meeting Amsterdam, Netherlands	poster presentation
04/2019	Experimental Biology Orlando, Florida, USA	poster presentation
06/2019	6th Summer Symposium of SFB 914	oral presentation

11 Affidavit



Affidavit

Mittmann, Laura Alice

Surname, first name

Street

Zip code, town

Country

I hereby declare, that the submitted thesis entitled

Excessive ageing of neutrophils in cancer accelerates tumor progression

is my own work. I have only used the sources indicated and have not made unauthorized use of services of a third party. Where the work of others has been quoted or reproduced, the source is always given.

I further declare that the submitted thesis or parts thereof have not been presented as part of an examination degree to any other university.

Munich, 30.06.2020

Laura Alice Mittmann

Place, date

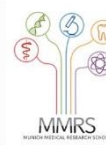
Signature doctoral candidate

12 Confirmation of congruency between printed and electronic version of the doctoral thesis



LUDWIG-
MAXIMILIANS-
UNIVERSITÄT
MÜNCHEN

Dean's Office
Medical



Confirmation of congruency between printed and electronic version of the doctoral thesis

Mittmann, Laura Alice

Surname, first name

Street

Zip code, town

Country

I hereby declare that the electronic version of the submitted thesis, entitled

Excessive ageing of neutrophils in cancer accelerates tumor progression

is congruent with the printed version both in content and format.

Munich, 30.06.2020

Laura Alice Mittmann

Place, date

Signature doctoral candidate